

**SOME ASPECTS OF GAMMA-RAY SCINTILLATION SPECTROMETRY  
USING CESIUM IODIDE CRYSTALS**

**CENTRE FOR NEWFOUNDLAND STUDIES**

**TOTAL OF 10 PAGES ONLY  
MAY BE XEROXED**

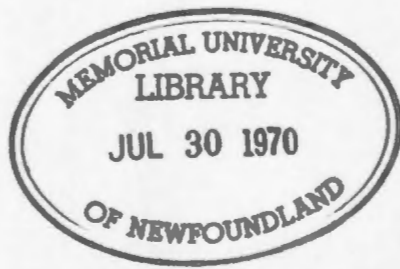
**(Without Author's Permission)**

**RAM DEO GOPAL PRASAD, M.SC. (RANCHI)**



213579

C.1





SOME ASPECTS OF GAMMA-RAY SCINTILLATION SPECTROMETRY  
USING CESIUM IODIDE CRYSTALS

by

© Ram Deo Gopal Prasad, M.Sc. (Ranchi)

Submitted in partial fulfilment  
of the requirements for the degree of Master of Science  
Memorial University of Newfoundland

March, 1970

## TABLE OF CONTENTS

CHAPTER		Page
ABSTRACT		1
I	INTRODUCTION	2
1.1	Gamma-ray Scintillation Spectrometry	2
1.2	The Absolute Detection Efficiency, the Photopeak Efficiency and the Photofraction	3
1.3	The Scaling Relations for the Absolute Detection Efficiency	7
1.4	Cesium Iodide and Sodium Iodide Crystals	10
1.5	The Present Project	12
II	REVIEW OF WORK ON NaI AND CsI CRYSTALS PERTAINING TO GAMMA-RAY SPECTROMETRY	14
III	THE EXPERIMENT	48
3.1	The Experimental Arrangement	48
(a)	The Electronic Set-Up	48
(b)	The Shielding Chamber	53
(c)	The Source Holder	55
3.2	The Measurement of the Crystal-to-Can-Top Distance	59
3.3	The Choice of the Radioactive Sources	64
3.4	The Acquisition of Data	66

CHAPTER		Page
IV	THE ANALYSIS OF SPECTRA AND THE PRESENTATION OF RESULTS	68
4.1	The Analysis of Spectra	68
(a)	The Number of Counts under a Photopeak of Gaussian Shape	68
(b)	Deviations from the Gaussian Shape of the Photopeaks	70
(c)	The Effect of the Sum-Spectrum	72
(d)	The Estimation of Errors	73
(e)	The Effect of the Absorbing Material between the Crystal and the Source	76
4.2	The Direct Experimental Results	79
(a)	The Sealed and Unsealed 2" x 2" CsI(Tl) Crystals	79
(b)	The Energy Resolution and the Typical Spectra	80
(c)	The Relative Photopeak Efficiencies	82
(d)	The Asymmetry Factor	91
4.3	The Evaluation of the Photofractions of CsI Crystals	100
V	DISCUSSION OF THE RESULTS	115
5.1	Comparison of our Experimental Photofraction Values with the Theoretical Values of Miller and Snow (1961)	115
5.2	The Asymmetry in the 3" x 3" CsI(Na) Crystal Spectra	118

CHAPTER		Page
5.3	Dependence of Photofractions on the Crystal-to-Source Distance	122
5.4	Photofractions of CsI Crystals using the Theoretical Values of Miller and Snow for the 3" x 3" NaI(Tl) Crystal	125
5.5	The Effect of the Possible Error in the Crystal-to-Source Distance	130
5.6	The Effect of the Finite Dimensions of the Sources	136
5.7	Photofractions of CsI and NaI Crystals	137
5.8	The Concluding Remarks	140
	ACKNOWLEDGEMENTS	142
	BIBLIOGRAPHY	143
	ADDITIONAL GENERAL REFERENCES	146

ABSTRACT

Photopeaks in four crystals, a 3" x 3" NaI(Tl), a 3" x 3" CsI(Na), a 2" x 2" CsI(Tl) and an unsealed 2" x 2" CsI(Tl) were experimentally investigated for ten gamma-ray energies in the energy range of 0.279 Mev to 3.25 Mev (using radioactive sources) and for a number of crystal-to-source distances from 1 cm to 10 cm. These measurements gave directly the relative photopeak efficiencies thus yielding new information about these CsI crystals. The photopeaks in the 3" x 3" CsI(Na) crystal were found to be unexpectedly asymmetric, and we analyzed our spectra from two points of view: (i) referring to the high energy half of the peaks and (ii) referring to the full peaks. The extent of asymmetry was investigated in detail. An important feature in our experimental set-up was the source-holder designed to facilitate accurate adjustments of the crystal-to-source distances (inside the lead chamber) with external manipulations only. We also determined the photofractions of the CsI crystals at 3 and 10 cm (and at 0 and 15 cm by extrapolation) assuming the experimental values of Heath (1964) for the photofraction of a 3" x 3" NaI(Tl). In this connection we used the "scaling relations" to compute the absolute detection efficiencies of the CsI crystals from the available information on the NaI crystals. The photofractions were found to be not too sensitively dependent on the crystal-to-source distance. We have compared our photofraction values with the theoretical values of Miller and Snow (1961) for the photofractions of the CsI crystals. Theoretical values were seen to be generally too large. Disagreement with the theoretical values was also seen in the comparison of the ratios of the photofractions of the 3" x 3" and the 2" x 2" CsI crystals.

CHAPTER I

INTRODUCTION

1.1 Gamma-ray Scintillation Spectrometry:

Since the early developments in the field of the scintillation spectrometry of gamma-rays, thallium activated sodium iodide (NaI(Tl)) crystals have been used almost to the exclusion of any other crystal. The reason is simple. The gamma-quanta are not detected directly but they first transfer, in their interaction with the material of the detectors, some or all of their energy to electrons either through the photo-electric effect or in a Compton collision or in a pair-production (provided the gamma-energy is greater than 1.02 Mev, which is the rest mass of the negatron-positron pair). The detection of gamma-quanta is in actual fact the detection of the energy transferred to the electrons. The observed count rate and the energy distribution spectrum are, of course, related to the strength of the gamma-source and the energy distribution of the incident gamma-rays, but the relationship is quite complicated. The relationship involves: (i) the cross-section of various types of events - namely, photo-electric effect, Compton effect and pair-production - which are dependent on the  $\gamma$ -ray energy and on the nature of the material, (ii) the size of the detector and (iii) the geometrical arrangement of the gamma source and the detector. Thus elaborate computations have to be performed to deduce the source strength from the observed energy spectrum even when the incident gamma-rays are mono-energetic. The NaI(Tl) crystals were recognized

as excellent gamma-ray detectors; hence, quite naturally these elaborate calculations have been performed for various selected shapes and sizes of NaI(Tl) crystals for different gamma-ray energies and with some selected geometrical arrangements. Though, later on, cesium iodide crystals came to be regarded as good gamma-ray detectors and, in some respects even preferable to NaI(Tl) detectors, there is a paucity of the needed elaborate computations applicable to cesium iodide crystals. We felt that the cesium iodide crystals should receive a greater attention in gamma-ray scintillation spectrometry, and we undertook the project of making direct experimental comparisons between NaI(Tl) and CsI detectors for different gamma energies and geometrical arrangements and thus obtaining a sort of conversion factor so that the already available information for the NaI(Tl) crystals can be used for the CsI detectors.

1.2 The Absolute Detection Efficiency, the Photopeak Efficiency and the Photofraction:

Before proceeding any further, it would be appropriate to explain some quantities - namely, the absolute detection efficiency, the photopeak efficiency and the photofraction.

Let a mono-energetic gamma source emitting  $N$  quanta (isotropically) give  $n$  counts (i.e. detectable scintillation events) in a scintillation detector situated in a certain geometrical arrangement with respect to the gamma source. The ratio  $\frac{n}{N}$  is the absolute

detection efficiency of that detector for the particular gamma-ray energy and for the particular geometry. Some of the observed counts correspond to the transfer of the total energy of the detected quantum to the detector, and these counts lie in the "total energy peak", more frequently referred to as the "photopeak" because the photo-electric effect implies a total transfer of the energy of the interacting gamma-quantum to the photo-electron (except for a possible X-ray escape peak), but it is understood that the "total energy peak" includes those events which also result in a total transfer of energy via a Compton collision followed by a photo-electric interaction of the Compton scattered photon within the detector, or via other suitable successive interactions yielding one count (event) corresponding to the eventual transfer of the total energy. Following the convention, we shall use the term "photopeak" for the "total energy peak". Let the number of counts in the photopeak be "p" while, as assumed earlier, the total number of observed counts is n. The ratio  $\frac{p}{n}$  is called the photofraction for the particular gamma-energy and the geometrical arrangement. The ratio  $\frac{p}{N}$  is called the photopeak efficiency. Thus,

$$\text{Photopeak efficiency} = \text{Absolute detection efficiency} \\ \times \text{Photofraction}$$

Related to the absolute detection efficiency one can define the "intrinsic efficiency" for a particular arrangement as the probability of getting a pulse anywhere in the spectrum if the gamma-ray is incident on the crystal. That is,

$$\text{Absolute detection efficiency} = \text{Intrinsic efficiency} \times \frac{\Omega}{4\pi}$$

where  $\frac{\Omega}{4\pi}$  is the "geometry factor", i.e. the fraction of the emitted gamma-rays which are actually incident on the crystal,  $\Omega$  being the solid-angle subtended by the crystal face with respect to the source.

Similarly, the "intrinsic photopeak efficiency" can be defined as

$$\text{Photopeak efficiency} = \text{Intrinsic photopeak efficiency} \times \frac{\Omega}{4\pi}$$

It may be remarked that some authors use slightly different names for the above quantities, e.g. "total efficiency" for "intrinsic efficiency".

The Monte-Carlo calculations, employing the known values of the cross-section of the relevant interactions, can give not only the computed values of the absolute detection efficiency and the photopeak efficiency but also the complete shape of the expected spectrum. Such computations have already been carried out for solid right cylindrical and well-type NaI(Tl) crystals of various sizes. (The references for solid right cylindrical NaI(Tl) crystals are Berger and Doggett (1956), Miller and Snow (1961), Gossett and Davisson (1961), Zerby and Moran (1961), Weitkamp (1963) and Snyder (1967).)

We shall confine our discussion to the point or the near-point sources only. The results are available for various crystal-to-source distances, the source being placed on the axis of the crystal. In addition to the computations for the NaI(Tl) crystals, some computations have been carried out for a few CsI(Tl) crystals (Miller and Snow (1961)), also. In Chapter II we shall give a detailed survey of the literature covering the relevant work on the solid right cylindrical NaI(Tl) and CsI(Tl or Na) crystals for point gamma sources. Our conclusion of the

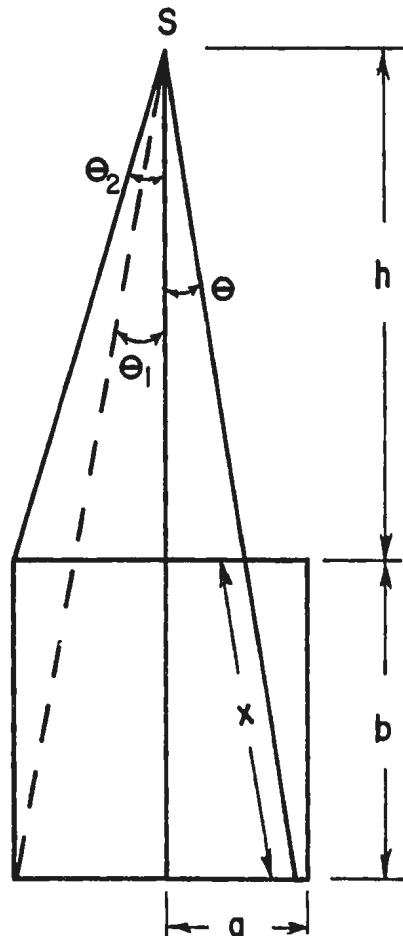
literature survey is that the computed values of the absolute detection efficiency are quite satisfactory, but the agreement between the theoretical and the experimental values of the photopeak efficiency (or equivalently of the photofraction) is not. From the point of view of using the scintillation detectors for gamma-rays, the experimentalist usually wants to know the photopeak efficiencies because it is more convenient to analyze simple spectra in terms of the photopeaks (Lazar et al (1956)). The following sentences explain the situation. We are interested only in those events which are caused by the interactions with the detector of gamma-rays incident on the detector directly from the source. There are, however, interactions of gamma-rays with the material in the neighbourhood of the detector also and a number of these secondary events are partially detected by the detector. These "unwanted pulses" contaminate the true spectrum. It is very fortunate, however, that most of these unwanted pulses lie outside the corresponding photopeak. Thus it is very convenient to get maximum information from the counts under the photopeak because then the exacting requirements to keep the complete spectrum free from the unwanted pulses (or to correct for the effect) can be relaxed.

It has been mentioned earlier that the theoretical values of the photopeak efficiencies have not proved very satisfactory so far and, therefore, the experimental determination of photofractions fills an important gap.

The absolute detection efficiencies can be computed without using the Monte-Carlo calculations. From a knowledge of the total

absorption coefficient one can theoretically evaluate the absolute detection efficiency by computing the probability that, in a given arrangement, a quantum emitted by the source will produce a "scintillation event" in the detector. For the sake of convenience, we shall refer to this method as the "integration method". Furthermore, one has simple scaling relations between the absolute detection efficiencies of different detectors if the dimensions are properly chosen. We shall devote the next section to the discussion of this aspect.

1.3 The Scaling Relations for the Absolute Detection Efficiency;



$$\theta_1 = \tan^{-1} \frac{a}{b+h}$$

$$\theta_2 = \tan^{-1} \frac{a}{h}$$

Fig. 1.1 Point Gamma Source S placed on the Axis of a Solid Right Cylindrical Detector of Radius 'a' and Thickness 'b'

For the crystal-source geometry shown in Fig. 1.1, the absolute detection efficiency  $\epsilon(E)$  for gamma-rays of energy  $E$  is given by

$$\epsilon(E) = \int_0^{\theta_2} (1 - e^{-\mu(E)x(\theta)}) \frac{2\pi \sin\theta \, d\theta}{4\pi} \quad \dots\dots (1.1)$$

where  $\frac{1}{4\pi} (2\pi \sin\theta \, d\theta)$  is the probability that an emitted quantum lies within the solid angle element between  $\theta$  and  $(\theta + d\theta)$ , and  $\mu(E)$  is the total absorption coefficient for the particular gamma-ray energy and the material of the detector.

$$\therefore \epsilon(E) = \frac{1}{2} \int_0^{\theta_2} (1 - e^{-\mu(E)x(\theta)}) \sin\theta \, d\theta = \frac{1}{2}(I_1 + I_2) \quad \dots (1.2)$$

$$\begin{aligned} \text{where: } I_1 &= \int_0^{\theta_1} (1 - e^{-\mu(E)x(\theta)}) \sin\theta \, d\theta \\ &= \int_0^{\theta_1} (1 - e^{-\mu(E)\frac{b}{\cos\theta}}) \sin\theta \, d\theta \quad \dots\dots (1.3) \end{aligned}$$

$$\text{and } I_2 = \int_{\theta_1}^{\theta_2} \left\{ 1 - e^{-\mu(E)\left[\frac{a}{\sin\theta} - \frac{h}{\cos\theta}\right]} \right\} \sin\theta \, d\theta \quad \dots\dots (1.4)$$

$$\text{We note that, } \theta_1 = \tan^{-1} \frac{a}{b+h} \quad \text{and } \theta_2 = \tan^{-1} \frac{a}{h} \quad \dots\dots (1.5)$$

If desired, one can write the expression for the intrinsic efficiency in a straightforward way,

$$\epsilon_{\text{int}}(E) = \frac{4\pi}{\Omega} \epsilon(E) \quad \dots\dots (1.6)$$

From the expression for the integrals  $I_1$  and  $I_2$  and for the limits  $\theta_1$  and  $\theta_2$ , it is obvious that if  $a$ ,  $b$ ,  $h$  are changed in the same proportion, i.e.,

$$\frac{a'}{a} = \frac{b'}{b} = \frac{h'}{h} = k \quad (\text{say}) \quad [\text{which also implies that the limits } \theta_1 \text{ and } \theta_2 \text{ are unchanged}]$$

and at the same time, by using a different material and/or different energy,  $\mu$  is changed such that

$$\frac{\mu'}{\mu} = \frac{1}{k}$$

so that

$$\mu'a' = \mu a, \quad \mu'b' = \mu b \quad \text{and} \quad \mu'h' = \mu h$$

then the integrals  $I_1$  and  $I_2$  evaluated for parameters  $\{a, b, h, \mu(E)\}$  and  $\{a', b', h', \mu'(E')\}$  have identical values. Thus for a crystal of dimension  $(a', b')$ , source-to-crystal distance  $h'$  and for a gamma-ray of energy  $E'$  having a total absorption coefficient  $\mu'(E')$ , we get the same absolute detection efficiency as for a crystal of dimension  $(a, b)$ , source-to-crystal distance  $h$  and for a gamma-ray of energy  $E$  having the total absorption coefficient  $\mu(E)$ . Thus if we have tables of the absolute detection efficiency for some crystal sizes and source-to-crystal distances, we can evaluate the absolute detection efficiency for many other crystals connected through the homothetic transformation  $a' = ka$ ,  $b' = kb$ ,  $h' = kh$ , provided that  $\mu(E)$  is replaced by  $\mu'(E') = \frac{\mu(E)}{k}$ . It should be noted that this "scaling" is not restricted to crystals of the same material as long as the absorption coefficients appropriate to the materials involved are used.

The usefulness of these scaling relations was first pointed out by Stanford and Rivers (1958). A few other works mention this simple but extremely useful feature of this expression for the absolute detection efficiency (Grosjean (1962), Vartanov and Samoiloov (1965)). It may be further noted that the above mentioned scaling relations hold for intrinsic efficiency as well because

$$\Omega = 2\pi \left[ 1 - \frac{h}{(h^2 + a^2)^{1/2}} \right]$$

is also invariant under the homothetic transformation.

In the light of the material presented in this section, the importance of knowing accurate values of the absorption coefficients as a function of energy cannot be overemphasized. In connection with the study of sodium iodide and cesium iodide crystals, the knowledge of the total absorption coefficient for gamma-rays of various energies in these two substances are of great importance. Results of extensive computations for various elements are available in Grodstein (1957), Storm et al (1958) and McGinnies (1959). The values for some compounds including NaI are also given in Grodstein's report. The values for CsI can be calculated from the elemental cross-sections.

#### 1.4 Cesium Iodide and Sodium Iodide Crystals:

If we compare CsI and NaI detectors of equal volumes, then of the two, the CsI detector has greater gamma-ray detection efficiency because the density of CsI ( $4.51 \text{ gm/cm}^3$ ) is greater than that of NaI

( $3.67 \text{ gm/cm}^3$ ). Moreover, because of a higher atomic number of cesium compared with that of sodium, the photo-electric cross-section in CsI is relatively more important than that of NaI, and this means a larger photofraction in the case of CsI. Thus, the photopeak efficiency of a CsI crystal is larger than that of a NaI crystal of equal volume because of two reasons: (i) a larger overall detection efficiency and (ii) a larger photofraction.

CsI has two other important advantages over NaI. Firstly, the latter is extremely hygroscopic whereas CsI is not and can be exposed to the atmosphere. Secondly, the hard soap-like properties of CsI make CsI crystals much less vulnerable to damage by mechanical shocks and mishandling than the NaI crystals. In addition to the above mentioned features, CsI has no potassium content, but NaI always has some such contamination and the consequent adverse effect on the signal to background ratio because of pulses due to  $\text{K}^{40}$ .

From the point of view of the scintillation characteristics, however, NaI(Tl) is a better crystal than CsI(Tl). The latter has only about 40 to 50% light output relative to that in NaI(Tl). Also, the decay constant of CsI(Tl) is  $1.2 \mu \text{ sec.}$  compared with the faster NaI(Tl) which has  $0.25 \mu \text{ sec.}$  decay constant. Recently produced CsI(Na) have improved the situation of CsI crystals because the light output in a CsI(Na) crystal is about 80% of that in a NaI(Tl) crystal and the decay constant is  $0.65 \mu \text{ sec.}$  Thus the CsI(Na) crystals do not appear to lag far behind the NaI(Tl) crystals in scintillation properties and have decided advantages over the NaI(Tl) mentioned earlier. For the

properties of the CsI(Tl) crystals, we refer to the work of Schmidt (1960) and for those of CsI(Na) we refer to the work of Brinckman (1965), Breiter and Schulz (1967) and Menefee et al (1967).

1.5 The Present Project:

We decided to determine experimentally the photofractions for those crystals which are good gamma-ray detectors [CsI(Na) and CsI(Tl)] but for which this information is lacking. Instead of following the conventional approach of measuring the ratio of area under the photopeak to the area under the complete spectrum, we decided to measure the photopeak efficiencies of the detectors under investigation in terms of the photopeak efficiency of a reference detector for which reliable experimental values were already available. The justification for this approach lies in the expectation that the relative photopeak efficiencies should be determined with great accuracy without having to take elaborate experimental precautions to minimize the number of unwanted counts in the observed spectrum (keeping in mind that most of these unwanted counts are outside the photopeak). More will be said later about these expectations. The work in this thesis covers the comparative study of

- (i) a 3" diameter x 3" height solid right cylindrical NaI(Tl) crystal (briefly referred to as a 3" x 3" NaI(Tl) crystal).
- (ii) a sealed 3" x 3" CsI(Na) crystal.
- (iii) a sealed 2" x 2" CsI(Tl) crystal.
- (iv) an unsealed 2" x 2" CsI(Tl) crystal.

All these crystals were purchased from the Harshaw Chemical Company and the first three belong to their standard line assemblies.

From the relative photopeak efficiencies and the calculated values of the absolute detection efficiency (using scaling relations), we have determined the photofractions for the CsI crystals accepting Heath's experimentally determined photofractions for a 3" x 3" NaI(Tl) crystal at 3.0 and 10.0 cm (Heath (1964)). The energy range covered by us was limited to the availability of suitable radioactive sources of near-point configuration. We carried out measurements at 0.279, 0.57, 0.662, 0.835, 1.064, 1.332, 1.837, 2.43, 2.615 and 3.25 Mev using the following sources:

- |                                      |                        |
|--------------------------------------|------------------------|
| (1) Hg <sup>203</sup>                | 0.279 Mev              |
| (2) Bi <sup>207</sup>                | 0.57 Mev and 1.064 Mev |
| (3) Cs <sup>137</sup>                | 0.662 Mev              |
| (4) Mn <sup>54</sup>                 | 0.835 Mev              |
| (5) Co <sup>60</sup>                 | 1.332 Mev              |
| (6) Y <sup>88</sup>                  | 1.837 Mev              |
| (7) Ra <sup>226</sup> plus daughters | 2.43 Mev               |
| (8) Th <sup>228</sup> plus daughters | 2.615 Mev              |
| (9) Co <sup>56</sup>                 | 3.25 Mev               |

CHAPTER II

REVIEW OF WORK ON NaI AND CsI CRYSTALS  
PERTAINING TO GAMMA-RAY SPECTROMETRY

We now proceed to review the already published work on the gamma-ray detection efficiencies and the photofractions of solid right cylindrical crystals of sodium iodide and cesium iodide; restricting ourselves mainly to point sources (without collimation) on the crystal axis. As mentioned in the first chapter, in this thesis when we refer to a crystal as a  $d \times t$  crystal, we mean a solid crystal of right cylindrical shape of diameter " $d$ " and thickness (or height) " $t$ ", i.e. a 2" x 3" crystal means a crystal of 2" diameter and 3" thickness.

We have already defined in the first chapter the relevant terms, (i) the absolute detection efficiency ( $\epsilon$ ), (ii) the photopeak efficiency ( $\epsilon_p$ ), (iii) the photofraction ( $f$ ), (iv) the intrinsic efficiency ( $\epsilon_{int}$ ) and (v) the intrinsic photopeak efficiency  $\epsilon_{p(int)}$ . It may be pointed out that some authors define the absolute detection efficiency by a quantity twice as large as our  $\epsilon$  because they take the ratio of the detected events to the gamma-quanta emitted by the source only in the hemisphere containing the detector. We will have occasion to mention some other terms, also, in the course of this review.

Lazar et al (1956) were one of the earliest to have studied NaI(Tl) crystals of various sizes, including a 3" x 3" crystal in which we are interested. They used the "integration method" to compute the

absolute detection efficiency for various crystal-to-source distances. They reported to have measured the photofractions for the different crystals they worked with, for two crystal-to-source distances. In this connection, they used sources emitting mono-energetic gamma-rays from 0.145 Mev to 1.114 Mev, and sources emitting two gamma-rays for 1.85 Mev and 2.76 Mev. The contribution to the total area from the lower energy gamma-rays, in the latter case, was determined by fitting a Gaussian shape to the full energy peaks observed for these radiations and using the value of the photofraction which had already been determined for that energy. Nuclear reactions were used for energies above 2.76 Mev and up to 7.48 Mev. Photofractions obtained at 2.14 Mev and 1.78 Mev by using radio-active isotopes and by using different reactions showed excellent agreement. Extreme care was taken to see that extraneous effects were minimum.

About the same time Wolicki et al (1956) extended the absolute detection efficiency calculations to several other NaI(Tl) crystals to cover the "standard crystals" of the Harshaw Chemical Co. available at that time.

Stanford and Rivers (1958), besides giving the intrinsic efficiencies of a number of NaI(Tl) crystals of various heights and diameter 1.5", pointed out the very useful scaling relations, already discussed in section 1.3, chapter I.

In 1958 Lazar reviewed the technique developed for the analysis of gamma-ray spectra at the Oak Ridge National Laboratory by the scintillation spectroscopy group over a number of years. They defined the peak

efficiency slightly differently from our photopeak efficiency. They defined it as the probability of obtaining a "full energy pulse" if a gamma-ray strikes the crystal. We have already referred to this quantity as the intrinsic peak efficiency or the intrinsic photopeak efficiency  $\epsilon_{p(int)}$ . That group determined  $\epsilon_{p(int)}$  by the relation

$$\epsilon_{p(int)} = \epsilon_{int} \times f \quad \dots (2.1)$$

where  $f$ , the photofraction, is the experimental quantity and  $\epsilon_{int}$  is the calculated value referred to in Lazar et al (1956). They have mentioned an accuracy of 3% for a 3" x 3" NaI(Tl) crystal. They determined the photofraction  $f$  for two crystal-to-source distances, 3.0 cm and 9.3 cm in the energy range 0.150 Mev to 7.50 Mev. They estimated that for large crystal-to-source distances (>10 cm), the photofraction was not distance dependent, but not so for smaller distances. In fact, they found that  $f$  may differ by as much as 10 to 20 % for 3.0 and 9.3 cm. As expected, both the photofraction and the photopeak efficiency approached unity (not linearly) for very low energies (<200 Kev).

One of the most quoted works in this connection is that of Heath. We refer to the report of Vegors, Marsden and Heath published in 1958 and a two volume report published by Heath in 1964. The latter is a complete revision of an earlier data compilation which was issued as an AEC R and D Report (IDO - 16408) in 1958. These reports include the computed values of the absolute detection efficiency  $\epsilon$  obtained by the "integration method" for a number of NaI(Tl) crystals for various

crystal-to-source distances. [While going over the tabulated values of  $\epsilon$  in the energy range and the crystal-to-source distances of our interest, we have spotted an error, which seems to be of typographical origin. In the 1958 report of Vegors et al on page no. 48 and again in the 1964 report of Heath in the table in Appendix II giving the "Calculated Detector Efficiency, 3" x 3" NaI, Point Source" the tabulated value of  $\epsilon$  for a crystal-to-source distance of 20.0 cms and an energy 0.566 Mev is 0.00547 whereas it should have been 0.0065 (perhaps 0.00647)]. The reports also include the results of very carefully carried out experiments on the direct determination of photofractions. The direct determination means the determination of the ratio of the area under the peak to the total area of the spectrum. Obviously, extreme care had to be taken in obtaining the true complete spectrum. In some cases, these directly determined values were compared with the ratio of the experimentally determined photopeak efficiencies to the calculated absolute detection efficiencies of Vegors et al (1958). The experimental determination of the photopeak efficiency involved calibrating the strength of the gamma-source and finding the number of counts under the photopeak. The calibration of the source strength was carried out by the  $4\pi\beta\text{-}\gamma$  coincidence technique. In all cases where such comparisons could be carried out, the values of the photofractions from the two methods agreed within better than 2%. Heath's values of photofraction for a 3" x 3" NaI(Tl) crystal are being reproduced in Table 2.1 and Fig. 2.1.

Table 2.1

Experimental Peak-to-Total Ratios for 3"x3" NaI Detector

[Ref: Heath (1964)]

Isotope	$E_{\gamma}$ (Mev)	Point Source	
		10 cm source distance integration*	3 cm source distance integration
Sc <sup>47</sup>	0.155	0.960	0.962
Ce <sup>139</sup>	0.166	0.950	
Cr <sup>51</sup>	0.323	0.820	0.813
Au <sup>198</sup>	0.4117		0.737
Be <sup>7</sup>	0.478	0.668	0.657
Cs <sup>137</sup>	0.6616	0.536	0.532
Nb <sup>95</sup>	0.766	0.500	0.504
Mn <sup>54</sup>	0.835	0.474	0.464
Zn <sup>65</sup>	1.114	0.395	0.388
Co <sup>60</sup>	1.332		0.357
Al <sup>28</sup>	1.78	0.290	0.295
Y <sup>88</sup>	1.837	0.280	
Na <sup>24</sup>	2.753		0.225
S <sup>37</sup>	3.13		0.207

\*Integration means the direct determination method explained above.

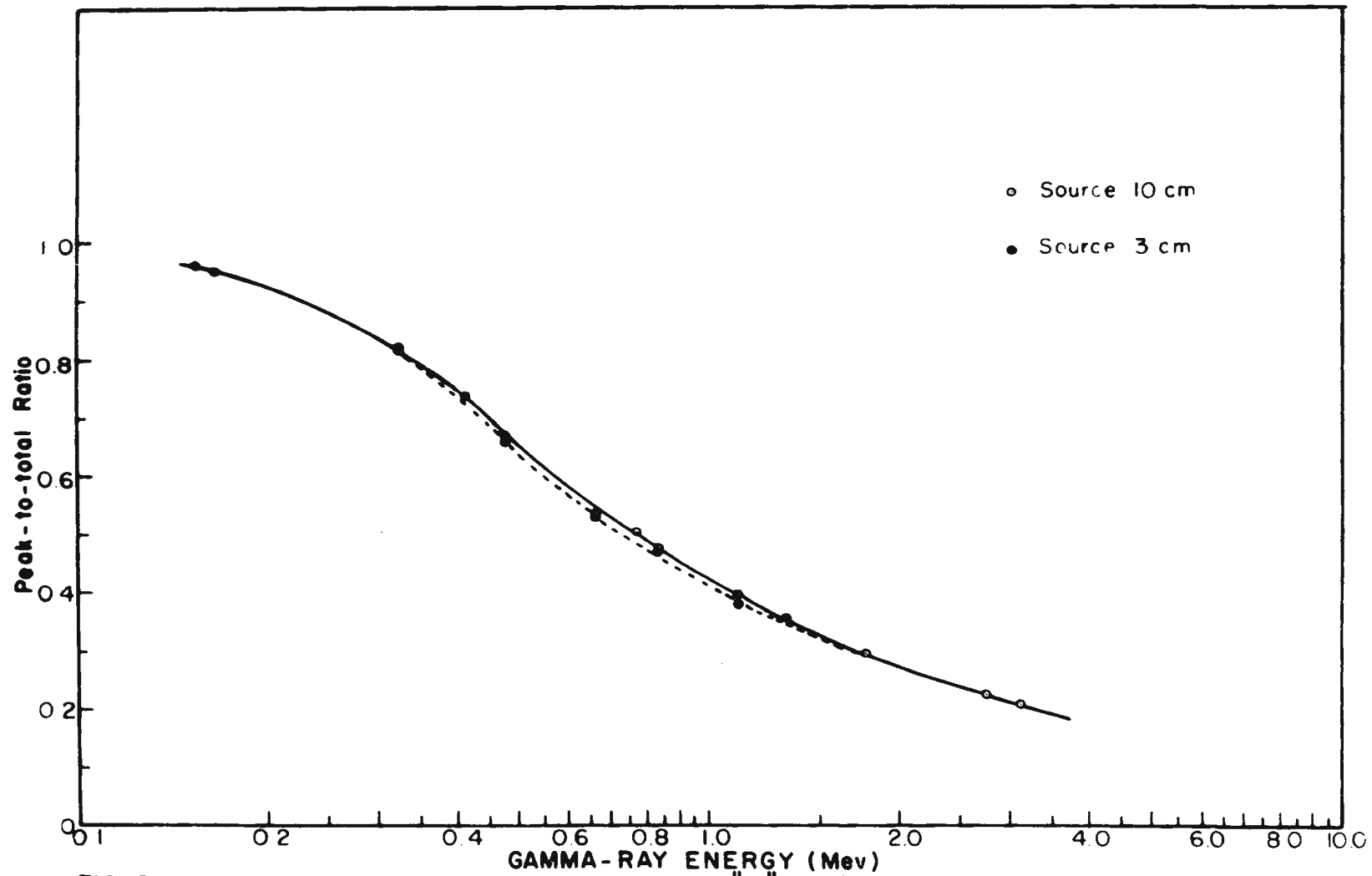


FIG. 2.1 Experimental Peak-to-total Ratio for 3x3" NaI(Tl) Detector Ref. Heath (1964)

The values are for two crystal-to-source distances, 10.0 cm and 3.0 cm . It is seen that the photofraction does not depend sensitively on the crystal-to-source distance whereas the earlier mentioned work of Lazar (1958) indicates a much larger difference between the values at 9.3 cm and 3.0 cm . It should be pointed out that Heath's results reproduced here are from the later report of 1964. The earlier report of Vegors et al (1958) also had included values of experimental photofractions but for fewer sources. Though Heath's experimental values of photofractions are probably the best available, it is difficult to estimate the uncertainties in the values quoted in the report. The values have been given up to three significant figures but that does not reflect the uncertainty in the values themselves. In the earlier report of Vegors et al (1958), results have been given of an experimental check of source strengths determined by two NaI(Tl) crystals 1 3/4" x 2" and 3" x 3". In the smaller crystal, the total number of counts in the whole spectrum was determined and in the 3" x 3" crystal only counts in the photopeak were determined and by using the values of the photofraction, the disintegration rate was determined. When the latter was compared with the disintegration rate obtained by using the smaller crystal, a discrepancy as much as 4.2% was observed. These discrepancies were considered to be within the experimental error.

During the period between the earlier reports and the revised reports of Heath some important works were published by a number of authors. Schmidt (1960) studied in some detail a 5" x 3.5" CsI(Tl)

mounted on a Dumont 6363 photo-tube. This was perhaps the first experimental work to be published on the gamma-spectrometry with a CsI(Tl) crystal. His studies showed a linear response of the CsI(Tl) crystal to low and high gamma-energies, an encouraging comparison of resolution with that of an 8" x 8" NaI(Tl) crystal and a larger photo-fraction in comparison to a 5" x 4" NaI(Tl) crystal. These photo-fractions were calculated by measuring the counts in the high energy half of the photopeak, doubling the number and dividing by the total number of counts detected. We reproduce his results in Fig. 2.2

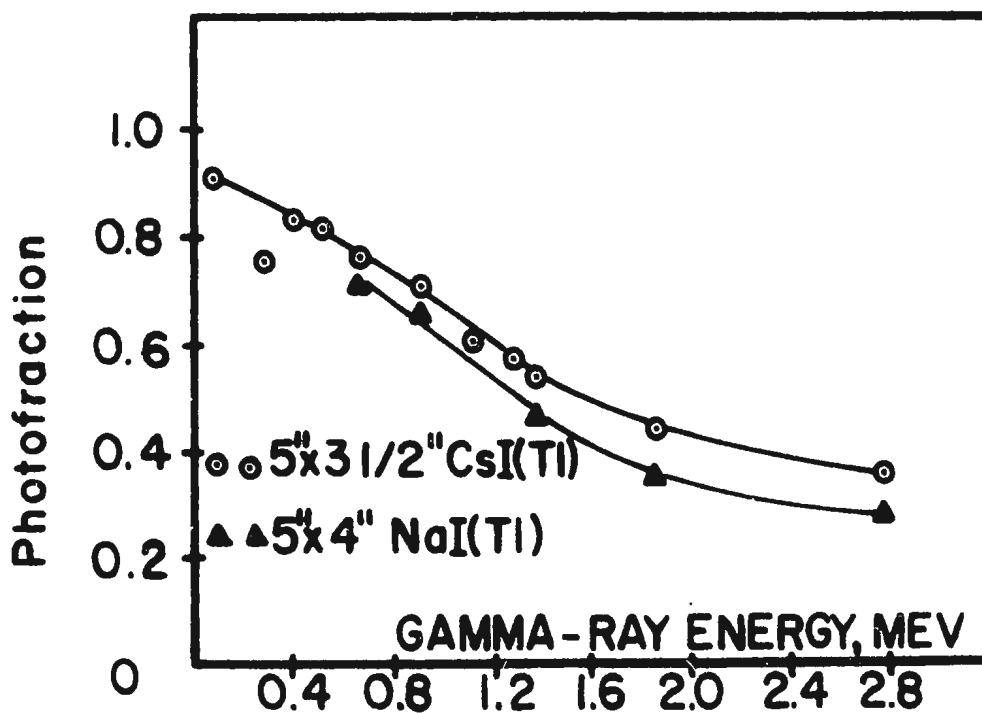


FIG. 2.2 CsI and NaI photofractions  
Ref. Schmidt(1960)

Although the CsI(Tl) crystal was 0.5 inch shorter in height, it gave a larger photofraction. The improvement of photofraction increased with energy.

About the same time Van Oostrum and Meijer (1961) determined the photopeak efficiency as a function of gamma-ray energy for a 3" x 3" NaI(Tl) crystal employing the so-called "two line method". The technique rests on using sources emitting gamma-rays of two energies of known relative intensity and thus determining the ratio of the photopeak efficiencies for these two energies. They used three such sources ( $\text{Na}^{22}$ ,  $\text{Y}^{88}$  and  $\text{Na}^{24}$ ) and from the three ratios they draw a smooth graph of photopeak efficiency in arbitrary units against gamma-ray energy. The graph was calibrated to give absolute values of photopeak efficiencies by using it for a source of known strength (in fact they used two sources  $\text{Au}^{198}$  and  $\text{Cs}^{137}$ ). The energy range of the graph was extended by using gamma-rays of higher energy from selected (p, $\gamma$ ) reactions suitable for this "two line method". In all they covered an energy range of 0.411 Mev to 5.8 Mev. They also determined the photofractions for some mono-energetic sources to check their results of the "two line method". The values of these photofractions are being reproduced in Table 2.2. We wish to point out that these values of the photofractions are generally lower than the expected values. For example: for  $\text{Cs}^{137}$ , they quote a value of 0.44, whereas one would expect it to be greater than 0.5. Their "two line method" values correspond to larger values of photofractions and are probably more reliable than the directly determined values given by them for mono-energetic sources.

TABLE 2.2

The Ratios of Full-Absorption Peak to Total Spectrum

[Ref: Van Oostrum and Meijer (1961)]

Gamma-ray energy (Mev)	Gamma-ray source	f
0.412	Au <sup>198</sup>	0.60
0.662	Cs <sup>137</sup>	0.44
1.11	Zn <sup>65</sup>	0.33
2.37	C <sup>12</sup> (p,γ) N <sup>13</sup> at Ep = 0.450 Mev	0.20
3.51	C <sup>12</sup> (p,γ) N <sup>13</sup> at Ep = 1.70 Mev	0.13
4.43	Po Be	0.12
5.88	Si <sup>29</sup> (p,γ) P <sup>30</sup> Ep = 0.326 Mev	0.073

Miller and Snow (1960) calculated the energy-loss spectra and response spectra for gamma-rays in CsI(Tl) and NaI(Tl) crystals by the Monte-Carlo method. The response spectra for CsI(Tl) crystals for various energies and a crystal-to-source distance of 10.0 cm show larger

photopeaks and a lower Compton distribution when compared with NaI(Tl) crystals of the same sizes and under identical geometrical conditions. The Monte-Carlo calculations give not only the absolute detection efficiency (or the intrinsic efficiency) but also the photofraction. It must be pointed out at this stage that the authors have used a term interaction ratio instead of intrinsic efficiency and that the interaction ratio also includes the Rayleigh Scattering which does not result in a scintillation event. In 1961, the results of the Monte-Carlo calculations carried out by these authors for interaction ratios and photofractions for CsI(Tl) and NaI(Tl) crystals of various sizes and energy up to 14.0 Mev together with the above mentioned work appeared in the form of a report. Again, in the same year, a condensed paper containing the results for interaction ratios and photofractions for CsI(Tl) and NaI(Tl) of various sizes and a crystal-to-source distance of 10.0 cm. for the former and 10.0 cm and zero for the latter was published. The interaction ratios and the photofractions for CsI(Tl) and NaI(Tl) are being reproduced in Tables ...2.3(a), 2.3(b) and 2.3(c). We now have "theoretical photofractions" of Miller and Snow, and "experimental photofractions" of Heath and some other workers. For a 3" x 3" NaI(Tl) crystal and for a crystal-to-source distance of 10.0 cm, the theoretical photofractions of Miller and Snow have been found to be generally higher than the experimental values of Heath. At 0.661 Mev, 1.332 Mev and 2.62 Mev, they are higher by ~ 5%, ~ 10% and ~ 14% from Heath's

values. We thus see that the discrepancy goes on increasing with increasing energy. The absolute detection efficiencies as calculated from the interaction ratios of these authors are in excellent agreement with those calculated by other workers for crystal-to-source distance of 10.0 cm except in the energy range 0.30 Mev to 0.60 Mev where these are very slightly higher (less than 2%).

TABLE 2.3(a)

Point Source 10 cm From CsI Crystal and on Crystal Axis

[Ref: Miller and Snow (1961)]

Crystal size, dia. x ht. (in.)	Energy (Mev)					
	0.279	0.661	1.330	2.620	4.450	6.130
	INTERACTION RATIOS					
3 x 3	0.853	0.679	0.562	0.493	0.473	0.477
2 x 2	0.841	0.621	0.496	0.421	0.404	0.410
1 x 1	0.787	0.434	0.353	0.289	0.274	0.279
$\frac{1}{2}$ x $\frac{1}{2}$	0.629	0.320	0.218	0.178	0.167	0.169
	PHOTOFRACTIONS					
3 x 3	0.890	0.649	0.477	0.331	0.244	0.207
2 x 2	0.865	0.546	0.373	0.237	0.159	0.115
1 x 1	0.779	0.393	0.235	0.114	0.059	0.033
$\frac{1}{2}$ x $\frac{1}{2}$	0.655	0.269	0.139	0.048	0.015	0.004

TABLE 2.3(b)

Point Source 10 cm from NaI-Crystal Face and on Crystal Axis

Crystal size, dia. x ht. (in.)	Energy (MeV)						
	0.142	0.279	0.661	1.170	1.330	2.620	4.450
	INTERACTION RATIOS						
8 x 8	0.969	0.882	0.754	0.687	0.670	0.606	0.586
6 x 6	0.957	0.864	0.712	0.632	0.622	0.549	0.524
4 x 4	0.943	0.829	0.654	0.576	0.552	0.472	0.459
3 x 3	0.936	0.811	0.619	0.525	0.509	0.428	0.405
2 x 2	0.932	0.780	0.564	0.468	0.435	0.360	0.345
1 x 1	0.930	0.700	0.416	0.332	0.305	0.247	0.224
½ x ½	0.902	0.520	0.266	0.198	0.187	0.145	0.134
	PHOTOFRACTIONS						
8 x 8	0.960	0.914	0.759	0.659	0.639	0.532	0.454
6 x 6	0.964	0.905	0.707	0.591	0.566	0.448	0.362
4 x 4	0.963	0.886	0.628	0.492	0.472	0.337	0.263
3 x 3	0.959	0.861	0.562	0.410	0.392	0.262	0.186
2 x 2	0.957	0.824	0.476	0.311	0.292	0.179	0.102
1 x 1	0.938	0.717	0.320	0.194	0.169	0.085	0.034
½ x ½	0.896	0.606	0.223	0.112	0.099	0.032	0.0051

continued .....

TABLE 2.3(b) (cont'd)

Crystal size, dia. x ht. (in.)	Energy (Mev)					
	6.130	7.100	8.00	10.00	12.00	14.00
	INTERACTION RATIOS					
8 x 8	0.579	0.590	0.585	0.598	0.611	0.612
6 x 6	0.525	0.527	0.529	0.535	0.548	0.557
4 x 4	0.444	0.451	0.457	0.464	0.476	0.485
3 x 3	0.405	0.407	0.408	0.416	0.427	0.435
2 x 2	0.338	0.341	0.345	0.349	0.365	0.370
1 x 1	0.222	0.223	0.229	0.232	0.242	0.249
$\frac{1}{2} \times \frac{1}{2}$	0.132	0.135	0.137	0.142	0.145	0.149
	PHOTOFRACTIONS					
8 x 8	0.424	0.404	0.387	0.361	0.339	0.302
6 x 6	0.325	0.308	0.299	0.266	0.241	0.210
4 x 4	0.211	0.192	0.172	0.149	0.122	0.094
3 x 3	0.138	0.118	0.102	0.088	0.063	0.048
2 x 2	0.070	0.056	0.041	0.035	0.023	0.010
1 x 1	0.015	0.0092	0.0069	0.0040	0.0013	0.0002
$\frac{1}{2} \times \frac{1}{2}$	0.0010	0.0007	0.0005	0.0001	0.0000	0.0000

TABLE 2.3(c)

Point Source on NaI-Crystal Face at Axis

Crystal Size, dia. x ht. (inc.)	Energy (MeV)						
	0.142	0.279	0.661	1.170	1.330	2.620	4.450
INTERACTION RATIOS							
8 x 8	1.000	1.000	0.966	0.914	0.897	0.810	0.802
6 x 6	1.000	0.996	0.930	0.849	0.828	0.750	0.714
4 x 4	1.000	0.979	0.833	0.728	0.705	0.597	0.572
3 x 3	1.000	0.955	0.740	0.627	0.603	0.499	0.467
2 x 2	0.999	0.874	0.598	0.479	0.456	0.379	0.345
1 x 1	0.976	0.657	0.370	0.281	0.262	0.212	0.192
½ x ½	0.865	0.422	0.210	0.152	0.145	0.112	0.102
PHOTOFRACTIONS							
8 x 8	0.912	0.879	0.764	0.666	0.626	0.531	0.455
6 x 6	0.913	0.880	0.709	0.589	0.572	0.441	0.361
4 x 4	0.916	0.870	0.627	0.479	0.460	0.320	0.252
3 x 3	0.913	0.845	0.557	0.411	0.377	0.251	0.177
2 x 2	0.919	0.796	0.457	0.314	0.294	0.172	0.101
1 x 1	0.912	0.702	0.319	0.186	0.173	0.078	0.028
½ x ½	0.879	0.595	0.221	0.114	0.092	0.031	0.0049

continued ....

TABLE 2.3(c) (cont'd)

Crystal size, dia. x ht. (in.)	Energy (Mev)					
	6.130	7.100	8.00	10.00	12.00	14.00
	INTERACTION RATIOS					
8 x 8	0.801	0.809	0.802	0.820	0.833	0.842
6 x 6	0.711	0.717	0.717	0.727	0.739	0.748
4 x 4	0.569	0.567	0.570	0.586	0.602	0.606
3 x 3	0.468	0.475	0.473	0.486	0.495	0.510
2 x 2	0.346	0.348	0.347	0.361	0.371	0.386
1 x 1	0.193	0.191	0.176	0.198	0.206	0.214
$\frac{1}{2}$ x $\frac{1}{2}$	0.102	0.102	0.104	0.105	0.111	0.115
	PHOTOFRACTIONS					
8 x 8	0.424	0.407	0.390	0.377	0.356	0.309
6 x 6	0.322	0.300	0.293	0.272	0.235	0.205
4 x 4	0.203	0.183	0.167	0.139	0.118	0.086
3 x 3	0.130	0.118	0.105	0.083	0.057	0.038
2 x 2	0.062	0.049	0.043	0.032	0.017	0.008
1 x 1	0.013	0.006	0.005	0.003	0.001	0.000
$\frac{1}{2}$ x $\frac{1}{2}$	0.0014	0.0004	0.0004	0.0001	0.0000	0.0000

For the crystal-source geometry shown in Fig. 1.1, Polevoi (1961) has expressed the absolute detection efficiency  $\epsilon(E)$ , analytically with an accuracy of not less than 5% as

$$\epsilon(E) = \frac{1}{2} \left\{ \beta \frac{\theta_1^2}{2} + \cos \theta_1 - \cos \theta_2 + \beta \frac{e^{-\mu(E)b}}{\mu(E)b} \left[ e^{-\mu(E)m} - 1 \right] - \frac{e^{-\mu(E)n\theta_2}}{\mu^2(E)n^2+1} \left[ e^{\mu(E)n\theta_2} (\mu(E)n \sin \theta_2 - \cos \theta_2) - e^{\mu(E)n\theta_1} (\mu(E)n \sin \theta_1 - \cos \theta_1) \right] \right\} \dots(2.2)$$

where

$$\left. \begin{aligned} \beta &= 1 - \frac{\theta_1^2}{12} \\ m &= \frac{1}{2} b \theta_1^2 \\ n &= \frac{b}{\left[ \cos \theta_1 (\theta_2 - \theta_1) \right]} \end{aligned} \right\} \dots(2.3)$$

In the conditions of the analytical approximation, the crystal-to-source distance  $h$  is related to crystal dimensions  $(a,b)$  by the following inequalities:

$$\frac{a}{h} \leq 2.5; \quad 0.55 \leq \frac{a}{h+b} \leq 0.84$$

i.e. the conditions are valid for  $.06 \times 4\pi \leq \Omega \leq 0.32 \times 4\pi$ .

He tested the correctness of his calculations by performing an experiment

with a 29 mm x 17 mm NaI(Tl) crystal and using the 411 Kev gamma-rays of Au<sup>198</sup>. He obtained

$$\frac{\epsilon(E) \text{ experimental}}{\epsilon(E) \text{ calculated}} = 1.01 \pm 0.05 .$$

Zerby and Moran (1961) carried out the Monte-Carlo calculations for the specific case of a point source placed at a distance of 10.0 cm on the crystal axis of a 3" x 3" NaI(Tl) crystal in the energy range 0.1 Mev to 6.0 Mev. These authors point out a major difference between their calculations and the previous ones in that they employed a statistical estimation and a weighting procedure rather than the analogue Monte-Carlo technique. The intrinsic efficiency and photofraction values of these authors are reproduced in Table 2.4. The absolute detection efficiencies as calculated from the intrinsic efficiencies are in good agreement with other similar works. However, the photofractions are slightly higher below 1 Mev and lower above 1 Mev from other works and, in particular, from Heath's. If the error flags are put, the agreement will appear much better. The uncertainties in the photofraction values are less than  $\pm 1\%$  at low energies but may be as much as  $\pm 11\%$  at 6.0 Mev. In contrast to the work of Miller and Snow, these authors have not included the Rayleigh Scattering in the transport of photons.

TABLE 2.4

Intrinsic Efficiency and Peak-to-total Ratio for a 3"x3" NaI(Tl)  
Point Source Located on the Crystal Axis 10 cm from one End.

[Ref: Zerby and Moran (1961) ↓

Source Energy (Mev)	Intrinsic Efficiency	Peak-to-Total Ratio
0.1	0.972	0.9919 ± 0.0004
0.15	0.927	0.9779 ± 0.0009
0.2	0.874	0.9520 ± 0.0016
0.25	0.825	0.9080 ± 0.0025
0.279	0.798	0.8845 ± 0.0030
0.3	0.781	0.8546 ± 0.0034
0.35	0.745	0.8120 ± 0.0041
0.4	0.714	0.7622 ± 0.0049
0.45	0.688	0.7078 ± 0.0054
0.5	0.666	0.6683 ± 0.0060
0.6	0.632	0.6014 ± 0.0068
0.661	0.615	0.5693 ± 0.0058
0.7	0.605	0.5538 ± 0.0073
0.8	0.583	0.5036 ± 0.0079
0.9	0.563	0.4692 ± 0.0083
1.114	0.530	0.3842 ± 0.0091
1.275	0.510	0.3413 ± 0.0095

..... continued

Table 2.4 (continued)

Source Energy (Mev)	Intrinsic Efficiency	Peak-to-Total Ratio
1.38	0.498	0.3262 ± 0.0079
1.6	0.478	0.3016 ± 0.0099
1.7	0.465	0.2862 ± 0.0101
2.14	0.445	0.2441 ± 0.0102
2.4	0.435	0.2143 ± 0.0104
2.76	0.424	0.1962 ± 0.0085
3.13	0.417	0.1650 ± 0.0088
3.57	0.411	0.1548 ± 0.0107
4.0	0.408	0.1345 ± 0.0109
5.0	0.405	0.1035 ± 0.0112
6.0	0.405	0.0918 ± 0.0113

Some authors have expressed their results of the determination of photopeak efficiencies in terms of a "correction factor"  $\delta$  applied to the intrinsic photopeak efficiency corresponding to a selected geometry. We know that the photopeak efficiency  $\epsilon_p$  is the product of the probability that a gamma-ray will be incident on the crystal and the probability that it will give a pulse in the full energy peak; i.e.,

$$\epsilon_p = \epsilon_p(\text{int}) \times \frac{\Omega}{4\pi} \quad \dots (2.4)$$

where  $\Omega$  is the solid angle subtended by the crystal face at the point source situated on the crystal axis. However, we can also write,

$$\epsilon_p = \epsilon_{ps(int)} \times \delta \times \frac{\Omega}{4\pi} \quad \dots (2.5)$$

where  $\epsilon_{ps(int)}$  is the intrinsic photopeak efficiency for a selected geometry. It must be pointed out that the "correction factor"  $\delta$  introduced this way depends both on the crystal-to-source distance and the gamma-ray energy.

Gunnink and Stoner (1961) determined the photopeak efficiency of a 3" x 3" NaI(Tl) for a crystal-to-source distance of 10.0 cm and for various energies using the method mentioned above. Samples of each isotope were assayed in the  $4\pi$  or  $4\pi\beta\text{-}\gamma$  coincidence counter to determine their absolute disintegration rate. The photopeak counting rate for these standardized sources was then taken at various positions with respect to the crystal. Sum peak efficiency was determined for the isotopes decaying through coincident gamma-rays. The experiment gives only the product of the photopeak efficiencies in this case. The photopeak efficiency for the individual gamma-rays was obtained by the method of successive approximations. They studied the variation of  $\delta$  with distance taking it to be unity for a crystal-to-source distance of 0.7 cm and ascribed this factor to the fact that the effective geometry of the crystal did not vary in the same way as the calculated geometry. The way they have treated this "correction factor"  $\delta$ , it appears that they have taken only the distance dependence of  $\delta$  into consideration,

whereas  $\delta$  should depend on energy, too. They estimate an error of  $\pm 3$  to 5% in the photopeak efficiency values.

Grosjean (1962) expressed the absolute detection efficiency of a cylindrical crystal in the case of an extended plane gamma-ray source as a sum of the point source absolute detection efficiency and terms depending on the finite size of the source. The gist of this work appeared as a note again in 1964. In 1965, a book titled "Table of Absolute Detection Efficiencies of Cylindrical Scintillation Gamma-Ray Detectors" by Grosjean and Bossaert appeared as an embodiment of the previous work as well as extensive computations done for NaI(Tl). This work is noteworthy in its own right, as it gives the absolute detection efficiencies of NaI(Tl) crystals of 64 different sizes, for 18 crystal-to-source distances and for gamma-ray energies from 0.01 Mev to 5.5 Mev. Their detection efficiencies for point sources are in excellent agreement with a number of other workers. Specifically, they make mention of this excellent agreement with that of Wolicki et al (1956) for point sources at all distances except for  $h = 0$ . For this distance, the absolute detection efficiencies in the table of Wolicki et al (1956) are unusually high. The authors illustrate this point by the following comparison (reproduced in Table 2.5) which corresponds to the gamma-ray energy having minimum absorption coefficient in NaI(Tl) (5-6 Mev). We further notice that this discrepancy goes on increasing with decreasing crystal dimensions being about 1% for a 5" x 4" crystal and about 14% for a  $\frac{1}{2}$ " x  $\frac{1}{2}$ " crystal.

TABLE 2.5

[Ref: Grosjean (1965)]

Crystal Radius $r$ (inches)	Crystal Thickness $t$ (inches)	$\epsilon_{po(int)}^{(E)}$ Wolicki et al	$\epsilon_{po(int)}^{(E)}$ Grosjean & Bossaert
5/2	4	0.320	0.317
3/2	3	0.238	0.233
7/8	2	0.163	0.157
7/8	1	0.155	0.141
7/8	$\frac{1}{2}$	0.123	0.114
1/2	$\frac{1}{2}$	0.0983	0.0834
1/4	$\frac{1}{2}$	0.0577	0.0507

During the period between Grosjean's first publication on the subject in 1962 and the publication of the book by Grosjean and Bossaert in 1965, a number of important works were published.

Korda et al (1963) have calculated the photopeak efficiency of a 29 mm x 15 mm NaI(Tl) crystal for point gamma sources between 60 Kev to 1.5 Mev in energy and placed at a distance of 36 mm. They report that the error in their calculations did not exceed 2%.

Weitkamp (1963), besides carrying out the Monte-Carlo calculations for intrinsic efficiencies and photofractions for NaI(Tl) detectors of

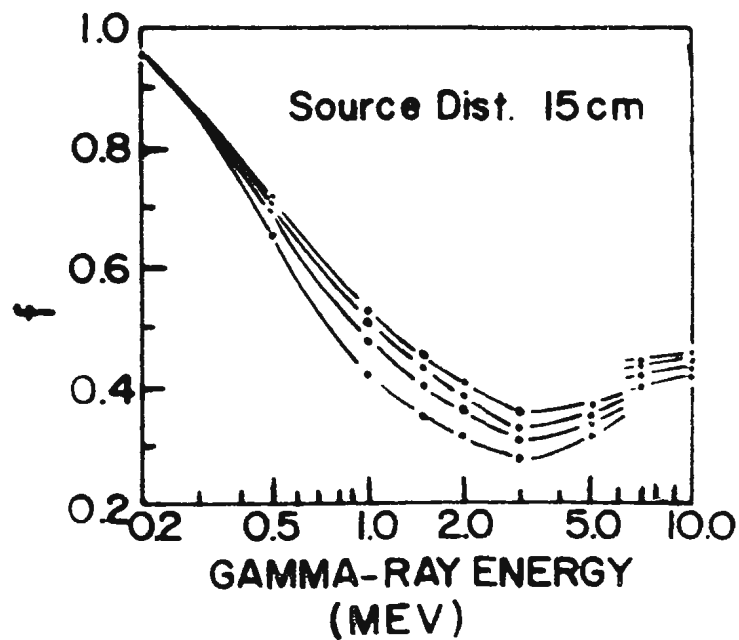
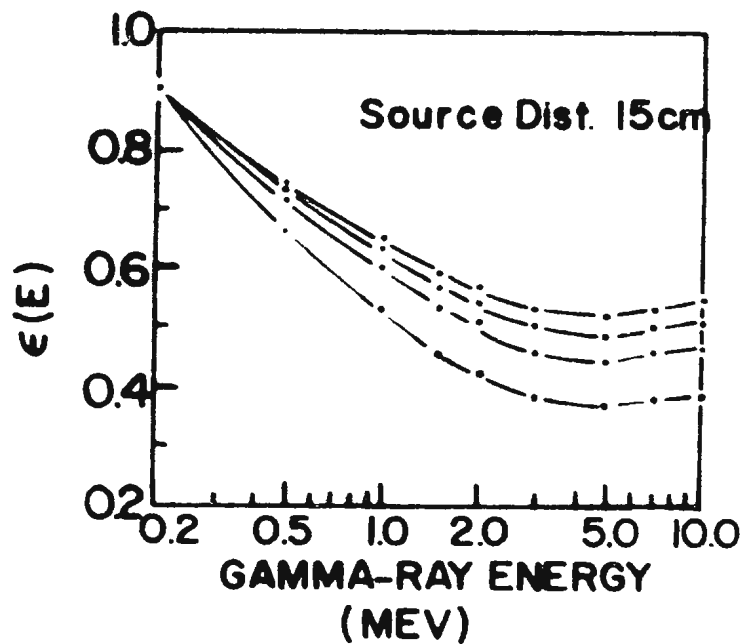


FIG. 2.3 Intrinsic efficiency and Photofraction for uncollimated radiation. Crystal dimensions:  $3'' \times L''$  ( $L = 5\frac{1}{2}''$ ,  $4''$ ,  $3''$ ,  $2''$ ;  $L$  values read from top)

Ref: Weitkamp (1963)

various sizes and for uncollimated gamma-rays of energy 0.2 Mev to 10.0 Mev from point sources at various distances on the crystal axis, determined experimentally the photofractions of a 4" x 6" NaI(Tl) crystal in the energy range 0.32 Mev to 2.76 Mev. Although, in his theoretical calculations, pair-production was treated thoroughly, no corrections were made for bremsstrahlung and escape of electrons from the crystal. His results for a crystal of diameter 3" and of different heights and for a crystal-to-source distance of 15.0 cm are being reproduced in Fig. 2.3. The minima in the intrinsic efficiency versus the energy and the photofraction versus energy curves do not occur for the same energy. In the former, it occurs at about 5.0 Mev whereas, in the latter, at about 3.0 Mev. He has an explanation for it. In this energy range, small Compton scattering angles and, therefore, small energy losses of the gamma-rays are quite frequent; thus, absorption of secondary gamma-rays is not likely and little energy will be transmitted to the crystal. Pair-production, on the other hand, yields secondary radiation of relatively low energy which may be easily absorbed within the crystal and, therefore, increases the photofraction in the energy region where its cross-section becomes relevant. The discontinuity in the photofraction versus energy curves has been ascribed to the energy dependence of the resolution. For uncollimated gamma-rays, his experimental photofraction values show good agreement with the theoretical values but, for collimated gamma-rays, the agreement is poor.

Green and Finn (1965), besides giving a short resume of the photopeak efficiency determinations, have studied:

(i) the variation of the intrinsic peak efficiency and the photopeak efficiency with energy, and

(ii) the variation of the "correction factor"  $\delta$  Eq. (2.5) with distance for different energies for NaI(Tl) crystals of different sizes, including a 3" x 3" NaI(Tl), and for point gamma-sources of energies in the range 0.279 Mev to 1.52 Mev.

Unlike Gunnink and Stoner (1961), these authors take  $\delta$  as unity for a crystal-to-source distance of 15.0 cm. Their observations may be summarized as:

(i) the intrinsic efficiencies of Vegors et al (1958), Heath (1964), Zerby and Moran (1961), and Gunnink and Stoner (1961) for a crystal-to-source distance of 10.0 cm from a 3" x 3" NaI(Tl) crystal agree fairly well but their own values are slightly lower, and

(ii) the variation of  $\delta$  with the crystal-to-source distance decreased with increasing crystal size and the crystal-to-source distance at which the minimum value of  $\delta$  occurs increases with increasing crystal size. This holds, of course, for any energy. We reproduce in Fig. 2.4 the  $\delta$  versus the crystal-to-source distance curves for an 8" x 4" NaI(Tl) crystal for 0.323 Mev, 0.478 Mev, 0.661 Mev and 0.84 Mev gamma-rays from the above reference. They further gave a detailed estimate of the errors involved in various measurements. They reported that the errors in the values of the intrinsic photopeak efficiencies with sources placed centrally on the crystal surface were about 3% and those due to setting of boundaries of the photopeak were less than 1%. When the sources were placed at a distance from the crystal face, the uncertainty

in the distance itself could be 2 mm and, hence, the error in  $\Omega/4\pi$  varied with distance. At about 20 cm, the error in  $\Omega/4\pi$  could be 2%, at 15 cm 3%, at 10 cm 4% and at 5 cm 8%. Hence, the error in the intrinsic photopeak efficiencies for different crystals could be 7%. The error in  $\delta$  itself could be as high as 6 to 8% for crystal-to-source distances greater than 10 cm and higher still for crystal-to-source distances less than this.

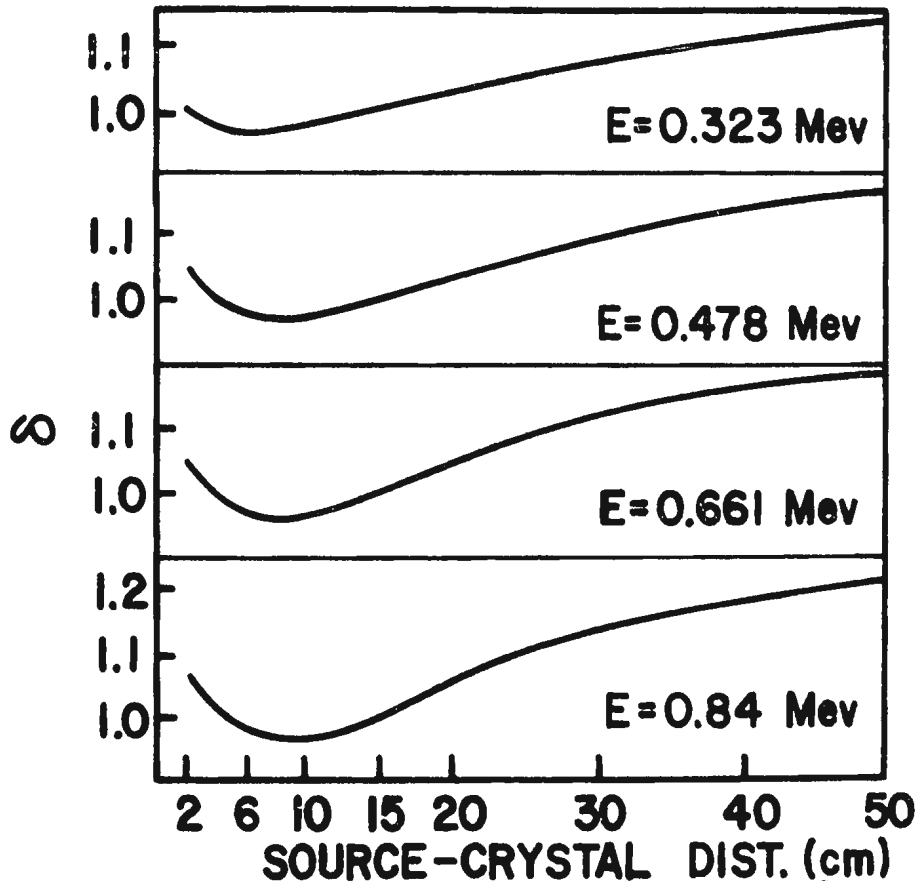


FIG.2.4  $\delta$  vs. Source-crystal dist. for  $8'' \times 4''$  NaI (TI)

Ref. Green and Finn (1965)

Coop and Grench (1965) determined the photopeak efficiency for a 3" x 3" and a 4" x 4" NaI(Tl) crystal for point sources of energies up to 3.0 Mev, at different distances along the crystal axes. The rather uncommon selection of distances makes it difficult to compare their work with other works. However, they could compare with the theoretical results of Miller and Snow (1961) for crystal-to-source distances of zero and 6" on the 4" x 4" crystal. At the 6" distance, the agreement was within 3% over the energy range 0.3 Mev to 1.2 Mev. At higher energies, the theoretical values were up to 10% greater than the experimental values. At zero distance, the theoretical values were 5 to 8% above the experimental values.

Leutz et al (1966) measured the photofractions of 8 NaI(Tl) crystals including a 3" x 3" one for crystal-to-source distances of 10.0 cm and 50.0 cm and point gamma sources of energy up to 2.620 Mev. They used three very distinct geometrical arrangements so that they could compare their results with some of the published works. The photofractions were found to be largest for narrow collimated gamma-rays. Their results were in good agreement with those of Heath (1964) up to 2.5 Mev, but there were considerable differences with those of Miller and Snow (1961). The latter values were 10 to 30% higher than their values. These authors found it difficult to calculate the error on the photofraction values; however, they estimated it to be less than  $\pm 5\%$  in the measurement by examining the deviations of the individual experimental points from the fitted curves.

Chinaglia and Malvano (1966) determined the photopeak efficiencies and photofractions of 3" x 3" NaI(Tl) crystals. According to them an error of  $\pm 5\%$  in the crystal-to-source distance will not destroy the quality of the results. Their results agree to within 4% with that of Heath (1964) and Zerby and Moran (1961) in the energy region where comparisons could be made.

Young et al (1966) experimentally measured the photofraction and the absolute detection efficiency for a 5" x 5" NaI(Tl) crystal for 2.5 cm . crystal-to-source distance for gamma-ray energies from 0.4 to 9.2 Mev from nuclear reactions, using a magnetic spectrometer to isolate nuclear states which decay by only one gamma transition and employing the appropriate coincident technique. The experimental absolute detection efficiency agreed with the theoretical value within  $\pm 5\%$ . There are no theoretical values of the photofractions available for this case to compare with the experimental values of these authors. However, we note that their values are somewhat higher than the experimental values of Leutz et al (1966) for the energy range 1.5 to 2.7 Mev, but Leutz et al have reported results for 10.0 cm crystal-to-source distance. Leutz et al did not carry out measurements at higher energies.

Snyder (1967) reviewed the situation in brief and compared some of the theoretical and the experimental photofractions for gamma-rays interacting with a 3" x 3" NaI(Tl) crystal, for a crystal-to-source distance of 10.0 cm and for different energies. We reproduce from

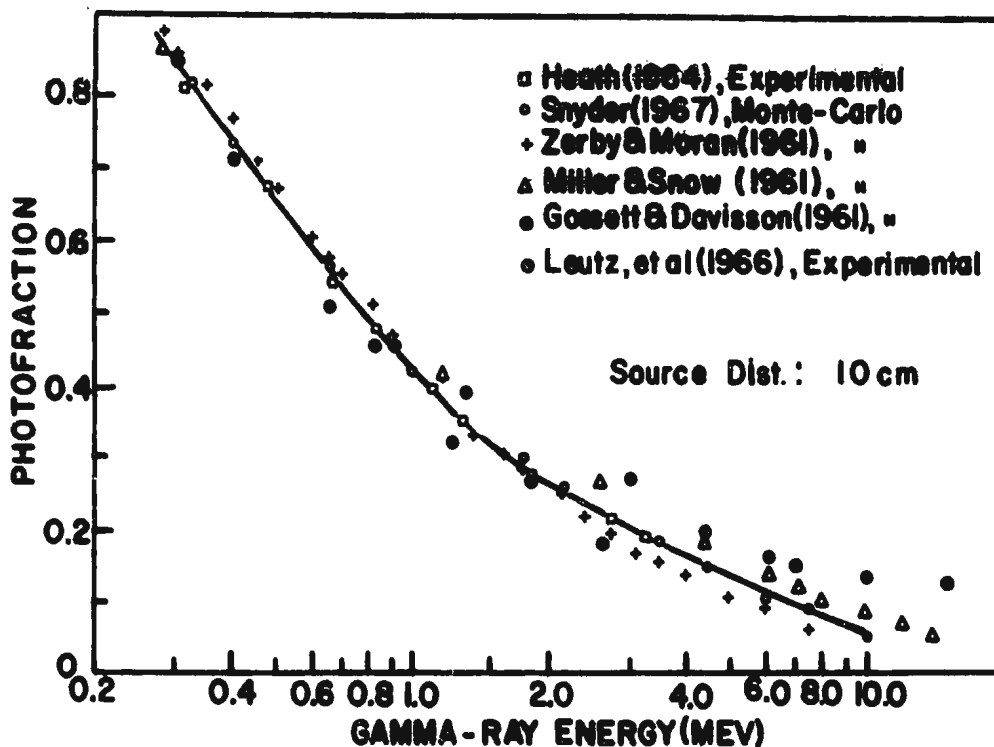


FIG. 2.5 Photofraction vs. Energy for a 3" x 3" NaI(Tl) crystal  
Ref. Snyder (1967)

the above reference, the photofraction versus the energy graph for a 3" x 3" NaI(Tl) crystal in Fig. 2.5. Concerning his calculated photofraction values by the Monte-Carlo method, he reported that these were in good agreement with that of Heath (1964) and of Zerby and Moran (1961) up to approximately 2.0 Mev.

A quick glance over the reproduced graph from Snyder's paper shows that the values of Gossett and Davisson (1961) and Miller and Snow (1961) are higher, Zerby and Moran (1961) and Leutz et al's (1966) are lower and Snyder's are in good agreement with Heath's values. Gossett and Davisson did not include simulation of electron or bremsstrahlung and this shows up in its divergence from other results.

Christaller (1967) has determined experimentally the photo-fractions of a 4" x 4" NaI(Tl) crystal for the crystal-to-source distances of 7.5 cm, 15 cm, 30 cm and 45 cm for the energy region 0.088 Mev to 2.75 Mev. Neither shielding nor collimator was used and the sources were of 3 mm diameter. They compared their experimental values with the theoretical photofractions published earlier and found that the theoretical values were too large, in some cases the deviation being as much as 60%. The errors in the experimental values were estimated by them to be  $\pm 4\%$ . Their results are being reproduced in Figs. 2.6 (a) to 2.6 (d).

Mishra and Sadasivan (1969) measured the photofractions for five different NaI(Tl) crystals of sizes ranging from 5" x 4" to 2" x 2" for the energy range 0.145 to 2.75 Mev. They seem to have taken good care in their experiments. They estimate an overall error of less than  $\pm 5\%$ . Further, their photofraction values for a 3" x 3" NaI(Tl) crystal seem to agree well with those of Heath (1964), except in the energy range where the difference may be due to a small uncertainty in the crystal-to-source distance. We reproduce their photofraction values in Table 2.6.

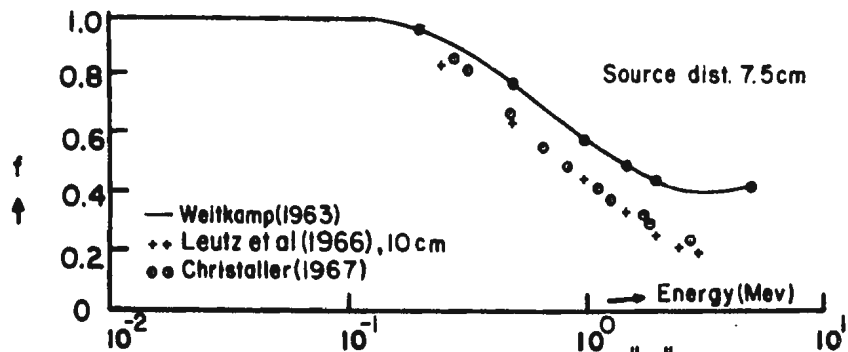


FIG. 2.6(a) Peak/total-ratio  $f$  for  $4 \times 4$  NaI(Tl)

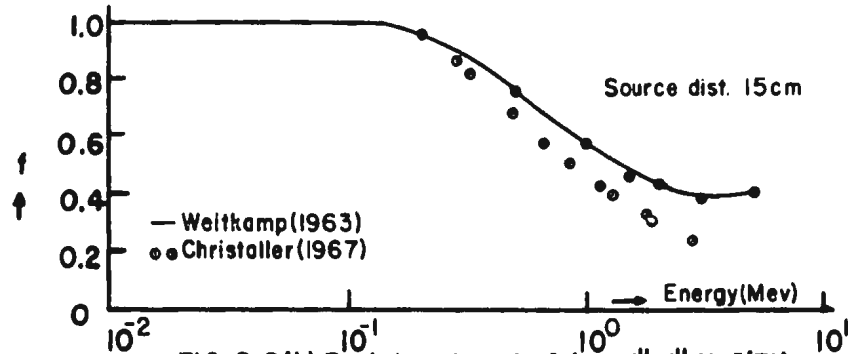


FIG. 2.6(b) Peak/total-ratio  $f$  for  $4 \times 4$  NaI(Tl)

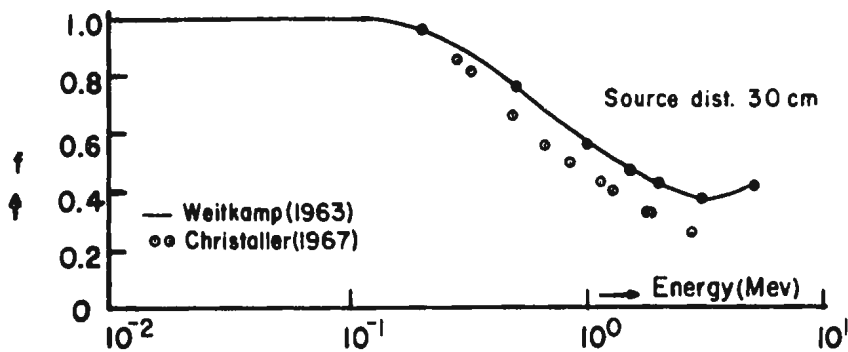


FIG. 2.6(c) Peak/total-ratio  $f$  for  $4 \times 4$  NaI(Tl)

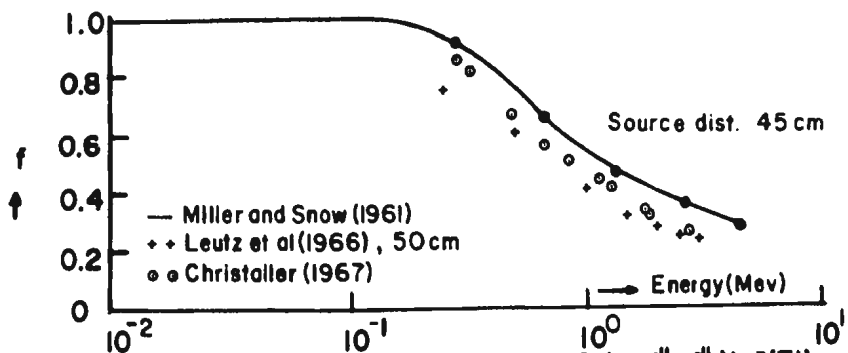


FIG. 2.6(d) Peak/total-ratio  $f$  for  $4 \times 4$  NaI(Tl)

Ref. Christaller (1967)

TABLE 2.6

Experimental Peak/Total Ratios for Five Different NaI(Tl) Crystals

Source Distance: 10 cm.

[Ref: Mishra & Sadasivan (1969)]

Energy (Mev.)	Crystal Size, dia x height (inch)				
	5 x 4	3 x 3	3 x 1	2.5 x 2.5	2 x 2
0.145	0.96	0.94	0.939	0.93	0.929
0.279	0.87	0.832	0.775	0.79	0.775
0.323	0.836	0.78	0.703	0.731	0.723
0.513	0.69	0.58	0.485	0.56	0.50
0.662	0.632	0.53	0.417	0.482	0.433
0.835	0.566	0.465	0.365	0.42	0.365
1.11	0.495	0.381	0.291	0.341	0.291
1.28	0.454	0.356	0.256	0.301	0.262
2.75	0.29	0.206	0.129	0.172	0.142

Possibilities of expressing photofractions for different crystal sizes, different geometrical arrangements and for different energies by empirical equations have also received some attention. A recent publication, Steyn and Andrews (1969) deserves mention. They have given empirical equations for a number of NaI(Tl) crystals but they have fitted separate equations to theoretical and experimental values of photofractions.

As stated at the beginning of this chapter, we have restricted our review to point or near point resources (without collimation) on the crystal axis. Narrow collimated beams, broad parallel beams and extended disc sources have been treated by several authors. We mention some of the references: Miller and Snow (1961), Kreger and Brown (1961), Jarczyk et al (1962) and Mundschenk (1966).

This completes the review of the work done in connection with NaI(Tl), CsI(Tl) and CsI(Na) crystals with special reference to a crystal size 3" x 3" and using point source geometry. The main points of this survey may be put as:

(i) The absolute detection efficiencies of NaI(Tl) crystals calculated either by the "Integration Method" or by the Monte-Carlo method agree excellently,

(ii) For the calculated photofractions of a 3" x 3" NaI(Tl) crystal and for a crystal-to-source distance of 10.0 cm, we have the works of Gossett and Davisson (1961), Miller and Snow (1961), Zerby and Moran (1961) and Snyder (1967).

For the experimentally determined photofractions for the same crystal size and the crystal-to-source geometry, we have the works of Heath (1964), Leutz et al (1966) and Mishra and Sadasivan (1969).

We observe that the experimental values of the photofraction seem to agree among themselves mostly within  $\pm 5\%$ , whereas the theoretical values may differ by more than that.

(iii) For the cesium iodide crystals, very little information exists as far as the photofractions are concerned.

CHAPTER III

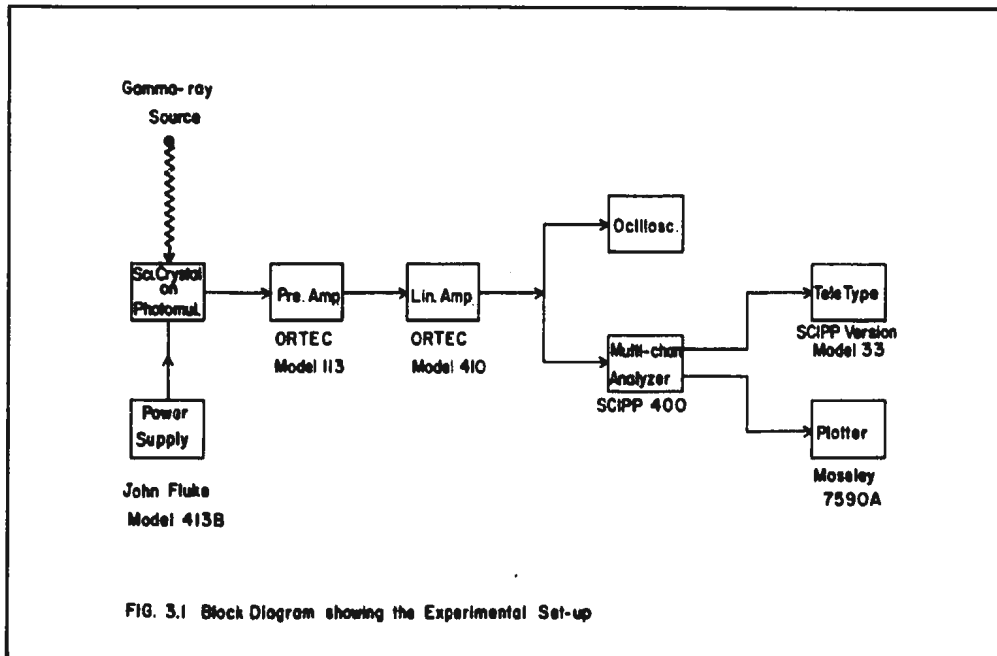
THE EXPERIMENT

3.1 The Experimental Arrangement:

We divide this section on the description of the experimental arrangement into three sub-sections dealing with the electronics, the shielding chamber and the source-holder.

(a) The Electronic Set-Up:

The nuclear electronics used in our measurements was simple and conventional. A block diagram is given in Fig. 3.1 and a photograph showing the actual arrangement in Fig. 3.2.



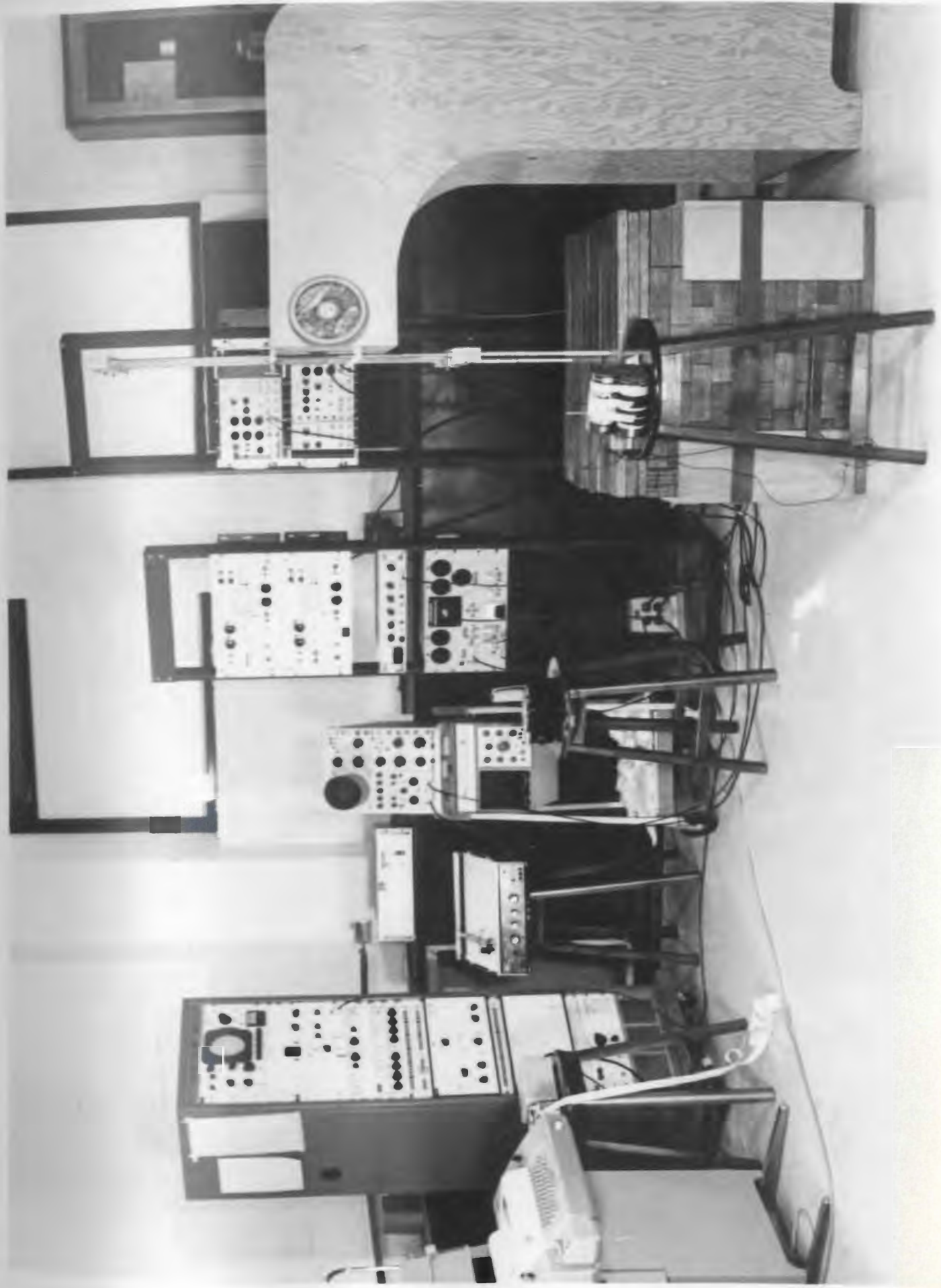


Fig. 3.2 The Actual Experimental Arrangement

The crystals were mounted on RCA 8054 photomultipliers. High viscosity silicone fluid ( $10^6$  centi-stokes) was used for the optical coupling between the crystal and the photomultiplier. Fig. 3.3 gives the high-voltage divider of the photomultiplier base.

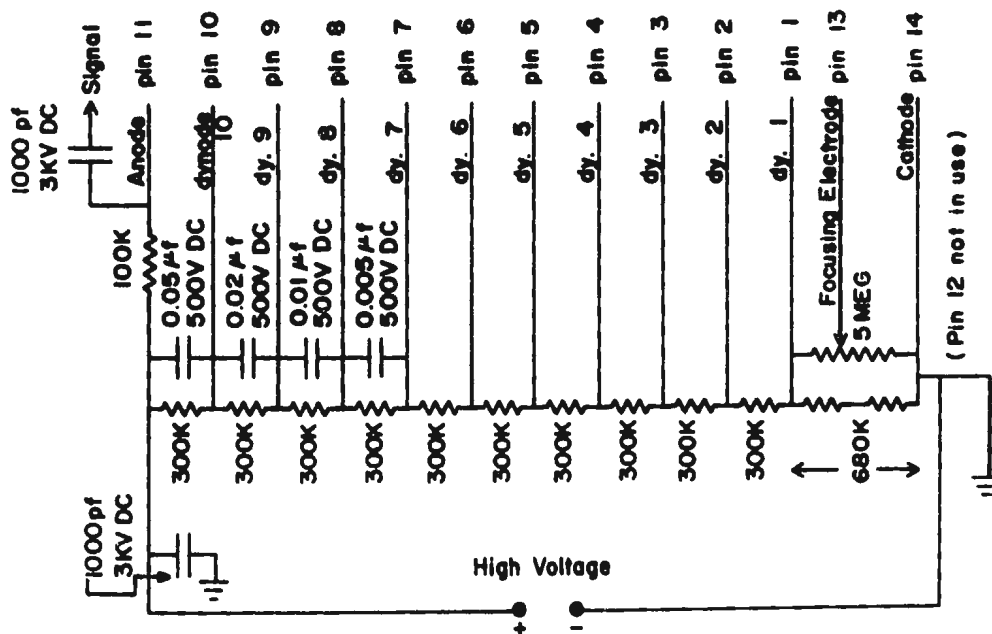


FIG. 3.3 High Voltage Divider of the Photomultiplier (RCA 8054) Base

The pulses from the photomultiplier were fed via an ORTEC Model 113 preamplifier into an ORTEC Model 410 linear amplifier. The amplified pulses were analyzed by a Victoreen "SCIPP 400" multi-channel pulse-height analyzer. The pulses were simultaneously monitored in a Tektronix Type 547 oscilloscope. In the next paragraph, a brief description of the pulse-height analyzer and its accessories is given. Concerning the high voltage supply to the photomultipliers, we designed an "adjustable high voltage distribution unit" so that up to four photomultipliers could be supplied by one high voltage power supply in such a way that the voltage on each photomultiplier could be adjusted individually.

Our "SCIPP 400" analyzer (Fig. 3.4) has 400 channels which can be divided into two or four sub-groups and has a built-in live/clock timer. Some of the additional "options" installed in our system are worth mentioning. It has a dead-time meter. An Auxilliary Data Register, a Digital Data Differentiation Programmer and a Digital Level Selector extend the arithmetic capabilities to permit (i) the peak integration, i.e. a quick determination of the total number of counts between any two selected channels, (ii) the curve integration of a spectrum in a sub-group and (iii) the digital subtraction or addition of spectra in two sub-groups (the operation can be repeated and certain suitable "fractions" can also be introduced). In addition, we have a "Router" so that different sub-groups can be used simultaneously for different detectors on a time shared basis. The READ-OUT and READ-IN accessories are as follows:

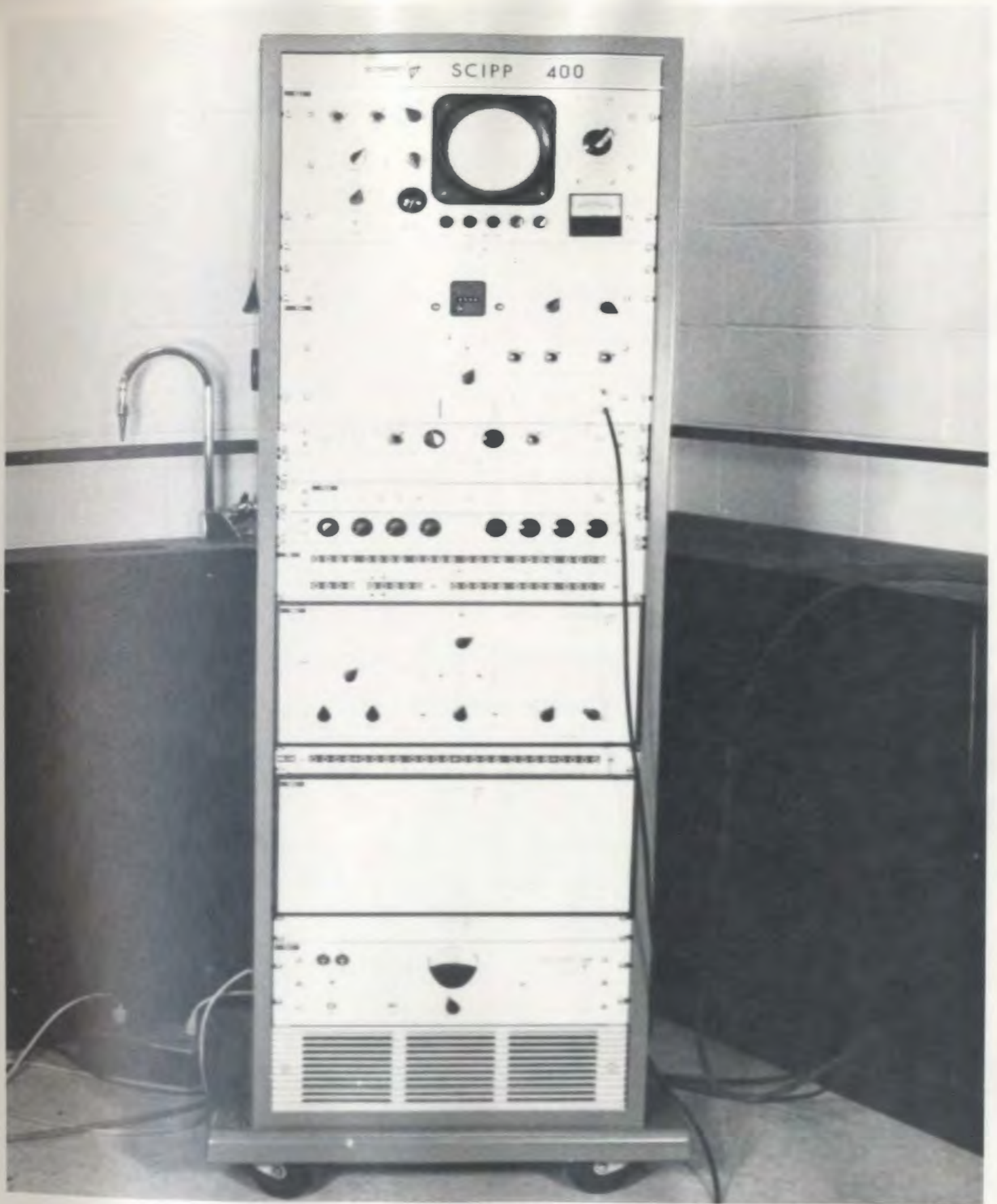


Fig. 3.4 Victoreen's "SCIPP 400" Multi-Channel Pulse-Height Analyzer

(i) The Teletype Keyboard Printer/Punch: This is a SCIIPP version Teletype Model 33 Page Printer. The speed of the Teletype is 1.4 channels per second. Incorporated within the Model 33 is a Paper Tape Punch that would punch the information onto a 1" wide tape at 10 characters per second in 8 level ASC II code without parity check. (Unfortunately, so far we have not been able to use these tapes directly in our "Computing Centre".)

(ii) The Plotter: A Victoreen modified Moseley 7590A plotter presents the analog output of the analyzer. We used the Model 17009B Hewlett-Packard character printers with this plotting system.

(iii) The C-X Reader: The C-X fast paper tape reader is used to read the punched paper tape information back into the analyzer memory at a speed of about 100 characters per second or 14 channels per second.

It may be mentioned in passing that the analyzer has a built-in manual read-out facility also. The multi-channel pulse-height analyzer with the accessories may be seen in Fig. 3.5.

(b) The Shielding Chamber:

Interlocking lead bricks of special design were used to erect the four walls of the shielding chamber. These walls were 3" thick. The maximum internal dimensions of the chamber were 24" x 24" cross-section and 20" in height. The dimensions of the chamber can be altered (decreased) in steps of a few inches by removing an appropriate



Fig. 3.5 Multi-Channel Pulse-Height Analyzer and its Accessories

number of lead bricks and, similarly, the chamber dimensions can be enlarged by acquiring an additional number of appropriate bricks. The flexibility has been made possible by a proper combination of the bricks of different sizes. The "corner" bricks and the bricks for the uppermost and the lower most layers were of appropriate design to facilitate the building of this type of chamber. 1" thick, 3" wide and 30" long lead bars were used for the floor and the roof of this chamber. In the final configuration, the floor was 1" thick and the roof was 3" thick. The shielding cut down the background counts in almost all the crystals by a factor of 10.

(c) The Source Holder:

In this sub-section, we describe in brief the source holding arrangement and the arrangement for varying the crystal to source distance with their special features.

(i) The Source Holding Arrangement: Gamma-ray sources were held on a plexiglass ring firmly attached to two nylon threads which stretched across the chamber and which were firmly fastened to a large aluminium frame held in position by an arrangement which we shall explain later. This reduced the amount of the material in the neighbourhood of the source, a desirable feature to minimize unnecessary scattering. Fig. 3.6 shows this source holding arrangement. As a matter of fact, the amount of material in the immediate vicinity of the sources could be further reduced if our requirements were really critical.

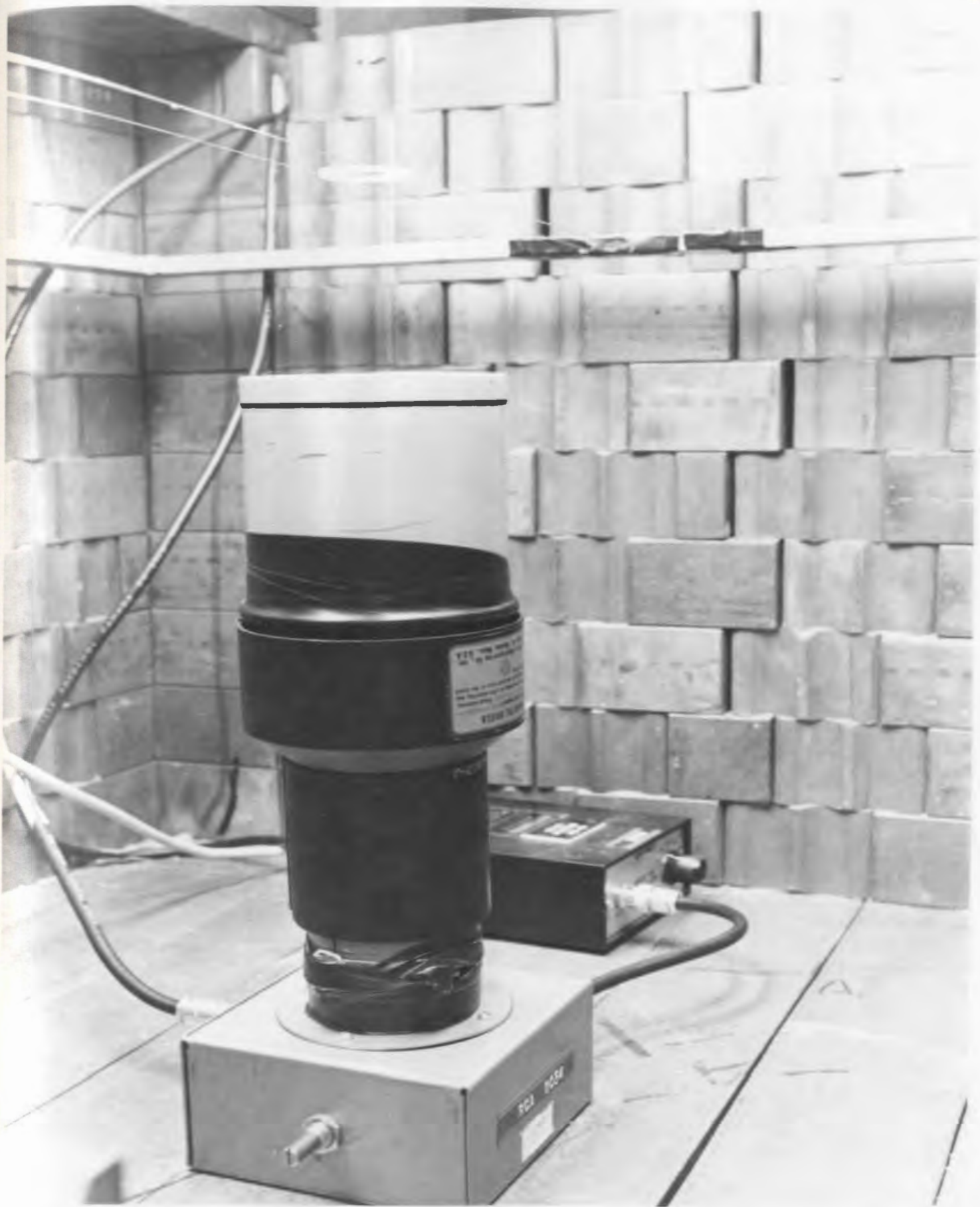


Fig. 3.6 The Source Holding Arrangement

(ii) The Arrangement to Vary the Crystal-to-Source Distance:

We decided that the source holding arrangement must have the facility for varying the crystal-to-source distance at will by external manipulations only so that the heavy lead roof of the chamber would not have to be removed (or even partially removed) every time that we desired to change the crystal-to-source distance. We also wanted to be able to position the source within a small fraction of a millimeter. After some preliminary experiments with simple arrangements, we decided to have the set-up shown in Fig. 3.7.

The large aluminium frame inside the lead chamber was attached to the two aluminium rods coming out of two holes in the roof. These two aluminium rods were in turn rigidly attached to a system of three steel rods. This whole assembly could be slid up or down and could be held in any desired position with reference to a scale attached near the central rod. This system was designed to allow a movement of about 20" and the length of the external rods was selected to accommodate this much displacement. The movement of the assembly was effected very smoothly by a system of three pulleys. A stable supporting wooden structure was designed to permit correct positionings of various parts of the assembly. The whole set-up was thoroughly checked by examining the reproducibility of spectra of excellent statistics. It should be noted that the readings on the external scale give only the amount of the displacement from one position to another. In order to obtain the absolute distance between the source and the crystal top (as a matter of fact, crystal container top), the external scale readings were

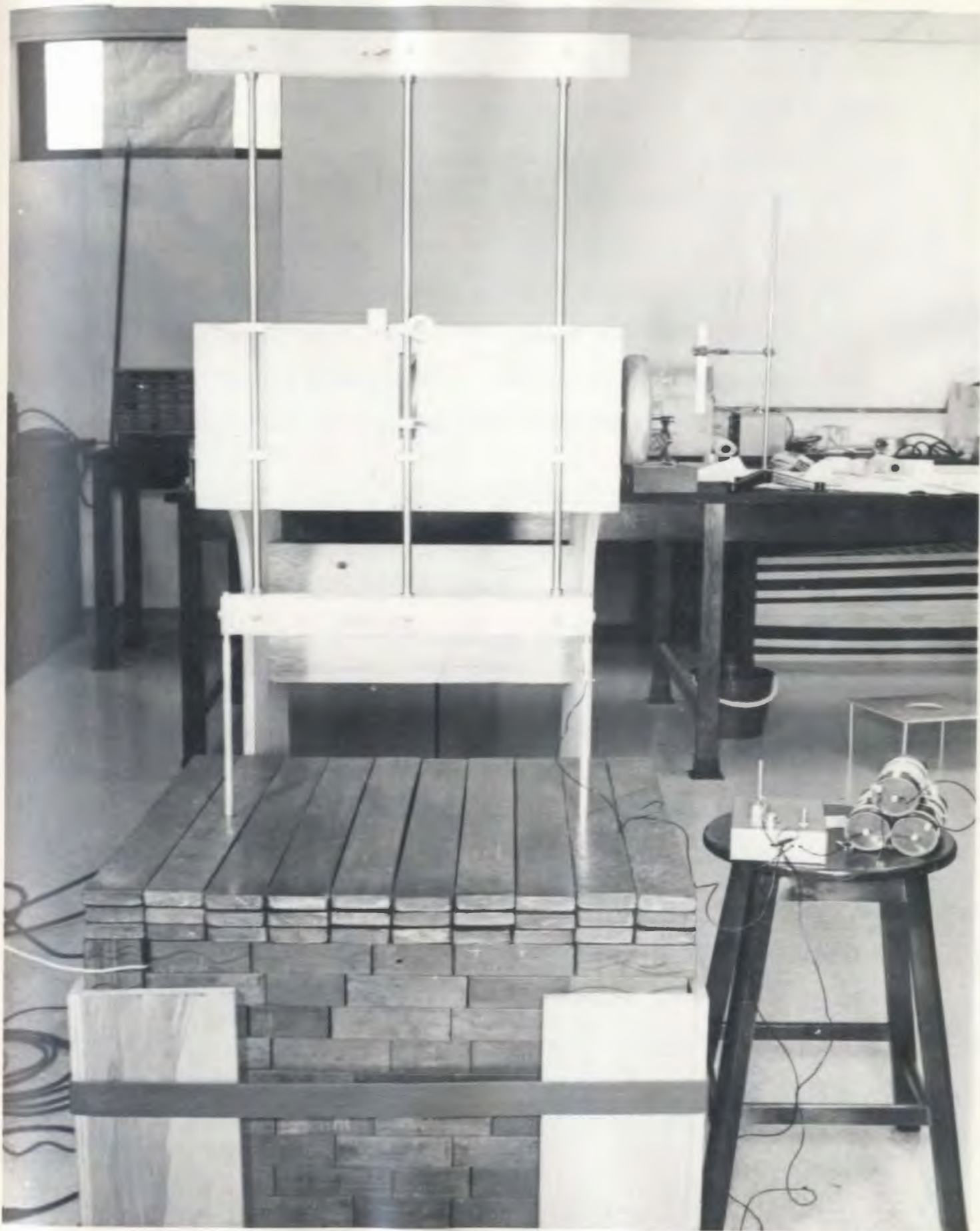
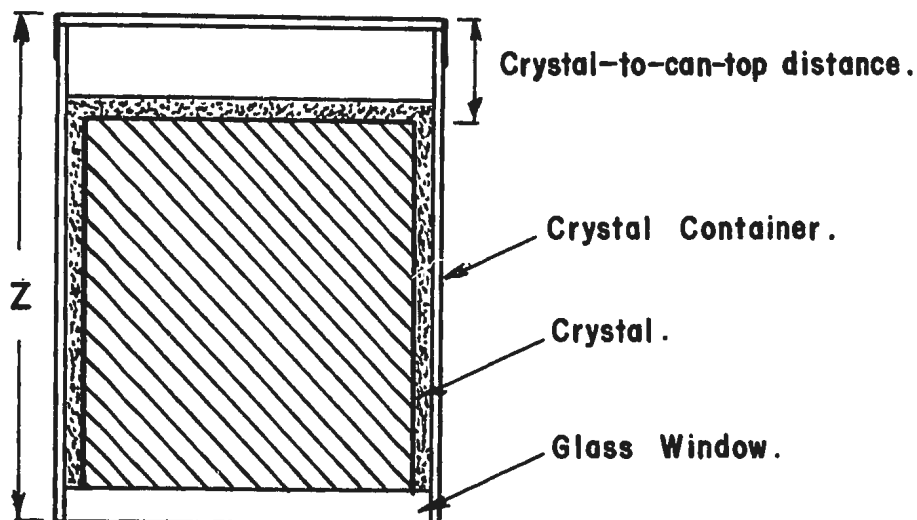


Fig. 3.7 The Source Holder

calibrated by reading it for a known distance between the source and the crystal top. The calibration procedure had to be simple but accurate because every time a new source was introduced or a crystal was changed, the calibration had to be checked again. The calibration was achieved by placing a metallic reference rod with a stable base on the top of the crystal container and bringing the source holder just in contact with the "reference rod". The moment of just contact was assured by a simple but very helpful electric bell circuit.

### 3.2 The Measurement of the Crystal-to-Can-Top Distance:

A correct knowledge of the crystal-to-source distance requires an accurate knowledge of the distance between the top surface of the crystal and the top outer surface of the crystal housing (we shall refer to this distance briefly as the "crystal-to-can-top distance"). The determination of the crystal-to-can-top distance presented some difficulties. Once we became sure about the precision of the quantities involved, we adopted the values obtained in simple, direct measurements as explained in the following sentences. The suppliers have assured us that the crystal thicknesses were precise to within  $\pm 0.005$ ". We also knew the thickness of the optical glass windows of the crystal assemblies. Measuring the total thickness  $Z$  (Fig. 3.8) and subtracting from it the combined thickness of the glass window and the crystal gave a reliable value of the crystal-to-can-top distance.



**FIG. 3.8**  
**THE CRYSTAL ASSEMBLY**

Before the adoption of these final values, we had used the "provisional" values based on certain considerations. The actual experimental data with the three crystals was collected for various crystal-to-source distances, giving us graphs showing the variations of the observed quantities with the crystal-to-source distances. Small corrections applied later to the crystal-to-can-top distances did not present any difficulty since the values for the correct distances could be read easily from the experimental graphs. These provisional values for the crystal-to-can-top distance were mainly on the basis of the general information supplied by the Harshaw Chemical Company on the method of the assembly of the crystals of these types. Unfortunately, this information did not give accurate values for the individual crystals (we think that the difficulty lies in maintaining identical conditions

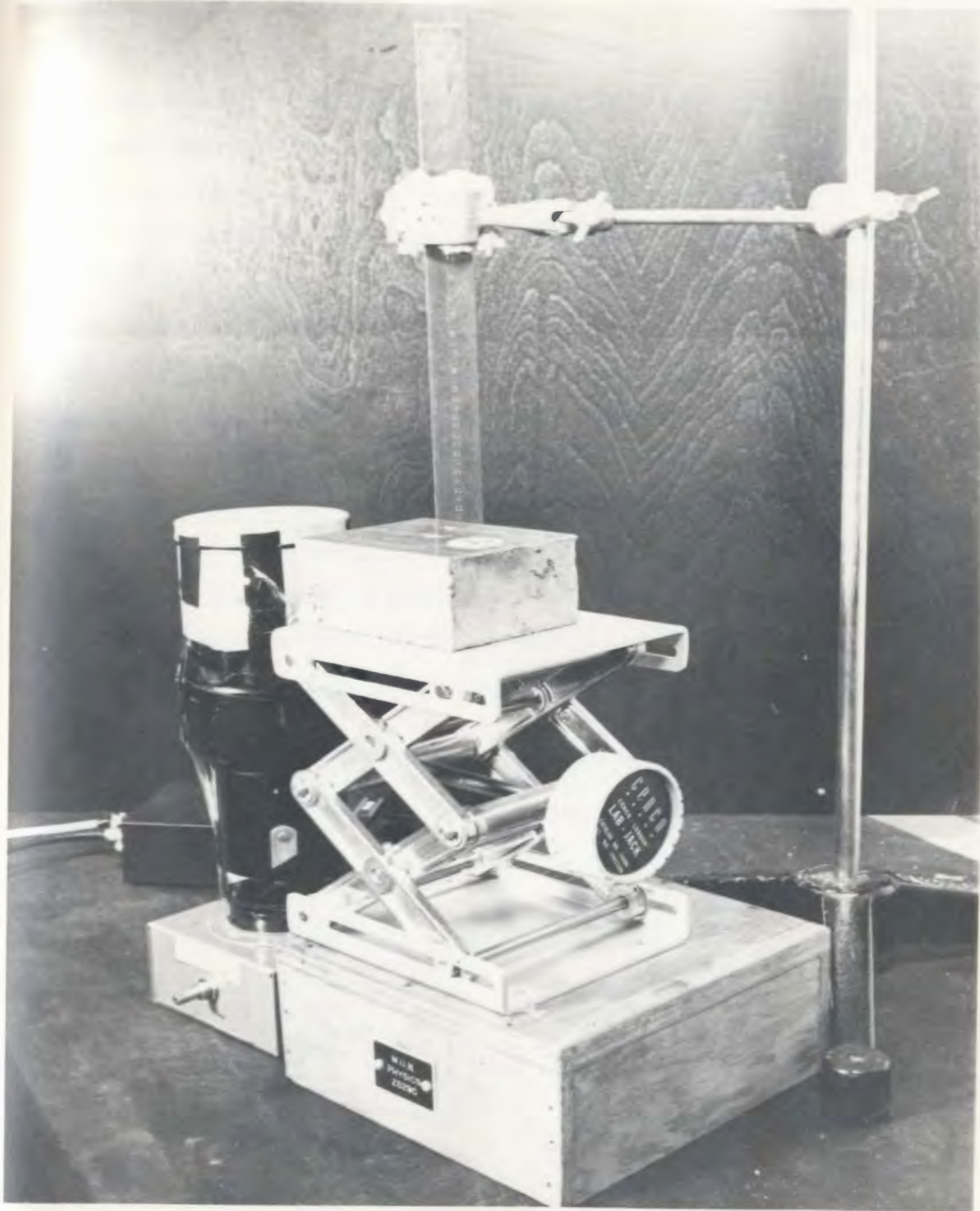


Fig. 3.9 The Arrangement for Measuring the Crystal-to-Can-Top Distance

during the sealing of the crystals and keeping some of the flexible substances that are used in the assembly to identical dimensions for all crystals of the same type.)

We also carried out our own measurements to estimate the crystal-to-can-top distances. The experimental arrangement is shown in Fig. 3.9. A strong source of gamma-rays was placed on a rectangular block of lead having flat, levelled surfaces and sharp edges whose height could be changed with the help of an adjustable jack and whose position could be read on a scale mounted just beside. The experiment was started with the source position sufficiently above the can surface. Changing the distance every time by 1 mm and collecting statistically good spectra, the number of counts in the spectra was determined. First there were very few counts and then the counts started increasing rapidly. In each case a graph of the type shown in Fig. 3.10 was obtained.

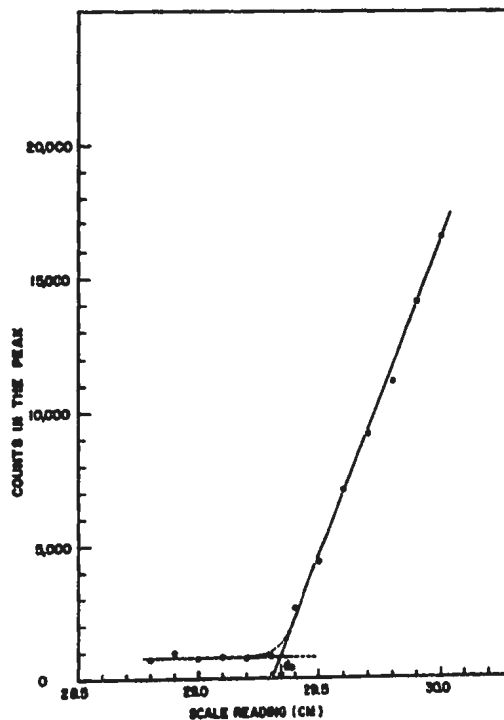


FIG. 3.10 A typical graph obtained with the arrangement shown in FIG. 3.9

The scale reading corresponding to the intersection of the tangents indicates a situation when the source just comes at the level of the crystal surface. The difference between the can-top reading and " $d_0$ " gives the crystal-to-can-top distance. The reliability of the method was checked by using an unsealed 2" x 2" CsI(Tl) crystal. Here, the position of the crystal top was known exactly (we used thin aluminium foils as a reflector which also served as a light tight seal). The deviation of the measured value of " $d_0$ " from the known position of the crystal top served to give an estimate of the accuracy of the measurements. The results indicated that the measured values could be uncertain by as much as 0.6 mm. It may be pointed out that the true crystal-to-can-top distance is expected to be somewhat less than the measured value because the count rate does not increase as abruptly as would be desirable, but deviations are estimated to be within the uncertainty of 0.6 mm as stated above. Our measured values agree within the estimated uncertainty with the values that we adopted finally. Table 3.1 gives the provisional values, the measured values and the finally adopted values.

Table 3.1. Values of the Crystal-to-Can-Top Distance

No.	Crystals	Provisional values,	Experimentally	
		based on information about crystal assembly	measured values, cm	Finally accepted values, cm
1.	3"x3" NaI(Tl)	0.619	$0.76 \pm 0.06$	0.70
2.	3"x3" CsI(Na)	0.669	$0.82 \pm 0.06$	0.79
3.	2"x2" CsI(Tl)	0.573	$0.48 \pm 0.06$	0.47

In the case of the 3" x 3" NaI(Tl) crystal and the 3" x 3" CsI(Na) crystal, we noted a "concavity" in the top surface of the crystal can. The values in the table are corrected for this effect to give the distances from the central region of the top.

### 3.3 The Choice of the Radioactive Sources:

We were restricted to suitable radioactive sources for gamma-rays of different energies. We used Hg<sup>203</sup> (47 d), Bi<sup>207</sup> (28 y), Cs<sup>137</sup> (30 y), Mn<sup>54</sup> (314 d), Co<sup>60</sup> (5.3 y), Y<sup>88</sup> (105 d), Ra<sup>226</sup> (1622 y), Th<sup>228</sup> (1910 y) and Co<sup>56</sup> (77.3 d) to cover an energy range of 0.279 Mev to 3.25 Mev, though Ra<sup>226</sup> and Co<sup>56</sup> did not satisfy our requirements adequately. Gamma-rays of still higher energies can be obtained only through suitable nuclear reactions for which we have no facilities available. Since we had to acquire sources from mainland Canada and the U.S.A., we were restricted to only those sources which had reasonably long half-lives (at least of the order of a few days).

Our first preference was for radioisotopes emitting mono-energetic gamma-rays but to cover the energy range adequately we had to accept some sources of complex spectra also. The following sources were mono-energetic: Hg<sup>203</sup> (0.279 Mev), Cs<sup>137</sup> (0.662 Mev) and Mn<sup>54</sup> (0.835 Mev). Bi<sup>207</sup>, having three prominent peaks (0.57 Mev, 1.064 Mev and 1.77 Mev), was used only for the first two peaks, i.e. 0.57 Mev and 1.064 Mev. The third peak was rejected because the troublesome sum peak due to the two lower peaks badly distorted the peak shape in the region of 1.6 Mev to 1.7 Mev. Co<sup>60</sup> (1.17 Mev and 1.332 Mev) was used for the

1.332 Mev peak. For higher energies  $Y^{88}$ ,  $Ra^{226}$ ,  $Th^{228}$  and  $Co^{56}$  were used. Out of these,  $Y^{88}$  and  $Th^{228}$  are well recognized sources for 1.837 Mev and 2.615 Mev, respectively. ( $Y^{88}$  has another peak at 0.90 Mev also.) A suitable  $Ra^{226}$  source was readily available because, concurrently, we were doing some work on the measurement of Radon-222 concentration in a number of water samples and a  $Ra^{226}$  source was acquired to make a comparative study of the near point  $Ra^{226}$  source and locally prepared distributed large volume sources containing  $Ra^{226}$ . In our present work we used the rather weak but high energy peak of  $Ra^{226}$  at 2.43 Mev. This was paid special attention because at that stage we had not been able to get a suitable Thorium-228 source. The gamma-ray spectra of  $Co^{56}$  was very complex but our interest was chiefly in the high energy gamma-rays and we found that the group of lines around 3.25 Mev could be used as a tolerable source of 3.25 Mev.

There was one more important consideration in the choice of the sources. We could not afford to have too many  $\beta$ -particles from these sources recorded within the photopeak of interest. Later on we shall comment about this in the case of  $Cs^{137}$  and  $Bi^{207}$  sources for which this consideration was needed.

All our sources except for  $Ra^{226}$  were thin disc type near point sources and in most cases the activity was confined to less than  $\frac{1}{4}$ " diameter area in the centre of the discs. (The  $Ra^{226}$  source was in the form of a double encapsulated tube with 0.5 mm screenage of 10% iridio platinum, external dimension of the tube - 1.65 mm diameter x 9.3 mm length.) However, later on we will be discussing the effect of the finite dimensions of the sources. Though we had intended to obtain all the sources from one supplier, we could not do this, so under compelling circumstances, we had to go to different suppliers.

Furthermore, all sources were not available to us at the same time and this necessitated some flexibility in our plans for the collection of experimental data.

### 3.4 The Acquisition of Data:

Before starting the final measurements, a series of preliminary experiments was carried out to examine thoroughly the reliability of the experimental set-up. We checked and were satisfied that the spectra collected under identical conditions agreed among themselves well within the statistical fluctuations. For these preliminary spectra, we used various gamma sources at various crystal-to-source distances.

We noticed that the gain in the photomultiplier used by us showed an undesirable dependence on the count rate, e.g. in some cases a change in the count rate by a factor of 10 caused a gain shift by about 5%. This effect required that the background subtraction from a particular spectrum should be carried out with due care, as the background count rate was much lower than the count rate with the sources. The overall gain in a particular measurement was checked by determining the position of the peak(s) with one or two suitable sources. To ensure that the background spectrum was compatible, this gain calibration was carried out at very low count rates and the gain was then readjusted as needed when the actual source spectrum was collected (at a different count rate).

For the actual measurements, spectra were accumulated in only 200 channels of the analyzer because use was made of the "Digital Data

Differentiation" and the "Curve Integration" facilities installed in our analyzer and to do that we needed to use the analyzer storage in two sub-groups.

The collection of the final spectra spread over a number of months because we had to depend on the availability of the gamma-ray sources. For each source and each crystal, three or four sets of spectra were accumulated at several crystal-to-source distances. These different "sets" were obtained with fresh calibrations including that of the crystal-to-source distances. The excellent agreement among such spectra ensured the "reproducibility" of the results. The collection of the compatible background spectra was interspersed with the accumulation of the spectra with the sources. To obtain the background spectra of reasonably good statistics, their accumulation was carried over much larger periods and then the normalized spectra were used for the background subtraction.

The results presented in this thesis are based on the final measurements requiring about 500 hours, excluding the time spent on the preliminary experiments and a much greater time spent on the analysis of the spectra and the derivation of the results. In all about 1500 spectra were accumulated and analyzed.

CHAPTER IV

THE ANALYSIS OF SPECTRA AND THE PRESENTATION OF RESULTS

4.1 The Analysis of Spectra:

The analysis of spectra demanded a number of important considerations such as a closer examination of the Gaussian shape of the photopeaks, the summing effect, the estimation of errors and the effect of the absorbing material between the crystal and the source. The following sub-sections will deal with these points in some detail.

(a) The Number of Counts under a Photopeak of Gaussian Shape:

In order to explain the procedure which we adopted to determine the number of counts under the photopeak in various spectra, we start with the spectra of mono-energetic sources ( $\text{Hg}^{203}$ ,  $\text{Cs}^{137}$ ,  $\text{Mn}^{54}$ ). As an example, consider the sample spectrum of  $\text{Mn}^{54}$  (Fig. 4.1) recorded in our 2" x 2" CsI(Tl) crystal.

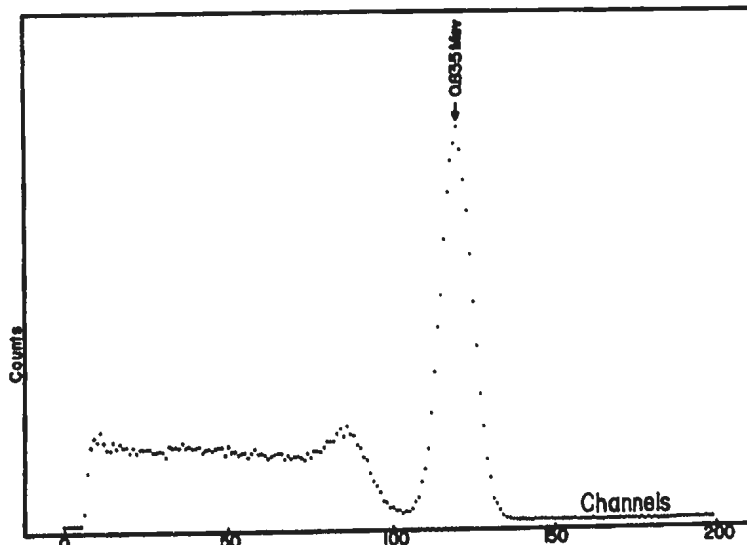


FIG. 4.1 Sample spectrum of  $\text{Mn}^{54}$  in 2"x2" CsI(Tl) crystal.

The peak shape is very nearly Gaussian. It is straightforward to integrate the number of counts under the peak and the result is only very slightly affected by the choice of the cut-off points near the low energy and the high energy tails of the peak. Had our main interest not been in the ratio of the counts in the photopeak using a CsI crystal to that in the photopeak using a 3" x 3" NaI(Tl) crystal, we would have paid greater attention to this question of the proper choice of the cut-off points. We examined thoroughly the variation of this ratio for different choices of cut-off points and found that if we used the same criteria for the two spectra under comparison, the ratio did not change very much. The photopeak in the 3" x 3" NaI(Tl) crystal was also nearly Gaussian and the ratio of the counts under the photopeaks could be determined equally well either by referring to counts only in the high energy half of the peaks or to the counts in the full peaks. The reason for thinking in terms of counts in the high energy half of the peaks was the well-known fact that the low energy tails of the peaks are not always very good because they extend into the region very close to the Compton edge. Furthermore, with sources emitting complex spectra it is usually possible to pick out convenient and acceptable peaks if one could refer to the counts in the high energy half alone. A sample spectrum of Co<sup>60</sup> (Fig. 4.2) illustrates this situation for the 1.332 Mev peak. It must, however, be stressed that this approach rests on the nearly Gaussian (symmetric) shape of the photopeaks. We found this to be reasonably true for our 2" x 2" CsI(Tl) and 3" x 3" NaI(Tl) crystals.

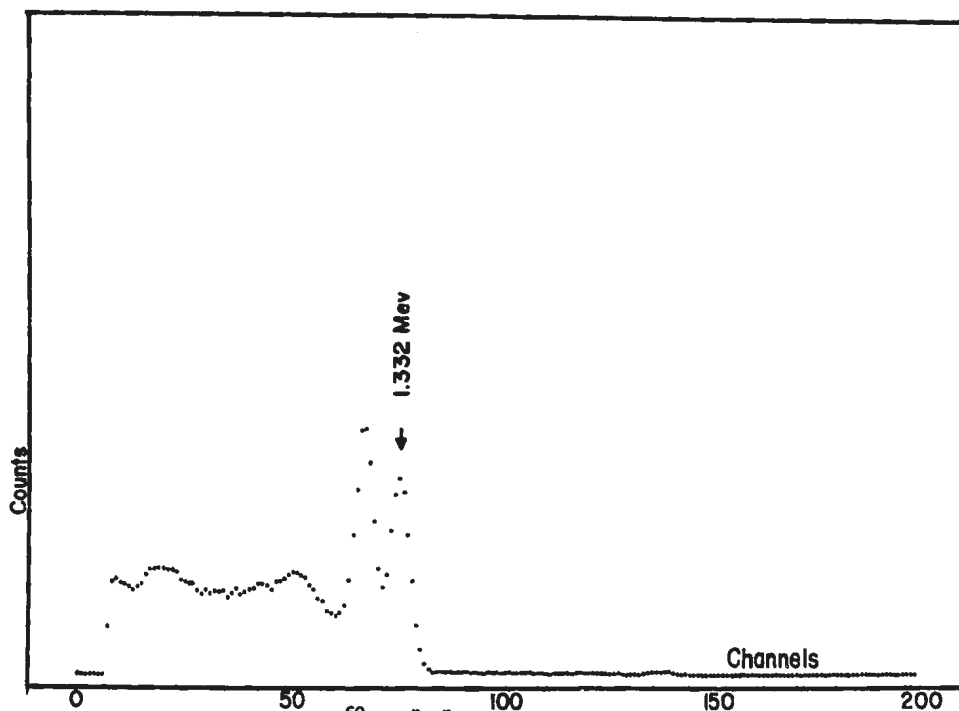


FIG. 4.2 Sample spectrum of  $\text{Co}^{60}$  in  $2'' \times 2''$  CsI(Tl) crystal

(b) Deviations from the Gaussian Shape of the Photopeaks:

Quite unexpectedly, our  $3'' \times 3''$  CsI(Na) showed significant departure from symmetry. The extent of this asymmetry and its consequences on the results will be discussed later at an appropriate place. However, we want to point out at this stage that the spectra obtained with our  $3'' \times 3''$  CsI(Na) crystal were analyzed both from the point of view of the counts in the high energy half of the peaks and the counts in the full peaks. The low energy cut-off points for some

spectra became very critical from the point of view of the error that could be introduced by making a mistake of one or two channels. A sample spectrum of  $Y^{88}$  for the 1.837 Mev peak (Fig. 4.3) illustrates this point.

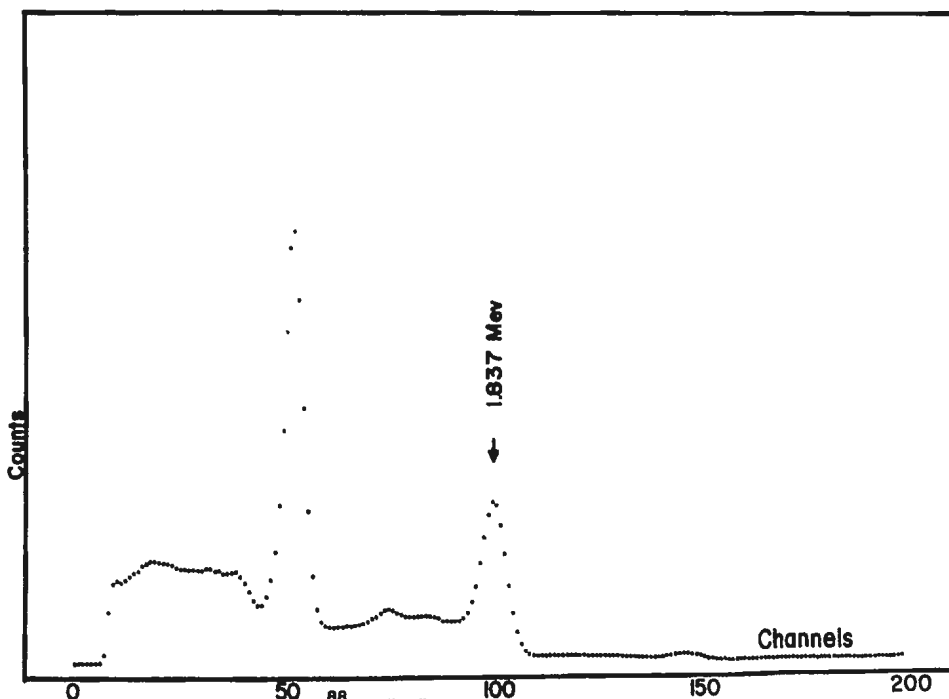


FIG. 4.3 Sample spectrum of  $Y^{88}$  in 3"x3" CsI(Na) crystal.

This situation arose with the gamma sources of high energies. This critical cut-off aspect, furthermore, convinced us of the desirability of analyzing the spectra with reference to the counts in the high energy half of the peaks as well. We have already stated earlier that the

spectra obtained with the 3" x 3" CsI(Na) crystal were analyzed both from the point of view of the counts in the high energy half of the peaks and the counts in the full peaks. As a matter of fact, the spectra obtained with other crystals were also analyzed from both points of view, but only in the case of 3" x 3" CsI(Na) were two different results obtained.

(c) The Effect of the Sum-Spectrum:

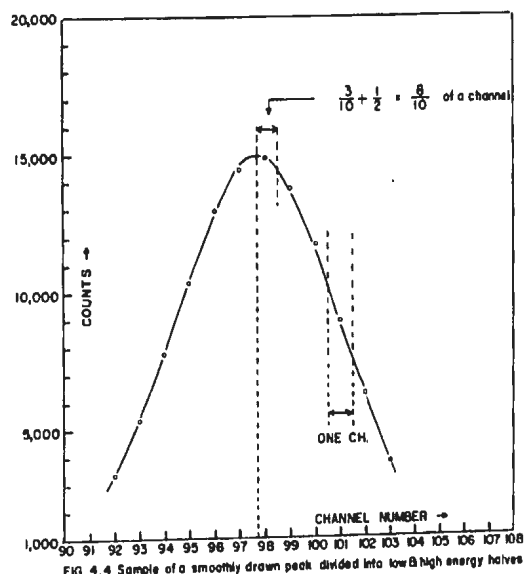
In the case of  $\text{Co}^{60}$ ,  $\text{Y}^{88}$ ,  $\text{Ra}^{226}$ ,  $\text{Th}^{228}$  and  $\text{Co}^{56}$  which are not mono-energetic, we used only the highest energy peaks. In these cases, the counts caused by the simultaneous detection of gamma-rays of different energies resulted in a sum-spectrum at the expense of some counts which should have appeared under the individual photopeaks. The relative intensity of the sum-spectrum is strongly dependent on the geometry. For large crystal-to-source distances, the contribution to the sum-spectrum is almost negligible but for distances of a few centimeters there is usually a significant number of counts in the "sum-spectrum". Remembering that we were dealing with the highest energy peaks and that we were interested only in the ratios, we carefully examined the difference in the ratios for the two extreme cases: (i) completely ignoring all counts beyond the observed photopeaks (some of which must be due to the "sum-spectrum" at the expense of the counts in the photopeaks) and (ii) treating all counts beyond the observed photopeaks as the counts belonging to the photopeaks. We were thus able to set an upper and a lower limit to the ratio of the counts under

the photopeaks in two spectra under comparison. We wish to emphasize the fact that these ratios could be determined with an uncertainty much less than the uncertainty in the number of counts in the individual spectra themselves. It should be noted that the effect of the counts in the "sum-peak" was considered with reference to the counts in the "full peaks" or equivalently with reference to twice the number of counts in the high energy half of the peaks. For the case of  $\text{Bi}^{207}$  when we used the lower energy peaks, we could not carry out the above mentioned procedure of taking into account the "summing effect". However, in the presentation of our results we have given due consideration to this aspect.

(d) The Estimation of Errors:

We now proceed to explain in some detail the procedure adopted for analyzing the spectra with particular reference to the estimation of errors involved. First, we shall discuss the determination of the number of counts in the high energy half of the peak.

In order to obtain the number of counts in the high energy half of the peak, the properly background subtracted spectra were plotted and smooth shapes were drawn by visual judgment. Fig. 4.4 is an illustration.



The vertical line from the highest point on the smoothly drawn peak divides it into the low and the high energy halves. Counts represented by points which are half a channel width or more away from this vertical line belong fully to the half portion in which they are plotted. The question arises about the only point near the peak which lies less than half a channel width away from this line. If the point happens to be right on the line, the counts represented by this point are divided equally between the two halves. More generally, however, the point in question does not lie on the line itself. Then the counts are divided in the appropriate ratio, e.g. if the point lies  $3/10$  of a channel away from the line, then the "half-peak" containing the point gets  $(\frac{1}{2} + 3/10) = 8/10$  of the counts and the remainder  $2/10$  of the counts go to the other half of the peak.

For a mono-energetic source, the uncertainty in the determination of the counts in the high energy half of the peak can be estimated as follows:

Excluding the point which is less than half a channel width away from the peak position, let the total number of counts in the remainder of the half-peak be  $N_1$ . Let the excluded point represent  $N_2$  counts and out of this let  $f_0 N_2$  counts belong to the half-peak under consideration. Thus the total number of counts in the half-peak on the high energy side is

$$N_0 = N_1 + f_0 N_2 \quad (4.1)$$

where  $N_1$  and  $N_2$  refer to properly background subtracted counts. For any estimation of uncertainty in  $N_0$ , we note that (assuming the background to be very small)  $N_1$  has a statistical fluctuation  $\sigma_1 = \sqrt{N_1}$  and, similarly,  $f_0 N_2$  has a statistical fluctuation  $\sigma_2 = f_0 \sqrt{N_2}$ . (If the background counts cannot be regarded as relatively insignificant, then the statistical fluctuation is given by  $\sqrt{N' + B/t}$ , where  $N'$  is the number of counts without the background subtraction and  $B$  is the number of background counts accumulated in "t" units of time relative to one unit of time for  $N'$ .) The fraction  $f_0$  itself has some uncertainty which in turn introduces some uncertainty; say  $\pm a$  in  $f_0 N_2$ . Furthermore, if an additional uncertainty of  $\pm N_3$  counts is estimated to be associated with the "cut-off" point of the tail of the high energy half of the peak, then the standard deviation  $\sigma_0$  of the total number of counts  $N_0$  in the high energy half of the peak is to a good approximation given by

$$\sigma_0 = \sqrt{N_1 + f_0^2 N_2 + a^2 + N_3^2} \quad . \quad (4.2)$$

The standard deviation of the ratio of counts in the half-peaks of any two spectra can be calculated easily.

If a number of independently collected spectra under identical conditions are taken, then a mean value of the ratio can be calculated with improved accuracy. This description of the error estimation ignores any complication due to "sum-spectrum" if the source is not mono-energetic. In that case, the estimated error is dominated by the uncertainty of the number of counts in the sum-peak and then it is more

appropriate to talk in terms of the upper and the lower limits of the ratio in question (as discussed earlier) because the above formula is not realistic. However, a mean value of  $N_0$  can still be determined so that the counts versus the distance graphs can be drawn but the "error" on the particular ratio must be in terms of the upper and the lower limits as discussed earlier.

In obtaining the "full-peak" counts, the uncertainties involved are due to the low energy cut-off, the high energy cut-off and the statistical fluctuations. In our experience, for high energy sources the low energy cut-off proved to be the biggest contributor to the uncertainty.

The effects of the finite dimensions of the source and of any error in the measurement of the crystal-to-source distance will appear at an appropriate place while discussing the results.

(e) The Effect of the Absorbing Material between the Crystal and the Source:

If measurements with each crystal are carried out with the same amount (i.e. thickness in  $\text{gm/cm}^2$ ) of the absorbing materials (between the source and the actual crystal), then for obtaining the ratio of the photopeak efficiencies, no correction is needed as far as the attenuation of gamma-rays is concerned. However, one has to pay due attention to the possibility of some of the electrons, if emitted by the particular source, being detected in the area of the photopeaks. Furthermore, if any difference does exist in the amount of the absorbing

materials for different crystals, appropriate corrections for different gamma-attenuations should be made.

According to the information supplied by the Harshaw Chemical Company about the crystal assembly, the gamma-rays had to pass through the materials as listed below for different crystals:

(A) 3" x 3" NaI(Tl) and 3" x 3" CsI(Na) Crystals:

(i) Immediately next to the crystal was a 0.005" thick aluminium sheet with sprayed aluminium oxide, maximum thickness 0.020". The thin sheet of aluminium had a mass of  $34.1 \text{ mg/cm}^2$  and the sprayed aluminium oxide  $20 \text{ mg/cm}^2$  (approximately) and (ii) the aluminium back cap 0.020" thick and had a mass of  $136.7 \text{ mg/cm}^2$ .

(B) 2" x 2" CsI(Tl) Crystal:

(i) packed aluminium oxide reflector approximately 1/16" thick of mass  $67 \text{ mg/cm}^2 \pm 10$ , (ii) polyethylene disc 0.006" thick of mass  $13.0 \text{ mg/cm}^2$ , (iii) sponge rubber pad (compressed) 1/8" thick of mass  $133.0 \text{ mg/cm}^2$  and (iv) aluminium back cap window 0.032" thick of mass  $218.8 \text{ mg/cm}^2$ .

First let us take up the possibility of the detection of electrons.  $\text{Cs}^{137}$  source was used for the 0.662 Mev gamma-rays. This source, however, also emits a continuous beta spectrum with 1.18 Mev end-point energy in 8% of the transitions (one should note that, unlike gamma-rays, all beta particles incident on the crystal are detected). The total amount of the absorber in the case of 3" x 3" crystals may be

considered as almost  $190 \text{ mg/cm}^2$  of aluminium, ignoring any absorption in the source disc itself. In passing through this much thickness of aluminium, the beta particles of the maximum kinetic energy 1.18 Mev are degraded to about 0.8 Mev. It should be noted that we are talking about the end-point energy and, naturally, very few electrons in the "degraded" beta spectrum would have the right energy to be detected in the photopeak region of the 0.662 Mev gamma-rays. We actually confirmed this fact by carrying out a simple experiment with the unsealed 2" x 2" CsI(Tl) crystal using absorbers of different thicknesses and concluded that if any correction were applied to the spectra obtained with the 3" x 3" crystals, it would be less than 1% of the counts in the photo-peaks. We did not apply any correction in this respect. For the 2" x 2" CsI(Tl) crystal (i.e. the sealed crystal), the absorbing material was as much as  $432 \text{ mg/cm}^2$  and no correction was needed. The  $\text{Bi}^{207}$  source was the only other source which needed an examination because of its beta emission with 0.77 Mev end-point energy. On the basis of simple calculations of the energy degradation of beta particles in passing through the absorbing materials, we found that no correction was needed as far as the 0.57 Mev peak was concerned.

Now, concerning the correction for different attenuation in the case of the 3" x 3" and the 2" x 2" crystals, we applied a correction using for all absorbers the total absorption coefficients for aluminium. The correction applied accounted for about 1 to 3% more attenuation in the case of the 2" x 2" CsI(Tl) crystal for gamma-rays of energies below 1.837 Mev.

#### 4.2 The Direct Experimental Results:

In this section we present the results obtained directly from the analysis of our spectra. We have used these results to obtain the values of photofractions for the CsI crystals as given in Section 4.3 on the evaluation of photofractions.

##### (a) The Sealed and Unsealed 2" x 2" CsI(Tl) Crystals:

We have already stated earlier that four crystals were used; namely, (i) a 3" x 3" NaI(Tl), (ii) a 3" x 3" CsI(Na), (iii) a 2" x 2" CsI(Tl) and (iv) an unsealed 2" x 2" CsI(Tl). The last crystal was investigated to detect any possible difference in the photopeak efficiency due to the absorption of the atmospheric moisture by the crystal over a prolonged period. (The presence of this crystal also helped in carrying out some preliminary experiments.) After taking into account the effect of the absorbing materials between the source and the crystal, we concluded that within the limits of the experimental error, the unsealed 2" x 2" CsI(Tl) had the same photopeak efficiency for the region investigated as that of the sealed 2" x 2" CsI(Tl) crystal, even though the resolution of the unsealed crystal was somewhat poorer than that of the sealed crystal (this may be due, perhaps, to poorer light collection in the case of the unsealed crystal). In order to avoid unnecessary duplication in the presentation of the results we shall not make any distinction between the unsealed and the sealed CsI(Tl) crystals.

(b) The Energy Resolution and the Typical Spectra:

The energy resolution of a scintillation spectrometer is a measure of the ability to distinguish between two gamma-rays closely spaced in energy. We have adopted the following convention in defining the resolution:

$$\text{Resolution (\%)} = \frac{\Delta E(\text{full width at half maximum})}{E(\text{peak energy})} \times 100$$

The values of the energy resolution of the 3" x 3" NaI(Tl), the 3" x 3" CsI(Na) and the 2" x 2" CsI(Tl) crystals appear in Table 4.1 and in the graphical form in Fig. 4.5.

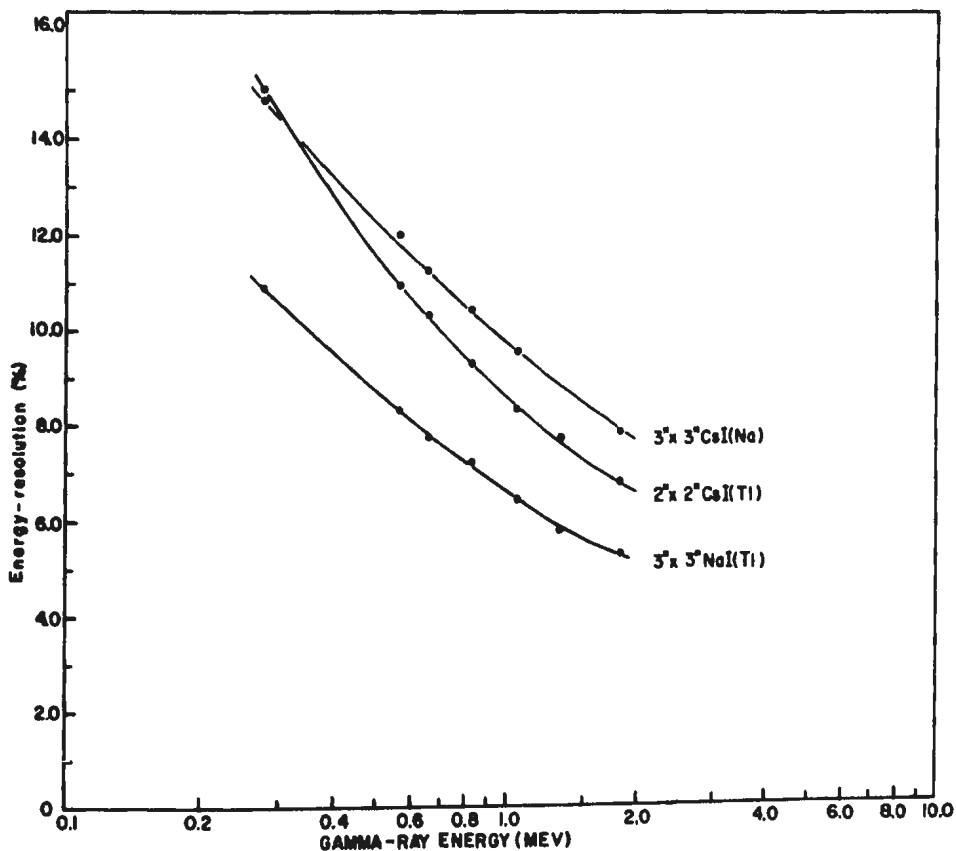


FIG. 4.5 Energy-resolution vs. Gamma-ray Energy

TABLE 4.1

Energy Resolution of Different Crystals

Gamma-ray Energy (Mev)	Resolution in %		
	3" x 3" NaI(Tl)	3" x 3" CsI(Na)	Sealed 2" x 2" CsI(Tl)
0.279	10.87	14.81	15.02
0.57	8.34	12.02	10.97
0.662	7.77	11.27	10.34
0.835	7.24	10.44	9.33
1.064	6.45	9.55	8.33
1.332	5.80	-	7.76
1.837	5.29	7.85	6.81

(NB: The blank space refers to the case where the calculation of that resolution was not possible.)

Typical spectra of various gamma-ray sources obtained with different crystals are shown in Figs. 4.6 (a) to 4.6 (i), 4.7 (a) to 4.7 (i) and 4.8 (a) to 4.8 (i). Some of the spectra selected for the illustration purposes are without background subtraction and others are background subtracted.

(c) The Relative Photopeak Efficiencies:

We now present the results in the form of photopeak efficiencies of the 2" x 2" CsI(Tl) and the 3" x 3" CsI(Na) crystals relative to that of the 3" x 3" NaI(Tl) crystal. The ratios for different energies and different crystal-to-source distances refer to the quantity

$$\frac{\left[ \text{Photopeak efficiency of the 2"x2" CsI(Tl) or the 3"x3" CsI(Na) Crystal} \right]}{\left[ \text{Photopeak efficiency of the 3"x3" NaI(Tl) crystal for the same gamma-ray energy and for the same crystal-to-source distance} \right]}$$

As stated earlier, for the 2" x 2" CsI(Tl) crystal we got the same value of the above ratio for the two methods of analysis: firstly, by referring to the counts under the high energy half of the photopeaks and, secondly, by referring to the counts under the full photopeaks (whenever it was possible to carry out the second method of analysis). However, for the 3" x 3" CsI(Na) crystal the ratio was found to depend on the method of analysis. Hence we present two values of the ratios for those spectra for which the second method of analysis was possible to carry out.

In the first method of analysis, the number of counts were read for the correct crystal-to-source distances from the experimentally

(Counts on linear scale)

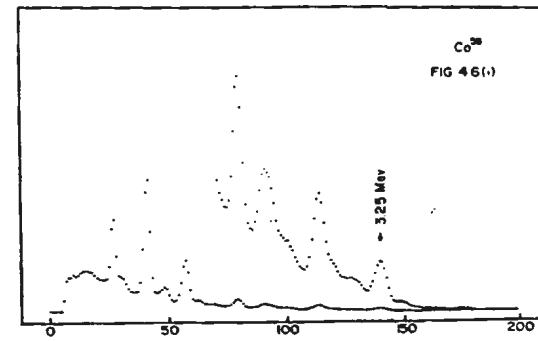
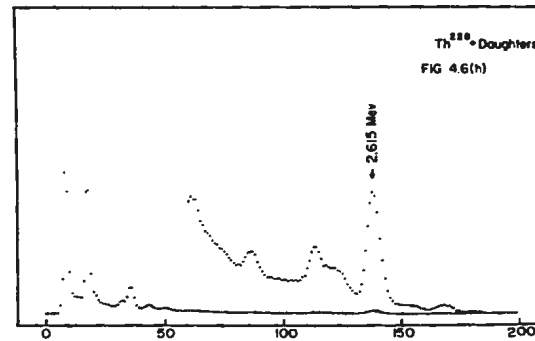
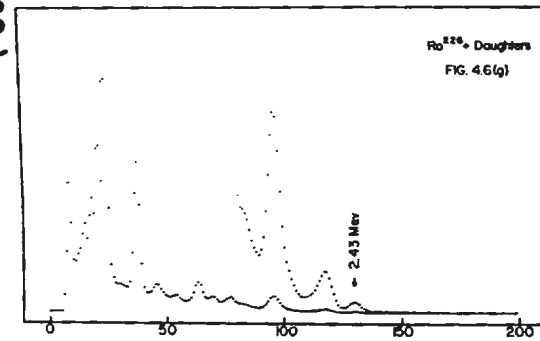
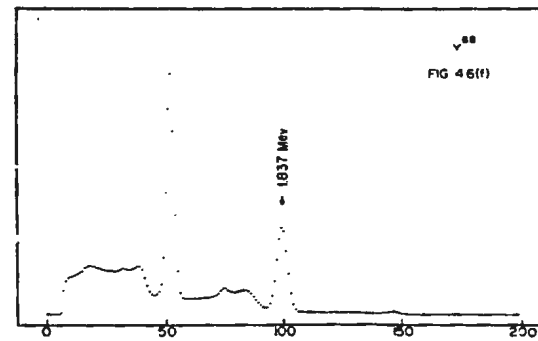
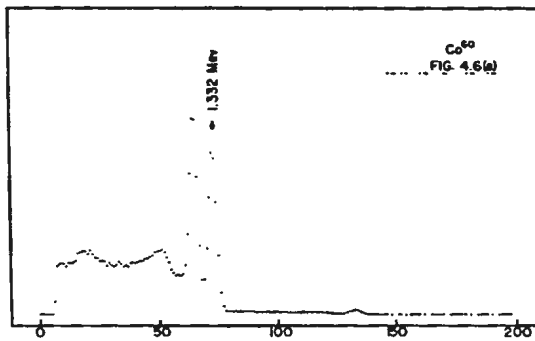
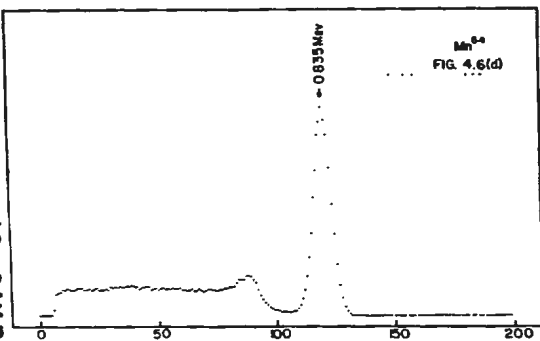
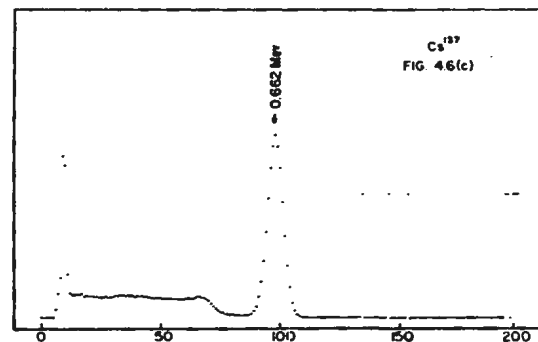
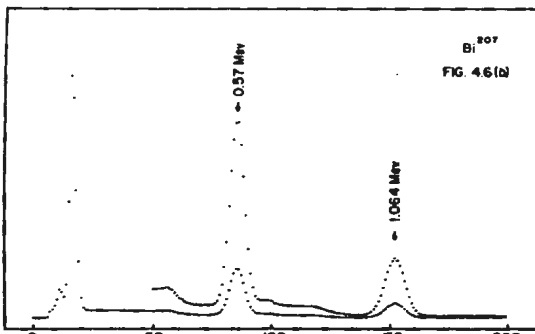
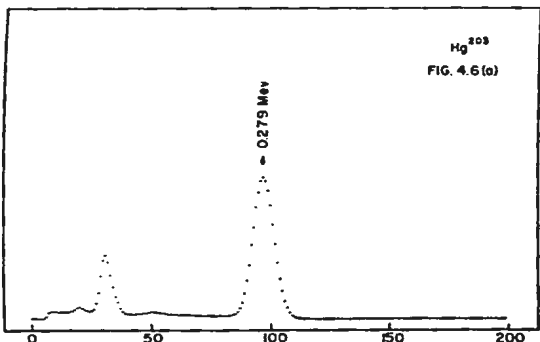


FIG. 4.6(a) to 4.6(i) Sample spectra  
Crystal : 3"x3" Na I(Tl) Source distance : 3.0 cm

( Counts on linear scale )

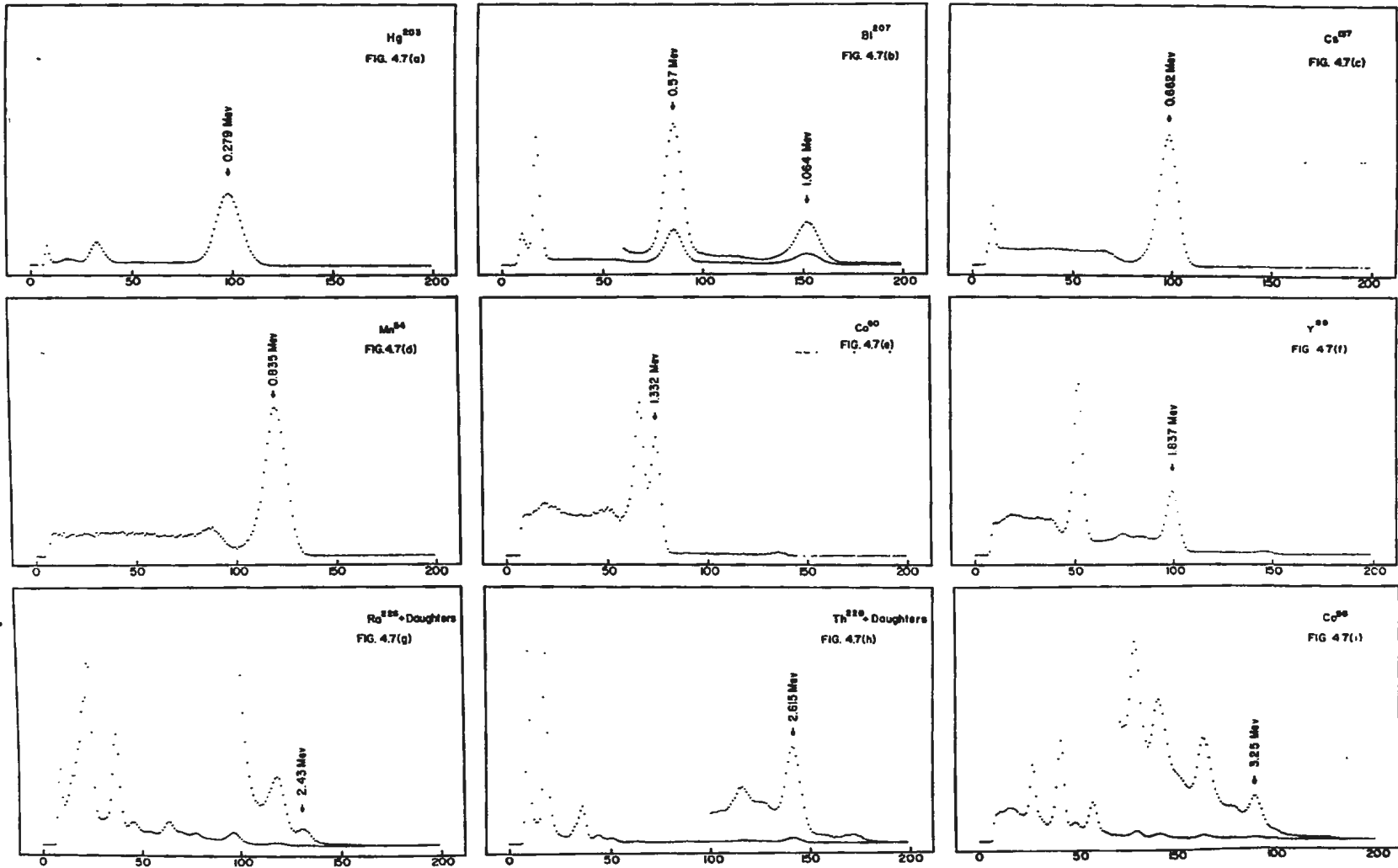
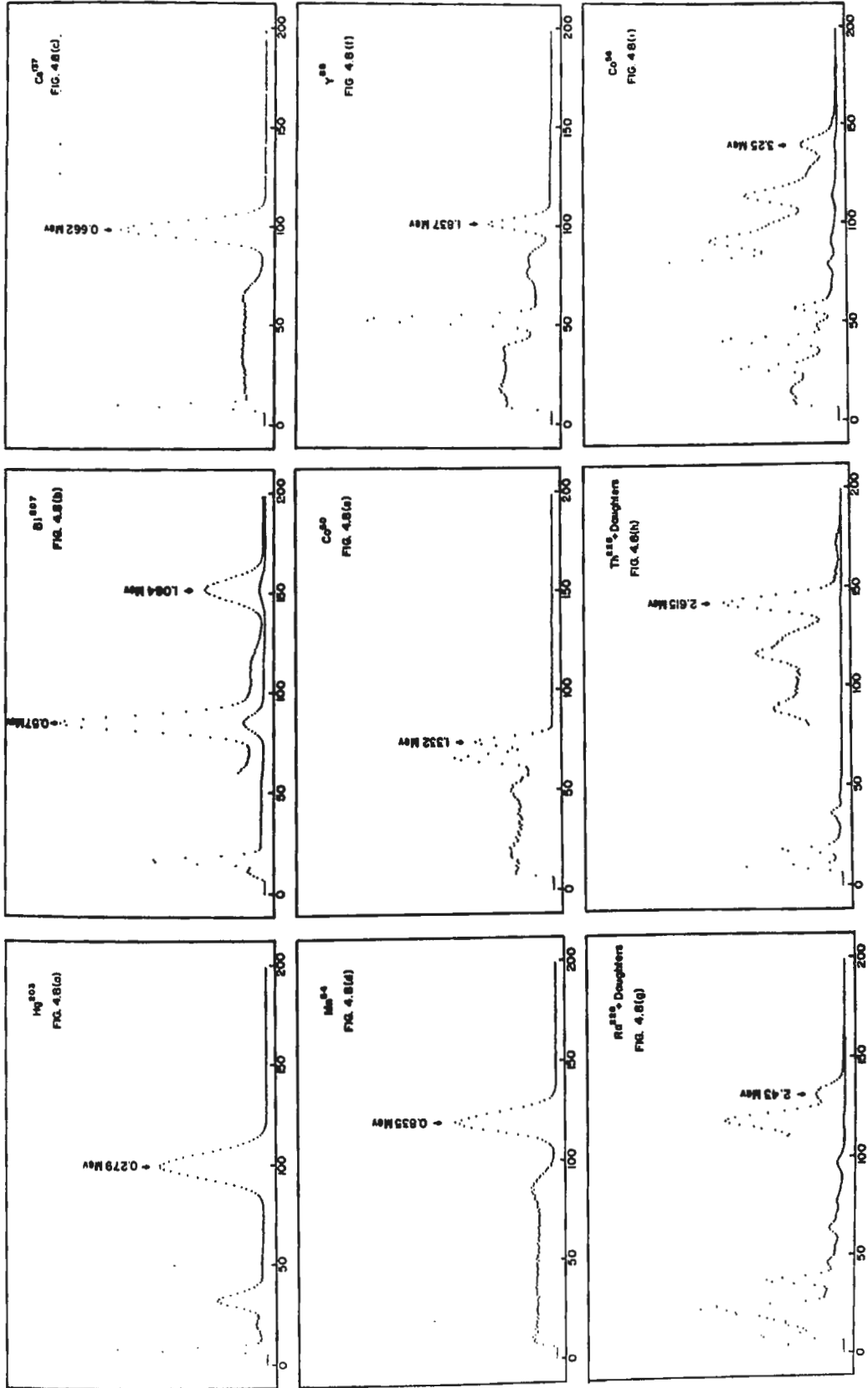


FIG. 4.7(a) to 4.7(i) Sample spectra  
Crystal: 3"x 3" CsI(Na)  
Source distance: 3.0 cm



( Counts on linear scale )

FIG. 4.8(a) to 4.8(i) Sample spectra  
Source distance : 3.0 cm  
Crystal : 2"x2" CsI(Tl)

obtained counts versus the distance graph (using provisional values of the crystal-to-can-top distances - see Section 3.2). The correction amounted to only 3% and, therefore, it is justified to estimate the uncertainty in the ratio from the corresponding spectra for the "uncorrected" distances.

In the second method of analysis, the ratios were obtained for the "uncorrected" distances and then the distance correction was applied assuming the same correction factor as for the first method of analysis. (We decided to carry out the second method of analysis for fewer distances and to use the small distance correction factor from the very carefully drawn earlier graphs based on the first method.)

In the case of Bi<sup>207</sup> spectra where we could not take into account any "summing effect", we estimate that for the 2" x 2" CsI(Tl) crystal for smaller crystal-to-source distances (less than 3 cm), there can be significant errors in our values, but for larger distances we believe that the observed values are within 5% or so of the true values and we have increased the estimated error on these values in the light of our experience with Co<sup>60</sup> and Y<sup>88</sup> for which the "possible sum-effects" are reflected in our estimated errors. For the 3" x 3" CsI(Na) crystal the situation is much more satisfactory because of nearly equal "summing effects" in the two crystals under comparison. We were again guided by our experience with Co<sup>60</sup> and Y<sup>88</sup> spectra.

In Table 4.2, we present the values of the relative photopeak efficiency for the 2" x 2" CsI(Tl) crystal. These values as a function of energy are presented in Fig. 4.9 and as a function of the crystal-to-source distance in Fig. 4.10. The relative photopeak efficiencies for

TABLE 4.2

Relative Photopeak Efficiency  $\left[ \frac{\epsilon_p \text{ of } 2'' \times 2'' \text{ CsI(Tl) crystal}}{\epsilon_p \text{ of } 3'' \times 3'' \text{ NaI(Tl) crystal}} \right]$   
 for the same energy and distance

No.	Crystal-to- Source Distance (cm)	Energy (Mev)				
		0.279	0.57	0.662	0.835	1.064
1.	1.0	0.821 ± 0.023	0.811 ± *	0.735 ± 0.017	0.693 ± 0.027	0.753 ± *
2.	1.5	0.757 ± 0.017	0.742 ± *	0.690 ± 0.015	0.657 ± 0.023	0.699 ± *
3.	2.0	0.706 ± 0.015	0.681 ± *	0.651 ± 0.014	0.618 ± 0.021	0.657 ± *
4.	2.5	0.666 ± 0.013	0.639 ± *	0.619 ± 0.013	0.588 ± 0.019	0.623 ± *
5.	3.0	0.626 ± 0.012	0.605 ± 0.038	0.591 ± 0.012	0.568 ± 0.016	0.593 ± 0.036
6.	3.5	0.603 ± 0.011	0.582 ± 0.040	0.571 ± 0.011	0.550 ± 0.016	0.571 ± 0.032
7.	4.0	0.584 ± 0.010	0.566 ± 0.034	0.556 ± 0.011	0.538 ± 0.015	0.553 ± 0.030
8.	4.5	0.569 ± 0.010	0.550 ± 0.034	0.544 ± 0.010	0.525 ± 0.014	0.538 ± 0.028
9.	5.0	0.559 ± 0.009	0.539 ± 0.030	0.534 ± 0.010	0.519 ± 0.013	0.526 ± 0.024
10.	6.0	0.542 ± 0.009	0.521 ± 0.023	0.518 ± 0.010	0.503 ± 0.013	0.506 ± 0.017
11.	7.0	0.528 ± 0.009	0.509 ± 0.023	0.502 ± 0.010	0.486 ± 0.014	0.489 ± 0.017
12.	8.0	0.517 ± 0.008	0.494 ± 0.023	0.485 ± 0.009	0.471 ± 0.013	0.478 ± 0.017
13.	9.0	0.511 ± 0.008	0.486 ± 0.024	0.475 ± 0.009	0.458 ± 0.012	0.471 ± 0.017
14.	10.0	0.507 ± 0.008	0.487 ± 0.024	0.474 ± 0.009	0.454 ± 0.012	0.464 ± 0.017

\*Errors are uncertain due to the summing effect.

continued .....

TABLE 4.2, continued

Relative Photopeak Efficiency  $\frac{[e_p \text{ of } 2'' \times 2'' \text{ CsI(Tl) crystal}]}{[e_p \text{ of } 3'' \times 3'' \text{ NaI(Tl) crystal}]}$   
 for the same energy and distance

No.	Crystal-to-Source Distance (cm)	Energy (MeV)				
		1.332	1.837	2.43	2.615	3.25
1.	1.0	0.696 ± 0.067	0.658 ± 0.045			
2.	1.5	0.656 ± 0.061	0.619 ± 0.040			
3.	2.0	0.606 ± 0.045	0.580 ± 0.036	0.560 ± 0.029		
4.	2.5	0.571 ± 0.040	0.557 ± 0.033			
5.	3.0	0.545 ± 0.036	0.531 ± 0.024	0.506 ± 0.034	0.505 ± 0.075	0.473 ± 0.063
6.	3.5	0.528 ± 0.034	0.510 ± 0.024			
7.	4.0	0.517 ± 0.032	0.495 ± 0.022	0.463 ± 0.040		
8.	4.5	0.506 ± 0.028	0.482 ± 0.021			
9.	5.0	0.505 ± 0.026	0.484 ± 0.019	0.460 ± 0.036	0.456 ± 0.038	0.439 ± 0.046
10.	6.0	0.485 ± 0.025	0.466 ± 0.018	0.457 ± 0.033		
11.	7.0	0.466 ± 0.026	0.454 ± 0.017	0.467 ± 0.039	0.431 ± 0.015	0.413 ± 0.035
12.	8.0	0.452 ± 0.025	0.446 ± 0.017	0.462 ± 0.045		
13.	9.0	0.455 ± 0.024	0.454 ± 0.016	0.434 ± 0.055	0.420 ± 0.014	0.420 ± 0.029
14.	10.0	0.453 ± 0.023	0.452 ± 0.016	0.431 ± 0.048	0.419 ± 0.015	0.431 ± 0.028

### VARIATION OF RELATIVE PHOTOPEAK EFFICIENCY WITH ENERGY

(different graphs for different distances)

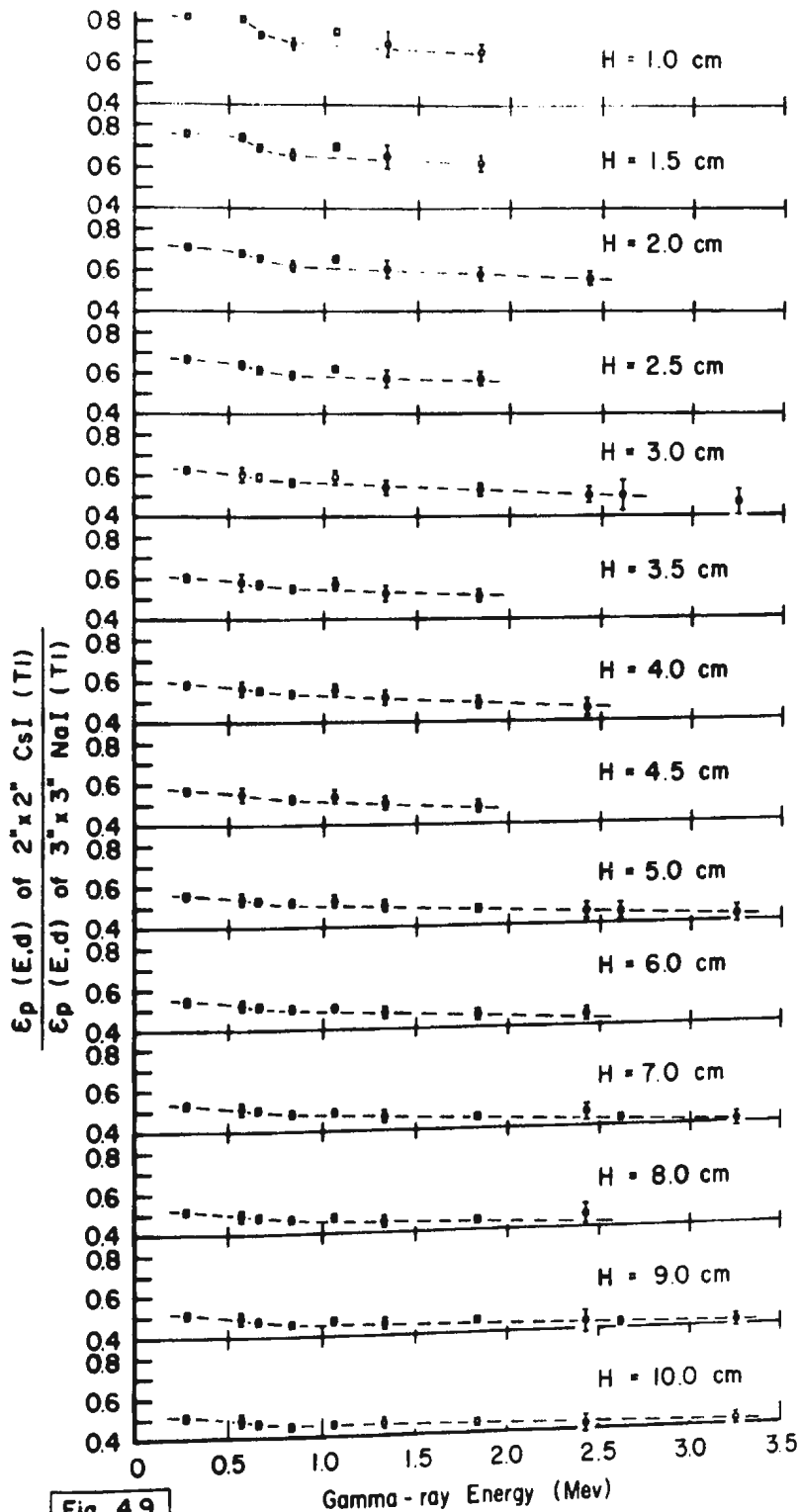


Fig. 4.9

Experimental values of the relative photopeak-efficiency of 2" x 2" CsI(Tl) crystal w.r.t. 3" x 3" NaI(Tl) crystal.

VARIATION OF RELATIVE  
PHOTOPEAK EFFICIENCY WITH DISTANCE  
(different graphs for different energies)

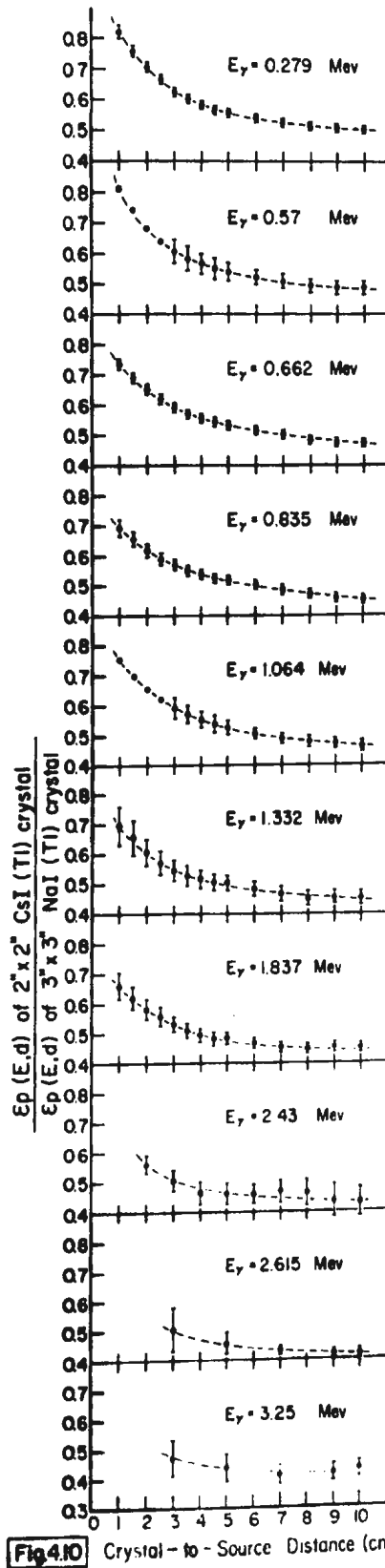


Fig. 4.10 Crystal-to-Source Distance (cms.)

Experimental values of the relative photopeak-efficiency of 2" x 2" CsI(Tl) crystal w.r.t. 3" x 3" NaI(Tl) crystal.

the 3" x 3" CsI(Na) crystal are presented in Tables 4.3 and 4.4 for the two methods of analysis. These values are plotted as a function of the energy in Fig. 4.11 and as a function of the crystal-to-source distance in Fig. 4.12. We have plotted results of both methods of analysis on the same graph and where the error bars on the corresponding points would have overlapped we have shown only half-error bars to avoid confusion. The values for intermediate energies and distances can be obtained from our results by appropriate interpolations.

(d) The Asymmetry Factor:

For the 3" x 3" CsI(Na) crystal, we have defined an asymmetry factor  $\Delta$  as

$$\Delta = \frac{\left[ \begin{array}{l} \text{Relative photopeak efficiency by the second method,} \\ \text{i.e. referring to counts under the full peaks} \end{array} \right]}{\left[ \begin{array}{l} \text{Relative photopeak efficiency by the first method,} \\ \text{i.e. referring to counts under the high energy half} \\ \text{of the peaks} \end{array} \right]}$$

Table 4.5 shows the values of the asymmetry factor  $\Delta$  for various gamma-ray energies and crystal-to-source distances. The variation of the asymmetry factor  $\Delta$  as a function of the energy appears in Fig. 4.13 and as a function of the distance in Fig. 4.14.

This completes the presentation of the experimental results obtained directly, both for 2" x 2" CsI(Tl) as well as 3" x 3" CsI(Na) crystals.

TABLE 4.3

Relative Photopeak Efficiency  $\frac{[\epsilon_p \text{ of } 3'' \times 3'' \text{ CsI(Na) crystal}]}{[\epsilon_p \text{ of } 3'' \times 3'' \text{ NaI(Tl) crystal} \text{ for the same energy and distance}]}$

(Photopeak considered as twice the high energy half of the peak)

No.	Crystal-to-Source Distance (cm)	Energy (Mev)				
		0.279	0.57	0.662	0.835	1.064
1.	1.0	1.055 ± 0.027	1.167 ± 0.028	1.174 ± 0.026	1.187 ± 0.046	1.151 ± 0.053
2.	1.5	1.083 ± 0.024	1.180 ± 0.029	1.197 ± 0.026	1.204 ± 0.044	1.166 ± 0.050
3.	2.0	1.084 ± 0.023	1.157 ± 0.029	1.192 ± 0.024	1.191 ± 0.040	1.167 ± 0.049
4.	2.5	1.079 ± 0.021	1.155 ± 0.029	1.194 ± 0.024	1.199 ± 0.038	1.174 ± 0.044
5.	3.0	1.068 ± 0.020	1.152 ± 0.029	1.191 ± 0.023	1.191 ± 0.034	1.165 ± 0.036
6.	3.5	1.080 ± 0.019	1.155 ± 0.031	1.177 ± 0.022	1.186 ± 0.033	1.160 ± 0.032
7.	4.0	1.081 ± 0.019	1.157 ± 0.032	1.177 ± 0.022	1.172 ± 0.032	1.153 ± 0.032
8.	4.5	1.077 ± 0.018	1.155 ± 0.032	1.174 ± 0.022	1.163 ± 0.031	1.152 ± 0.032
9.	5.0	1.073 ± 0.018	1.149 ± 0.030	1.168 ± 0.022	1.164 ± 0.031	1.154 ± 0.026
10.	6.0	1.069 ± 0.017	1.140 ± 0.030	1.162 ± 0.021	1.166 ± 0.030	1.151 ± 0.026
11.	7.0	1.067 ± 0.017	1.137 ± 0.030	1.163 ± 0.021	1.148 ± 0.031	1.143 ± 0.026
12.	8.0	1.068 ± 0.017	1.130 ± 0.031	1.140 ± 0.021	1.134 ± 0.031	1.134 ± 0.025
13.	9.0	1.074 ± 0.017	1.128 ± 0.031	1.144 ± 0.021	1.130 ± 0.031	1.122 ± 0.027
14.	10.0	1.070 ± 0.017	1.129 ± 0.033	1.145 ± 0.021	1.141 ± 0.030	1.111 ± 0.025

..... continued

TABLE 4.3, continued

$$\text{Relative Photopeak Efficiency} \frac{\left[ \epsilon_p \text{ of } 3'' \times 3'' \text{ CsI(Na) crystal} \right]}{\left[ \epsilon_p \text{ of } 3'' \times 3'' \text{ NaI(Tl) crystal} \right.}$$

$$\left. \text{for the same energy and distance} \right]$$

(Photopeak considered as twice the high energy half of the peak)

No.	Crystal-to- Source Distance (cm)	Energy (Mev)				
		1.332	1.837	2.43	2.615	3.25
1.	1.0	1.184 ± 0.096	1.165 ± 0.073			
2.	1.5	1.207 ± 0.095	1.188 ± 0.074			
3.	2.0	1.201 ± 0.076	1.187 ± 0.072	1.405 ± 0.097		
4.	2.5	1.186 ± 0.076	1.199 ± 0.073			
5.	3.0	1.185 ± 0.068	1.186 ± 0.052	1.333 ± 0.085	1.237 ± 0.051	1.390 ± 0.061
6.	3.5	1.191 ± 0.066	1.176 ± 0.056			
7.	4.0	1.190 ± 0.066	1.171 ± 0.051	1.316 ± 0.074		
8.	4.5	1.184 ± 0.056	1.162 ± 0.069			
9.	5.0	1.173 ± 0.054	1.144 ± 0.043	1.311 ± 0.060	1.172 ± 0.048	1.303 ± 0.055
10.	6.0	1.148 ± 0.055	1.137 ± 0.043	1.311 ± 0.080		
11.	7.0	1.138 ± 0.058	1.131 ± 0.043	1.264 ± 0.076	1.124 ± 0.049	1.208 ± 0.051
12.	8.0	1.129 ± 0.059	1.126 ± 0.042	1.232 ± 0.086		
13.	9.0	1.119 ± 0.053	1.109 ± 0.039	1.157 ± 0.084	1.126 ± 0.055	1.184 ± 0.053
14.	10.0	1.120 ± 0.056	1.086 ± 0.038	1.140 ± 0.102	1.130 ± 0.055	1.220 ± 0.073

TABLE 4.4

Relative Photopeak Efficiency  $\frac{[\epsilon_p \text{ of } 3'' \times 3'' \text{ CsI(Na) crystal}]}{[\epsilon_p \text{ of } 3'' \times 3'' \text{ NaI(Tl) crystal}]}$   
 for the same energy, distance ]

(Photopeak considered as the full peak)

No.	Crystal-to-Source Distance (cm)	Energy (Mev)					
		0.279	0.662	0.835	1.064	1.837	2.615*
1.	1.0	1.073 ± 0.015	1.236 ± 0.019	1.248 ± 0.027	1.246 ± 0.043	1.238 ± 0.089	
2.	2.0	1.103 ± 0.015	1.266 ± 0.018	1.261 ± 0.027	1.281 ± 0.040	1.258 ± 0.087	
3.	3.0	1.082 ± 0.016	1.268 ± 0.020	1.270 ± 0.029	1.282 ± 0.036	1.265 ± 0.086	1.290 ± 0.109
4.	5.0	1.089 ± 0.016	1.254 ± 0.021	1.266 ± 0.031	1.296 ± 0.027	1.260 ± 0.084	1.238 ± 0.081
5.	8.0	1.083 ± 0.016	1.225 ± 0.021	1.261 ± 0.033	1.301 ± 0.031	1.253 ± 0.089	
6.	10.0	1.075 ± 0.016	1.226 ± 0.022	1.249 ± 0.036	1.283 ± 0.034	1.258 ± 0.091	1.208 ± 0.075

\*Values for the crystal-to-source distances of 7.0 and 9.0 cm and for gamma-ray energy 2.615 Mev are 1.225 ± 0.076 and 1.216 ± 0.077, respectively.

### VARIATION OF RELATIVE PHOTOPEAK EFFICIENCY WITH ENERGY

(different graphs for different distances)

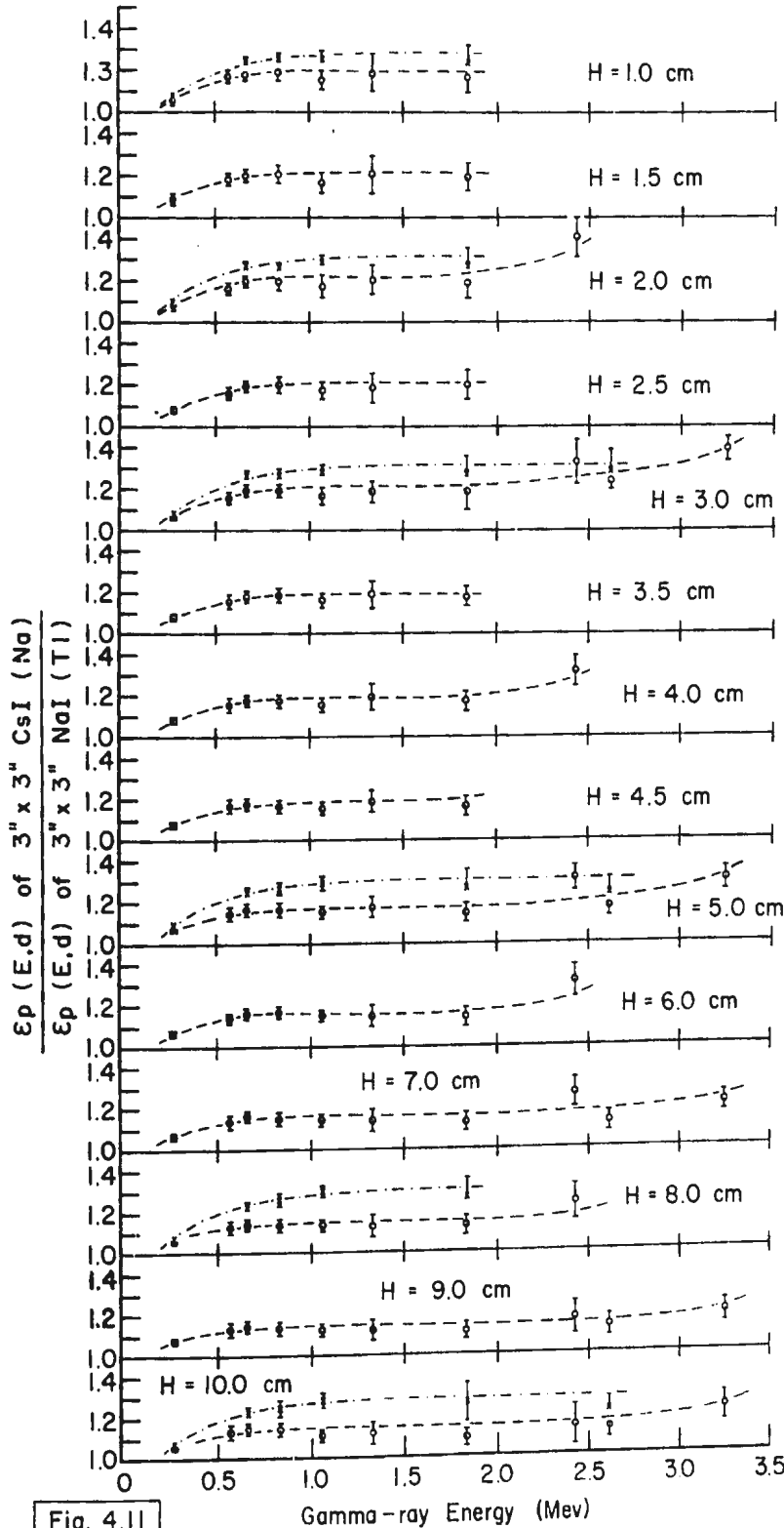
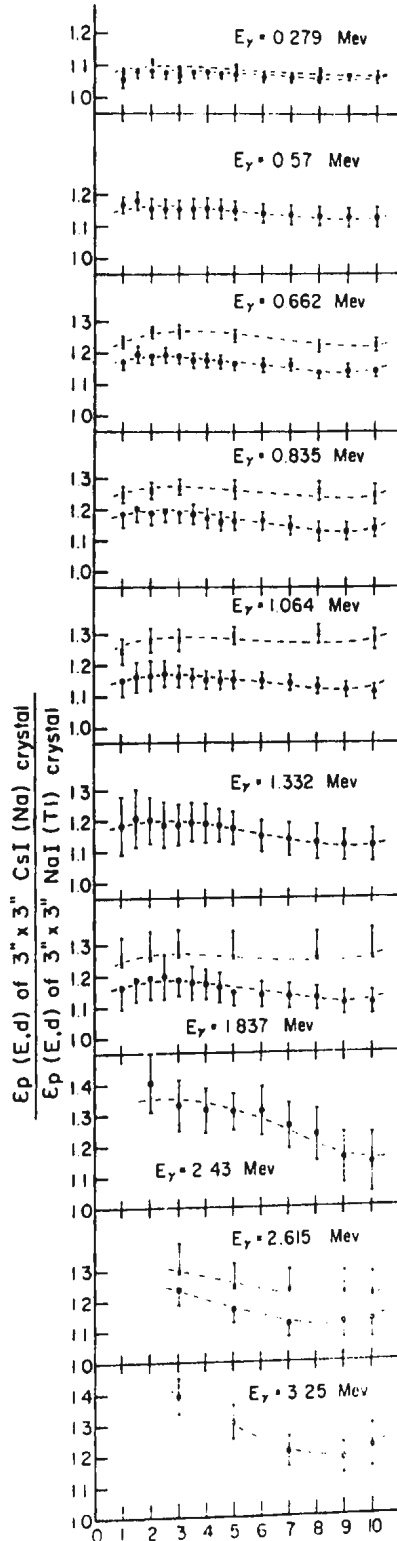


Fig. 4.11

Experimental values of the relative photopeak-efficiency of  $3'' \times 3''$  CsI(Na) crystal w.r.t.  $3'' \times 3''$  NaI(Tl) crystal.

VARIATION OF RELATIVE  
PHOTOPEAK EFFICIENCY WITH DISTANCE

(different graphs for different energies)



[Fig 4.12] Crystal-to-Source Distance (cm)

Experimental values of the relative photopeak-efficiency of 3"x3" CsI (Na) crystal w.r.t. 3"x3" NaI (TI) crystal.

TABLE 4.5

 $\Delta$ , Asymmetry Factor\*

(3" x 3" CsI(Na))

No.	Crystal-to-Source Distance (cm)	Energy (Mev)					
		0.279	0.662	0.835	1.064	1.837	2.615**
1.	1.0	1.017 ± 0.030	1.053 ± 0.029	1.052 ± 0.047	1.083 ± 0.063	1.062 ± 0.102	
2.	2.0	1.018 ± 0.026	1.062 ± 0.027	1.059 ± 0.043	1.098 ± 0.058	1.059 ± 0.098	
3.	3.0	1.013 ± 0.024	1.065 ± 0.027	1.067 ± 0.039	1.100 ± 0.046	1.067 ± 0.088	1.044 ± 0.097
4.	5.0	1.015 ± 0.023	1.074 ± 0.026	1.088 ± 0.040	1.123 ± 0.035	1.100 ± 0.084	1.057 ± 0.081
5.	8.0	1.014 ± 0.022	1.075 ± 0.027	1.112 ± 0.043	1.148 ± 0.038	1.113 ± 0.090	
6.	10.0	1.005 ± 0.022	1.071 ± 0.027	1.094 ± 0.043	1.155 ± 0.040	1.158 ± 0.094	1.073 ± 0.063

$$*\Delta = \frac{\left[ \begin{array}{l} \text{Relative photopeak efficiency by the second method,} \\ \text{i.e. referring to counts under the full peaks} \end{array} \right]}{\left[ \begin{array}{l} \text{Relative photopeak efficiency by the first method,} \\ \text{i.e. referring to counts under the high energy half} \\ \text{of the peaks} \end{array} \right]}$$

\*\*Values for the crystal-to-source distances of 7.0 and 9.0 cm and for gamma-ray energy 2.615 Mev are  $1.094 \pm 0.083$  and  $1.080 \pm 0.087$ , respectively.

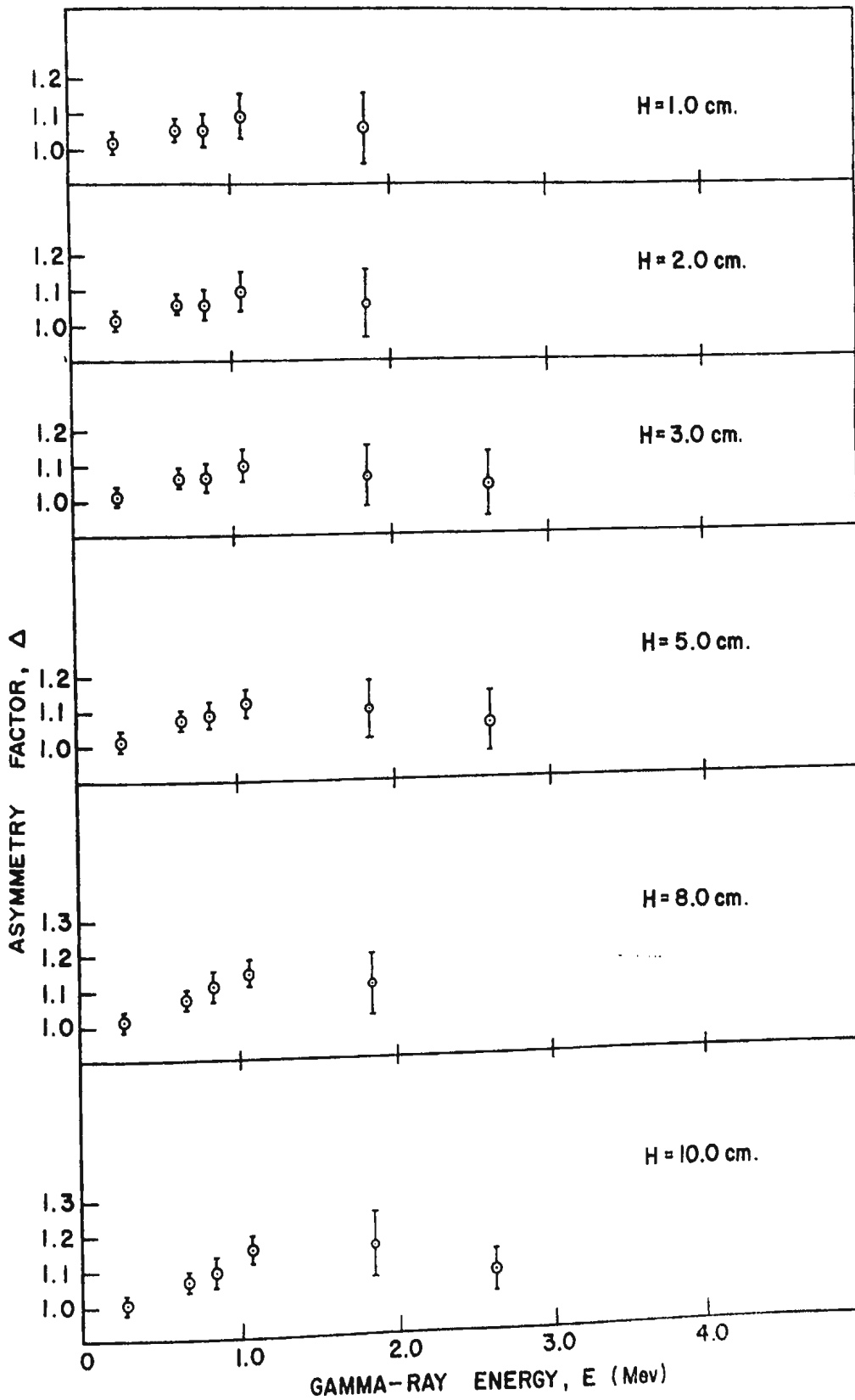


FIG. 4.13 Variation of Asymmetry factor  $\Delta$  with Energy

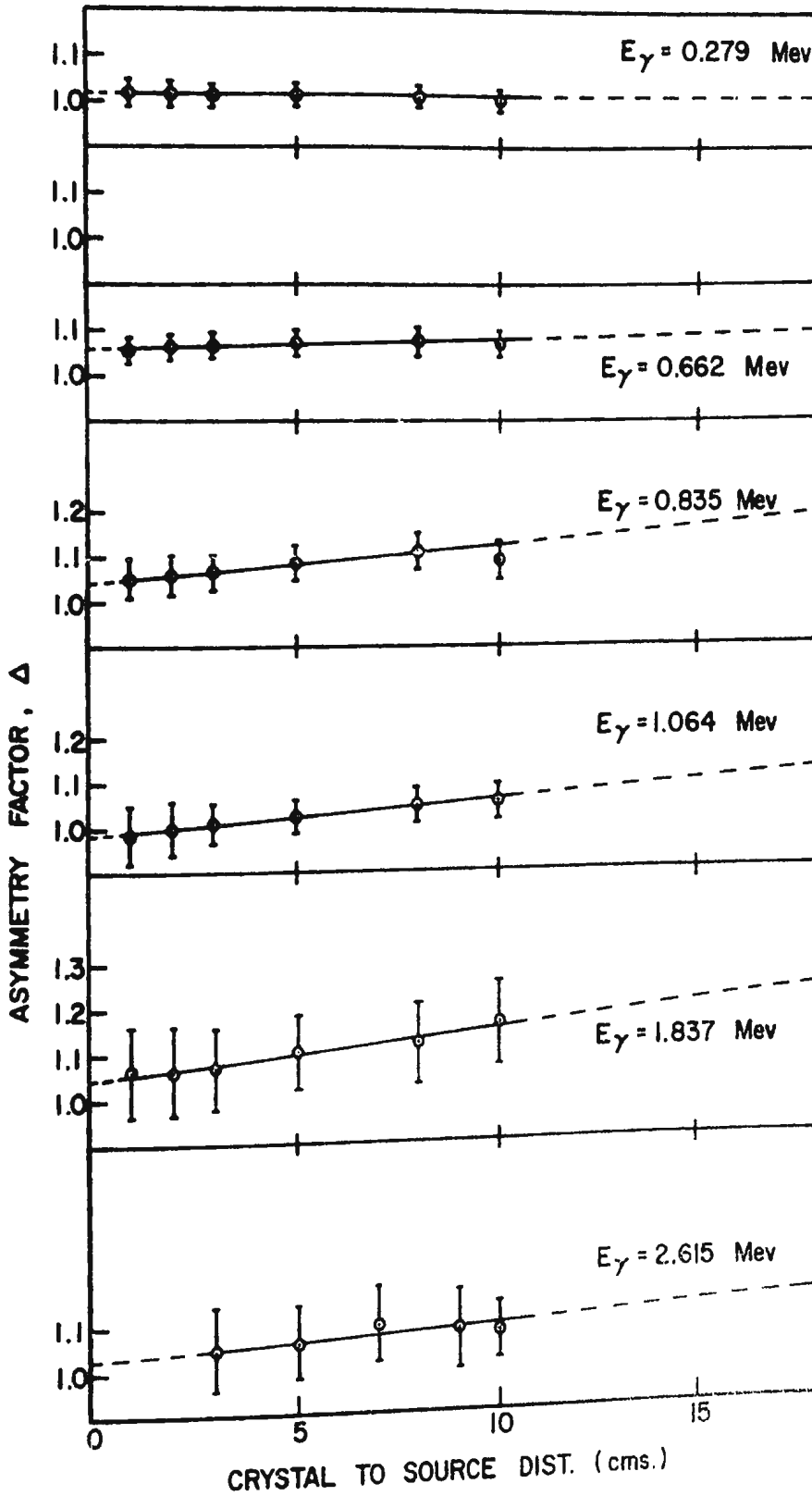


FIG. 4.14 Variation of Asymmetry factor  $\Delta$  with Distance

4.3 The Evaluation of the Photofractions of CsI Crystals:

We have already stated that one of the main objectives of our investigations was to evaluate the photofractions of cesium iodide crystals in terms of the photofractions of a 3" x 3" NaI(Tl) crystal for which we accepted Heath's (1964) experimental values. Table 4.6 shows the symbols used by us to denote the various quantities.

TABLE 4.6

Symbols for the Quantities of Interest

Quantity	3"x3" NaI(Tl)	2"x2" CsI(Tl)	3"x3" CsI(Na)
Absolute detection efficiency for a crystal-to-source distance of 'd' cm	$\epsilon_0$ (dcm)	$\epsilon_2$ (dcm)	$\epsilon_3$ (dcm)
Photopeak efficiency for a crystal-to-source distance of 'd' cm	$\epsilon_{p_0}$ (dcm)	$\epsilon_{p_2}$ (dcm)	$\epsilon_{p_3}$ (dcm) referring to high energy half of the peaks
Photofractions for a crystal-to-source distance of dcm	$f_0$ (dcm)	$f_2$ (dcm)	$f_3$ (dcm) referring to high energy half of the peaks $f'_3$ (dcm) referring to full-peak counts

If for a particular quantity (say,  $\epsilon_{p_0}$ ) we wish to specify the energy of the gamma-rays (say, E Mev) as well, then we denote the quantity by  $\epsilon_{p_0}(d, E)$ . Now,

$$\epsilon_{p_2}(d, E) = f_2(d, E) \epsilon_2(d, E) \quad (4.1)$$

$$\text{and } \epsilon_{p_0}(d', E) = f_0(d', E) \epsilon_0(d', E) \quad (4.2)$$

$$\text{Thus, } f_2(d, E) = \frac{\epsilon_0(d', E) f_0(d', E)}{\epsilon_2(d, E)} \times \frac{\epsilon_{p_2}(d, E)}{\epsilon_{p_0}(d', E)} \quad (4.3)$$

The ratio  $\frac{\epsilon_{p_2}(d, E)}{\epsilon_{p_0}(d', E)}$  was our measured quantity. Heath's (1964) values of  $f_0(d', E)$  are for 3 cm and 10 cm crystal-to-source distances, i.e.

$d'$  is either 3 cm or 10 cm. We could have used our experimental values  $\frac{\epsilon_{p_2}(d, E)}{\epsilon_{p_0}(d', E)}$  for different  $d$  and  $d'$  but the experimental ratios were found to have, in general, better accuracy for  $d = d'$ . Thus, for 3 cm and 10 cm, we have

$$f_2(3 \text{ cm}, E) = \frac{\epsilon_0(3 \text{ cm}, E) f_0(3 \text{ cm}, E)}{\epsilon_2(3 \text{ cm}, E)} \times \frac{\epsilon_{p_2}(3 \text{ cm}, E)}{\epsilon_{p_0}(3 \text{ cm}, E)} \quad (4.4)$$

$$\text{and } f_2(10 \text{ cm}, E) = \frac{\epsilon_0(10 \text{ cm}, E) f_0(10 \text{ cm}, E)}{\epsilon_2(10 \text{ cm}, E)} \times \frac{\epsilon_{p_2}(10 \text{ cm}, E)}{\epsilon_{p_0}(10 \text{ cm}, E)} \quad (4.5)$$

Similarly, we have  $f_3(3 \text{ cm}, E)$  and  $f'_3(3 \text{ cm}, E)$  for 3 cm and  $f_3(10 \text{ cm}, E)$  and  $f'_3(10 \text{ cm}, E)$  for 10 cm.

From extrapolations of our experimental graphs we were also able to evaluate, in some cases, the photofractions for  $d = 0$  cm and  $= 15$  cm. We used the following relations:

$$f_2(0, E) = \frac{\epsilon_o(3 \text{ cm}, E) f_o(3 \text{ cm}, E)}{\epsilon_2(0, E)} \times \frac{\epsilon_{p_2}(0, E)}{\epsilon_{p_o}(3 \text{ cm}, E)} \quad (4.6)$$

$$\text{and } f_2(15 \text{ cm}, E) = \frac{\epsilon_o(10 \text{ cm}, E) f_o(10 \text{ cm}, E)}{\epsilon_2(15 \text{ cm}, E)} \times \frac{\epsilon_{p_o}(15 \text{ cm}, E)}{\epsilon_{p_o}(10 \text{ cm}, E)} \quad (4.7)$$

It should be noted that for calculating  $f_2(0, E)$  and  $f_2(15 \text{ cm}, E)$ , for the reference crystal  $3'' \times 3''$  NaI(Tl) we used Heath's values for the quantities involved at 3 cm and 10 cm, respectively. This kept the errors on the experimental quantities  $\frac{\epsilon_{p_2}}{\epsilon_{p_o}}$  low. Similarly, we evaluated  $f_3(0, E)$ ,  $f'_3(0, E)$  and  $f_3(15 \text{ cm}, E)$ ,  $f'_3(15 \text{ cm}, E)$ . The values of absolute detection efficiencies for the  $3'' \times 3''$  NaI(Tl) crystal were obtained by interpolation from the tabulated values of Heath (1964). As already mentioned earlier in Chapter I, Section 1.3, the scaling relations were used to calculate the absolute detection efficiencies of the CsI crystals for various distances. In addition to the absolute detection efficiency of the NaI(Tl) crystal, we needed the total gamma-ray absorption coefficient curves for the NaI and the CsI. We carried out some calculations using the tables of Grodstein (1957) and of Storm et al (1958) but generally we found it quite satisfactory to use the already published curves which we are reproducing in Figs. 4.15 and 4.16. (One can also use the booklet prepared by the Harshaw Chemical Co. (1965).) Though we could have calculated the

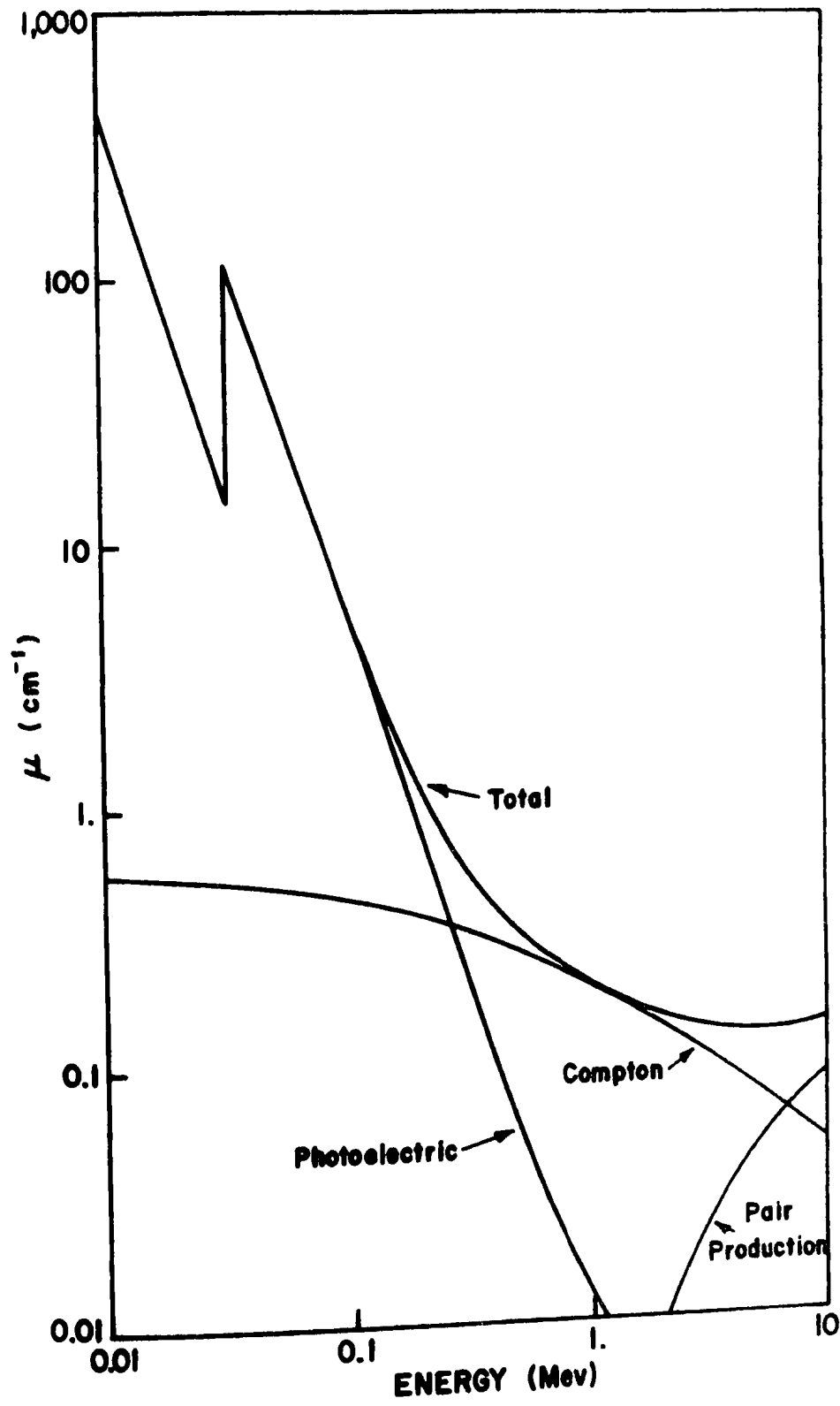


FIG. 4.15 Absorption cross-sections of NaI vs. energy.

Ref:- Heath (1964)

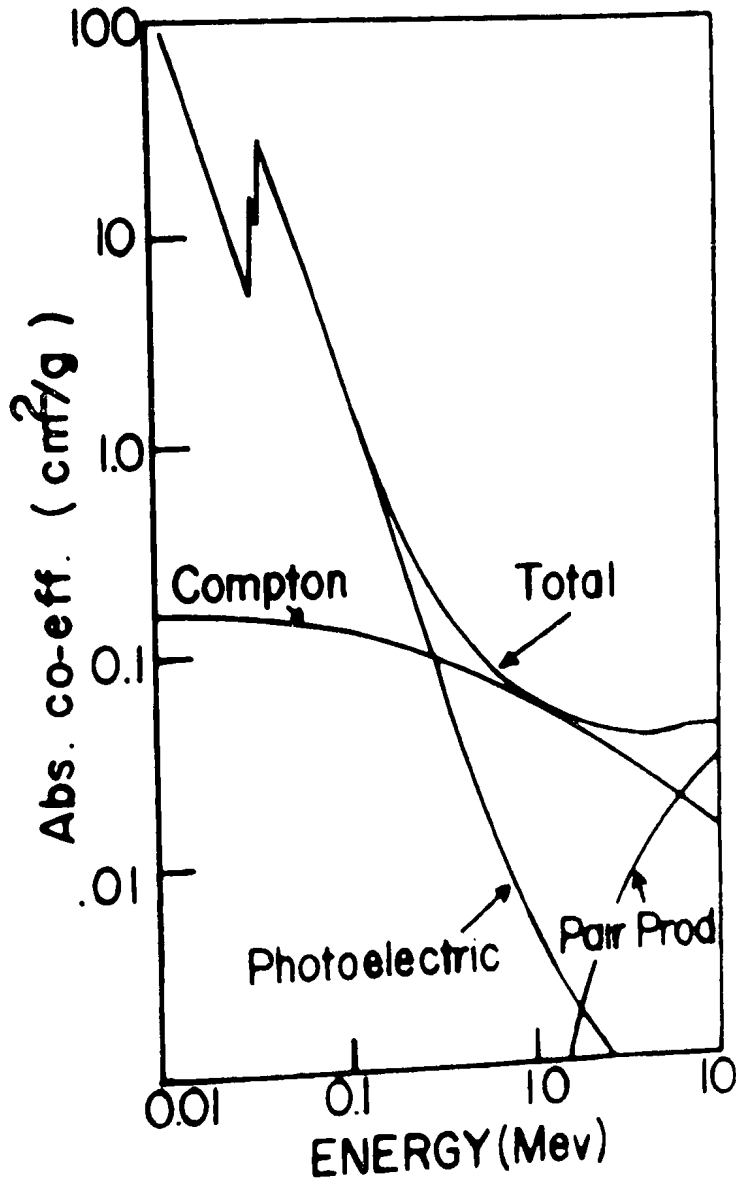


FIG 4.16 Absorption cross-sections of CsI(Na) vs. energy

Ref. Menefee et al (1967)

NOTE:  $\mu(\text{cm}^{-1}) = \text{Absorption coefficient in } \frac{\text{cm}^2}{\text{g}} \times \text{density of CsI in } \frac{\text{g}}{\text{cm}^3}$ .

absolute detection efficiency of the 2" x 2" CsI(Tl) crystal from the values for the 3" x 3" NaI(Tl) crystal, it was desirable to scale the values from those of the 2" x 2" NaI(Tl) crystal so as to have a scaling factor of unity for the crystal-to-source distances. We obtained the values of the absolute detection efficiency for a 2" x 2" NaI(Tl) crystal from Grosjean (1965). Our calculated values of the absolute detection efficiency of the 2" x 2" and the 3" x 3" CsI crystals are being presented in Tables 4.7 and 4.8, respectively.

TABLE 4.7

The Absolute Detection Efficiencies of the 2" x 2" CsI(Tl) Crystal

Gamma-ray Energy, Mev	Crystal-to-source distance			
	0	3 cm	10 cm	15 cm
0.279	0.4722	0.0862	0.01292	0.00614
0.57	0.3620	0.0619	0.01022	0.00503
0.662	0.3400	0.0580	0.00965	0.00478
0.835	0.3115	0.0534	0.00896	0.00443
1.064	0.2815	0.0485	0.00822	0.00407
1.332	0.2600	0.0446	0.00762	0.00378
1.837	0.2385	0.0408	0.00704	0.00350
2.43	0.2208	0.0377	0.00655	0.00326
2.615	0.2180	0.0372	0.00647	0.00322
3.25	0.2110	0.0360	0.00627	0.00313

TABLE 4.8

The Absolute Detection Efficiencies of the 3" x 3" CsI(Na) Crystal

Gamma-ray Energy, Mev	Crystal-to-source distance			
	0	3 cm	10 cm	15 cm
0.279	0.4926	0.1528	0.027975	0.01362
0.57	0.4240	0.1175	0.023225	0.01175
0.662	0.4055	0.1116	0.022275	0.01134
0.835	0.3818	0.1040	0.021000	0.01075
1.064	0.3540	0.0968	0.019515	0.01004
1.332	0.3310	0.0898	0.018475	0.00945
1.837	0.3090	0.0825	0.017300	0.00888
2.43	0.2898	0.0765	0.016225	0.00838
2.615	0.2865	0.0758	0.016070	0.00830
3.25	0.2785	0.0735	0.015650	0.00810

We give the photofractions of the 2" x 2" CsI(Tl) crystal for various energies and crystal-to-source distances in Table 4.9. It must be mentioned here that photofractions for zero and 15.0 cm were obtained on the basis of the extrapolations of the counts versus distance graphs and, because of the uncertainty in the extrapolated values, it became difficult to assign errors to these photofractions. However, we estimate these values to be correct within  $\pm 15\%$ . The plots for the photofractions for various energies and for the crystal-to-source distances of 3.0 cm and 10.0 cm are given in Figs. 4.17 and 4.18.

TABLE 4.9

Photofractions of a 2" x 2" CsI(Tl) Crystal

No.	Gamma-ray Energy, Mev	Photofractions			
		0	3.0 cm	10.0 cm	15.0 cm
1.	0.279	0.7*	0.860 ± 0.016	0.873 ± 0.014	0.7*
2.	0.57		0.594 ± 0.037	0.600 ± 0.030	0.56*
3.	0.662	0.43*	0.539 ± 0.011	0.530 ± 0.010	0.43*
4.	0.835	0.38*	0.455 ± 0.013	0.453 ± 0.012	0.40*
5.	1.064		0.407 ± 0.025	0.402 ± 0.015	0.34*
6.	1.332		0.327 ± 0.022	0.350 ± 0.018	0.27*
7.	1.837		0.258 ± 0.012	0.271 ± 0.010	0.23*
8.	2.43		0.218 ± 0.015	0.226 ± 0.025	0.16*
9.	2.615		0.210 ± 0.031	0.211 ± 0.008	
10.	3.25		0.169 ± 0.023	0.188 ± 0.012	

(NB: Blank spaces refer to the cases where the calculation was not possible either because of summing effect or because of difficulty in extrapolation.)

\*Values obtained on the basis of extrapolation with estimated uncertainty of about 15%.

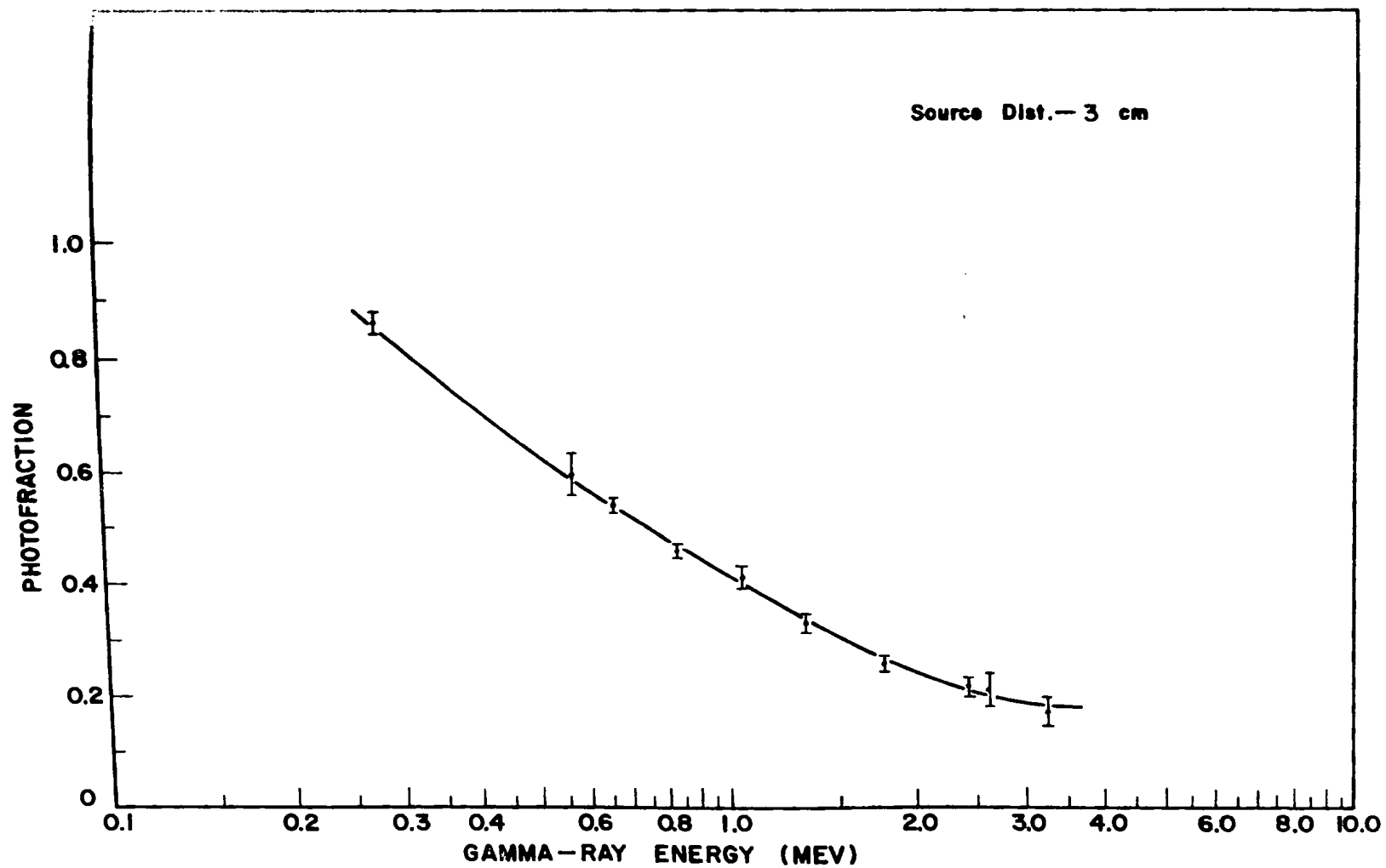


FIG. 4.17 Experimental photofraction of a 2"x2" CsI(Tl) crystal.

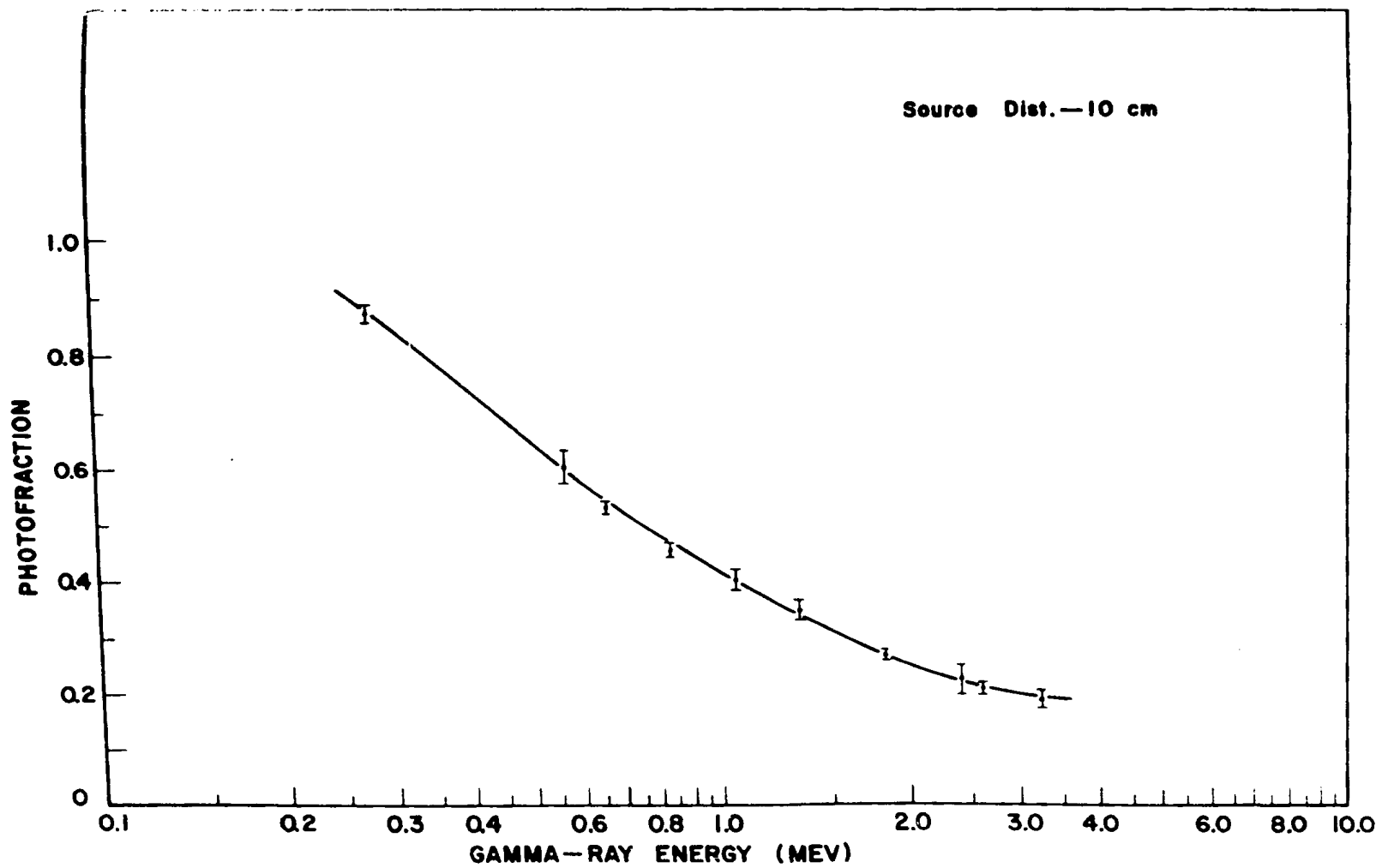


FIG. 4.18 Experimental photofraction of a 2"x2" CsI (Tl) crystal.

For the 3" x 3" CsI(Na) crystal, we have two sets of the photofraction values corresponding to the two methods of analysis. The values of the photofraction when the photopeak was defined as twice the high energy half of the peak for various energies and crystal-to-source distances are given in Table 4.10. Table 4.11 gives the photofraction values when the photopeak was considered to be the full peak. As expected, the values of the photofraction for the latter case are larger. Figs. 4.19 and 4.20 show graphically the photofractions for various energies and for the crystal-to-source distances of 3.0 cm and 10.0 cm. The graphs are self-explanatory and represent results of both methods of analysis. Again, the extrapolated values for 0 and 15 cm may have as much as  $\pm 15\%$  uncertainty. The extrapolated values corresponding to the second method of analysis involved extrapolations for the appropriate values of the asymmetry factor also.

TABLE 4.10

Photofractions of a 3" x 3" CsI(Na) Crystal

(Photopeak Considered as Double the High Energy Half of the Peak)

No.	Gamma-ray Energy, Mev	Photofractions			
		0	3.0 cm	10.0 cm	15.0 cm
1.	0.279	0.7*	0.828 ± 0.016	0.851 ± 0.014	0.8*
2.	0.57		0.595 ± 0.015	0.613 ± 0.018	0.57*
3.	0.662	0.47*	0.565 ± 0.011	0.555 ± 0.010	0.5*
4.	0.835	0.4*	0.490 ± 0.014	0.485 ± 0.013	0.43*
5.	1.064		0.401 ± 0.012	0.406 ± 0.010	0.38*
6.	1.332		0.354 ± 0.020	0.357 ± 0.018	0.34*
7.	1.837		0.285 ± 0.012	0.265 ± 0.010	0.23*
8.	2.43		0.283 ± 0.018	0.241 ± 0.022	0.15*
9.	2.615		0.253 ± 0.010	0.231 ± 0.011	
10.	3.25		0.243 ± 0.011	0.213 ± 0.013	

(NB: Blank spaces refer to the cases where the calculation was not possible either because of summing effect or because of difficulty in extrapolation.)

\*Extrapolated values with estimated uncertainties of about 15%.

TABLE 4.11

Photofractions of the 3" x 3" CsI(Na) Crystal

(Photopeak Considered as Full-Peak)

No.	Gamma-ray Energy, Mev	Photofractions			
		0	3.0 cm	10.0 cm	15.0 cm
1.	0.279	0.7*	0.839 ± 0.012	0.855 ± 0.013	0.8*
2.	0.662	0.5*	0.601 ± 0.009	0.594 ± 0.011	0.57*
3.	0.835	0.4*	0.523 ± 0.012	0.531 ± 0.015	0.5*
4.	1.064		0.441 ± 0.012	0.467 ± 0.012	0.42*
5.	1.837		0.304 ± 0.021	0.307 ± 0.022	0.30*
6.	2.615		0.263 ± 0.022	0.247 ± 0.015	0.25*

(NB: Blank spaces refer to the cases where it was not possible to calculate because of the summing effect.)

\*Extrapolated values with estimated uncertainties of about 15%.

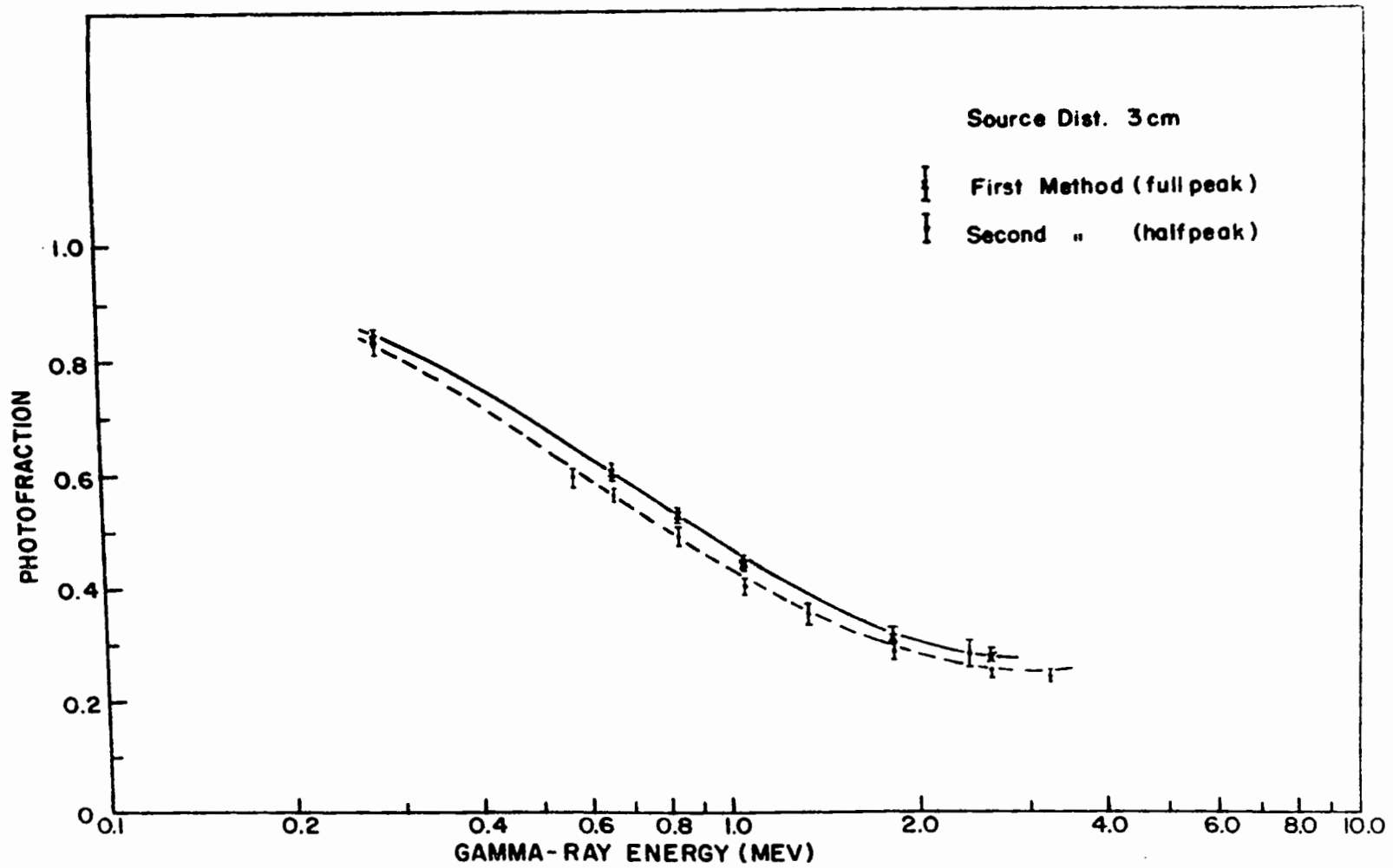


FIG. 4.19 Experimental photofraction of a 3"x3" CsI(Na) crystal

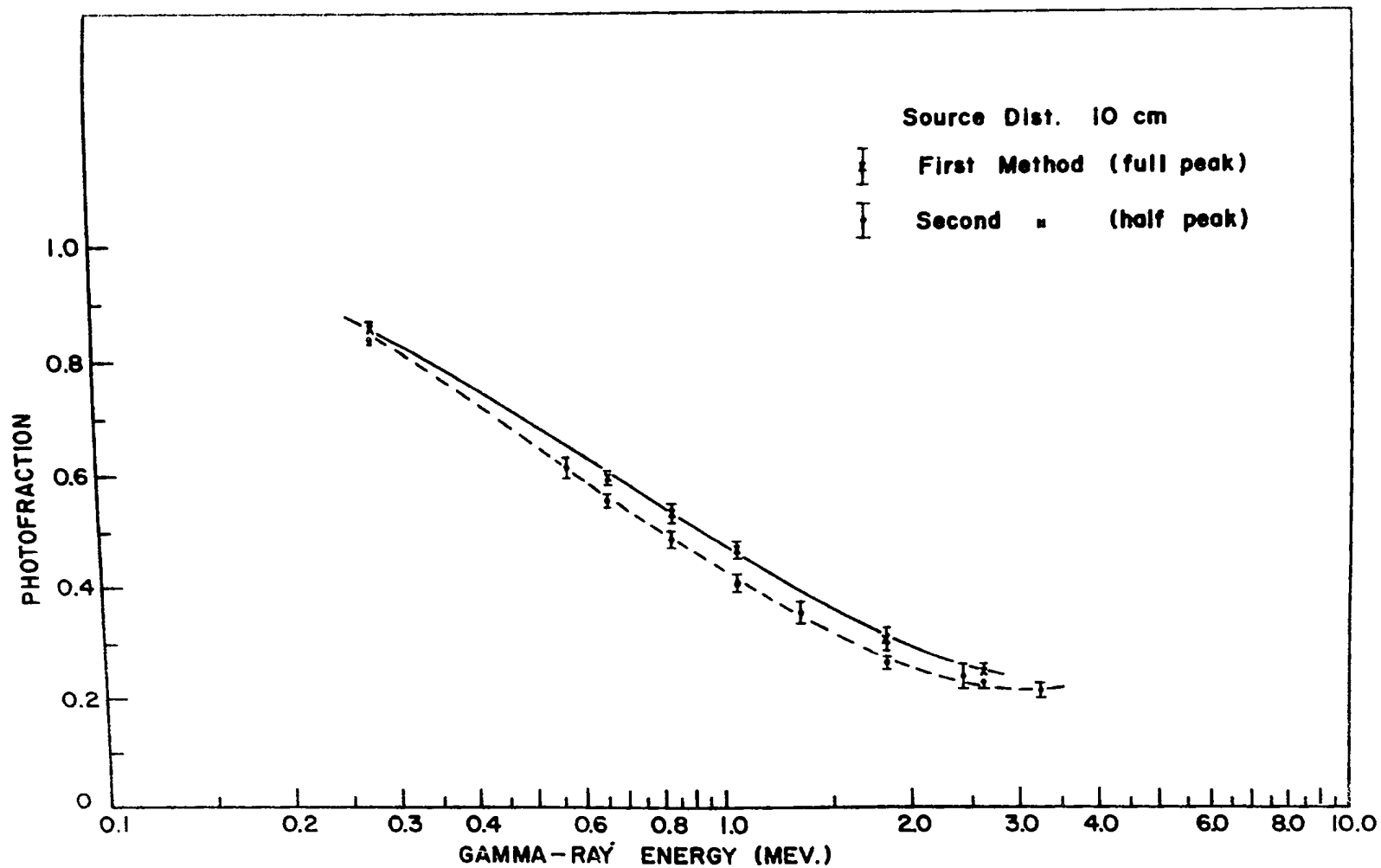


FIG. 4.20 Experimental photofraction of a 3"x3" CsI (Na) crystal.

CHAPTER V

DISCUSSION OF THE RESULTS

5.1 Comparison of Our Experimental Photofraction Values with the Theoretical Values of Miller and Snow (1961):

Fig. 5.1 shows a comparison of the photofractions of a 2" x 2" CsI(Tl) crystal evaluated by us for a crystal-to-source distance of 10 cm with the theoretical values computed by Miller and Snow (1961). Fig. 5.2 shows a similar comparison for our 3" x 3" CsI(Na) crystal with the theoretical photofractions of Miller and Snow but, in this case, we quote two values for some energies for which we were able to analyze the spectra by two methods (see Section 4.1 (b)). Quite clearly, the theoretical values are higher than our experimental values but the discrepancy is more pronounced for the 3" x 3" CsI(Na) crystal. For the 2" x 2" CsI(Tl) crystal, the theoretical and the experimental values are almost the same for 0.279 Mev but with increasing energy the experimental values go on decreasing in comparison to the theoretical values but near the high energy end of our graph it is difficult to establish any particular trend. For 0.661 Mev, 1.332 Mev and 2.615 Mev, the experimental values are lower by  $\sim 3\%$ ,  $\sim 6\%$  and  $\sim 11\%$ , respectively. For the 3" x 3" CsI(Na) crystal, the experimental values are always lower than the theoretical values and, even for the second method of analysis of the spectra, the photofractions are lower by  $\sim 4\%$ ,  $\sim 9\%$  and  $\sim 25\%$  for 0.279 Mev, 0.661 Mev and 2.615 Mev, respectively.

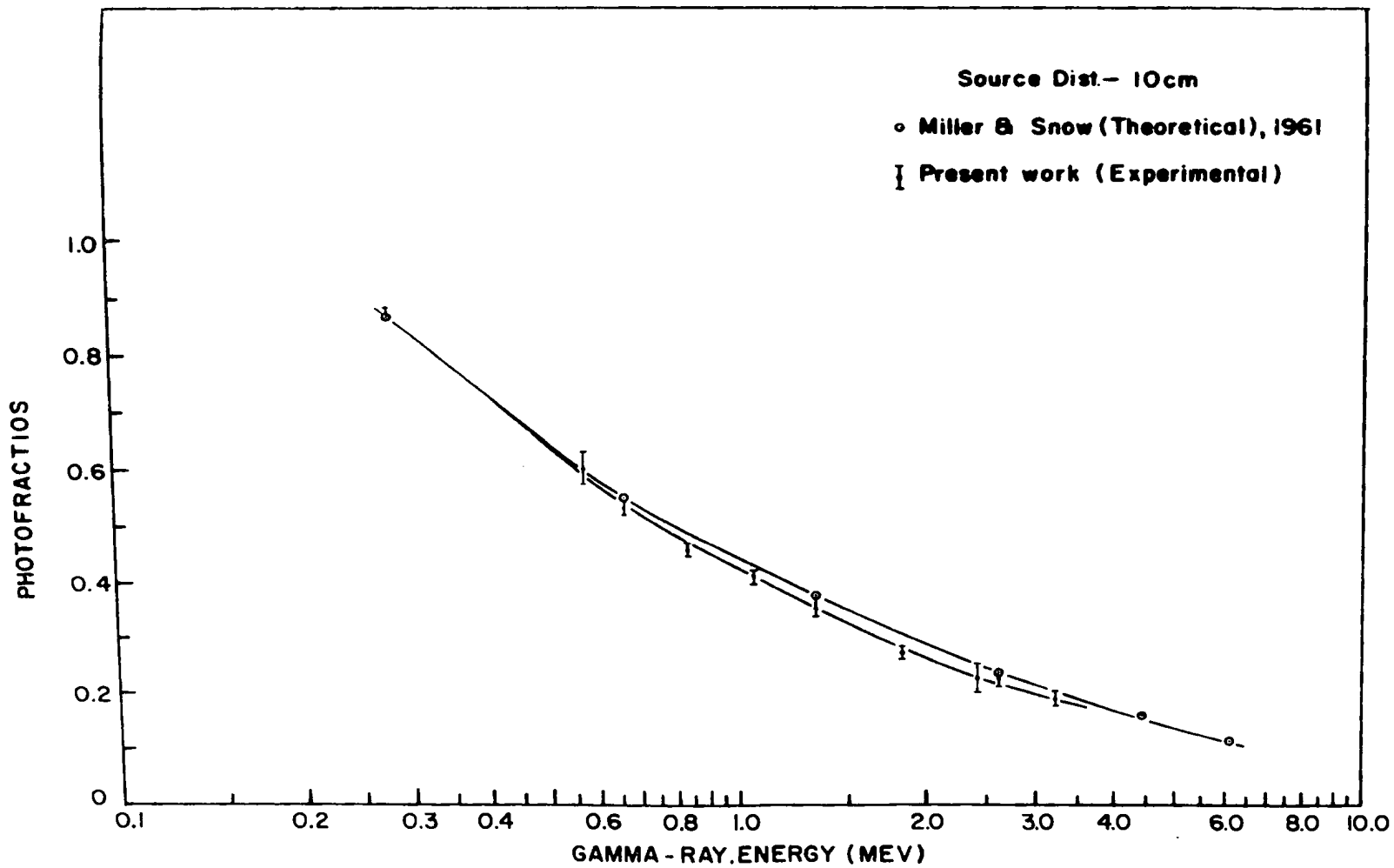


FIG. 5.1 Experimental and theoretical photofractions of 2"x2" CsI(Tl) crystal

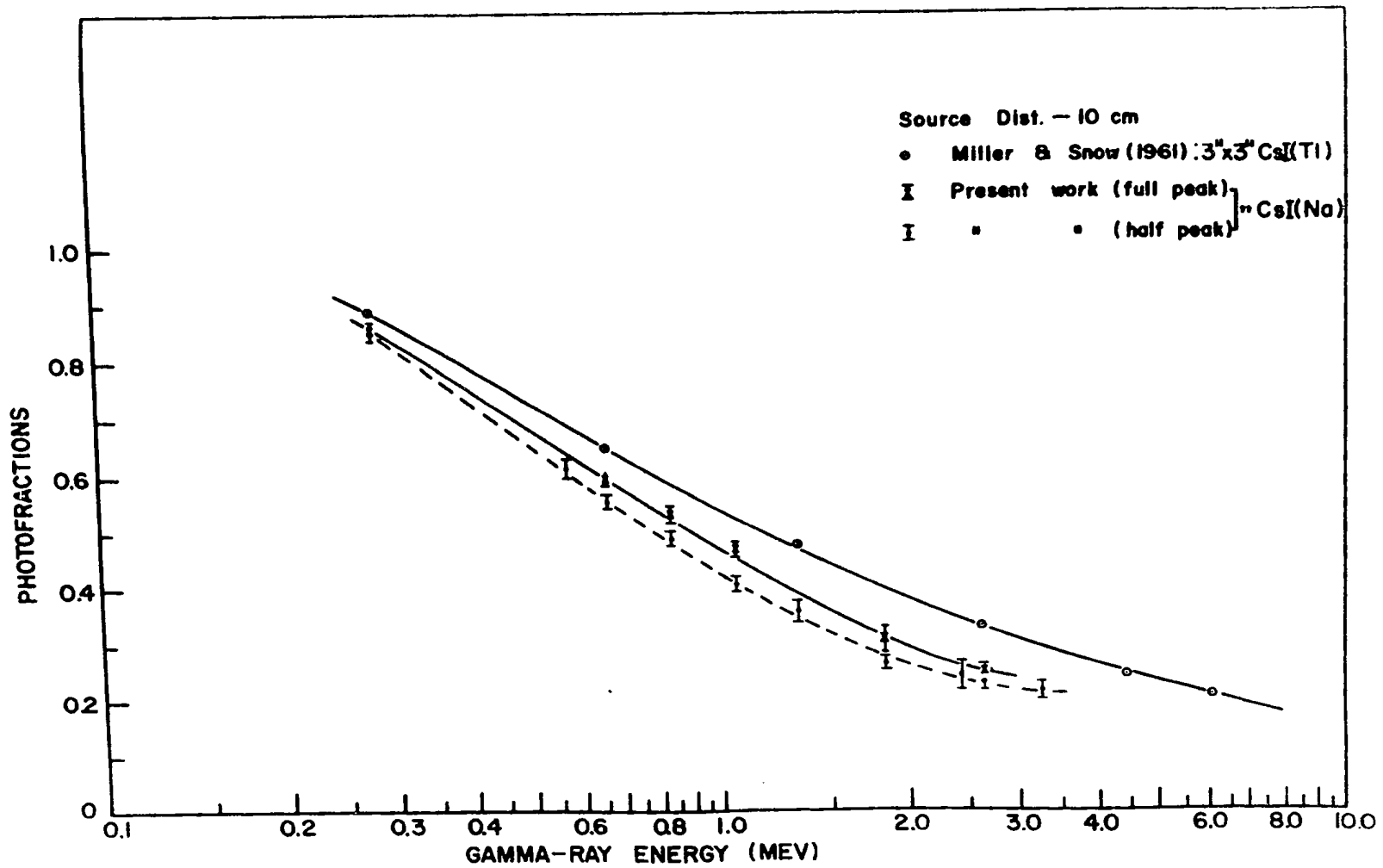


FIG. 5.2 Experimental and theoretical photofractions of 3"x3" CsI crystals.

In Fig. 5.3, we show a comparison of the theoretical values of the ratio  $\frac{\text{Photofraction of the } 3'' \times 3'' \text{ CsI crystal}}{\text{Photofraction of the } 2'' \times 2'' \text{ CsI crystal}}$  with the values obtained from our results. The values appear in Table 5.1. We give two values of the ratio for some energies based on two results for the  $3'' \times 3''$  CsI(Na) crystal. We find that the values of the ratio derived from our results are lower than the theoretical values of Miller and Snow and that this discrepancy increases with energy.

#### 5.2 The Asymmetry in the $3'' \times 3''$ CsI(Na) Crystal Spectra:

If we accept the values of the photofractions of the  $3'' \times 3''$  CsI(Na) crystal arrived at by the first method of analysis (i.e. referring to the counts in the high energy half of the peaks), then the photofractions for the  $3'' \times 3''$  and the  $2'' \times 2''$  CsI crystals are very nearly the same which is rather unlikely to be the case. The second method of analysis, referring to the counts under the full peaks, gives higher photofractions for the  $3'' \times 3''$  CsI(Na) crystal (though still the ratios  $\frac{f \text{ for } 3'' \times 3'' \text{ CsI(Na)}}{f \text{ for } 2'' \times 2'' \text{ CsI(Tl)}}$  are smaller than the ratios obtained on the basis of computed values of photofractions by Miller and Snow) and it would be more logical to discuss the results for the  $3'' \times 3''$  CsI(Na) crystal based on the second method of analysis only. However, because of the practical convenience implied in the first method of analysis, importance should be attached to the results based on that method. It is obviously very important that care should be taken in referring to the values of the photofractions for any crystal which gives photopeaks with significant asymmetry. More investigations need to be carried out for large size crystals from this point of view.

TABLE 5.1

Photofraction of 3" x 3" CsI(Na) Crystal

Photofraction of 2" x 2" CsI(Tl) Crystal

Gamma-ray Energy (Mev)	Present Work		Miller and Snow (1961)
	First Method	Second Method	
0.279	0.975 ± 0.022	0.979 ± 0.022	1.029
0.57	1.022 ± 0.059		
0.662	1.047 ± 0.027	1.121 ± 0.030	1.189
0.835	1.071 ± 0.040	1.172 ± 0.045	
1.064	1.010 ± 0.045	1.162 ± 0.053	
1.332	1.020 ± 0.073		1.279
1.837	0.978 ± 0.052	1.133 ± 0.091	
2.43	1.066 ± 0.153		
2.615	1.095 ± 0.067	1.171 ± 0.084	1.397
3.25	1.133 ± 0.100		
4.45			1.535
6.13			1.800

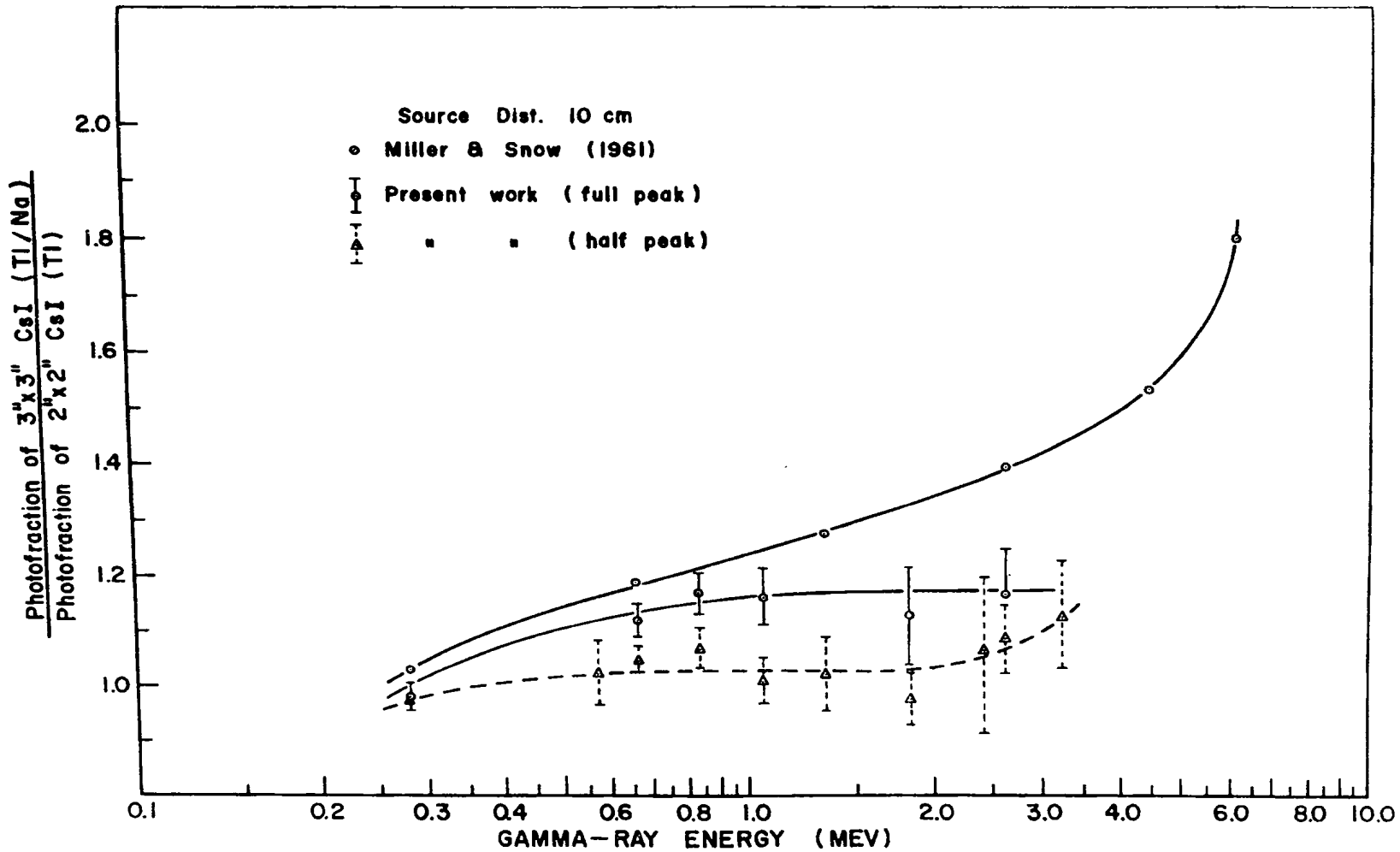


FIG. 5.3 Comparison of experimental and theoretical photofraction ratios of CsI crystals.

The extent of the observed asymmetry in the 3" x 3" CsI(Na) crystal has already been given in the two figures in Chapter IV, Fig. 4.13 giving the variation of the asymmetry factor  $\Delta$  with energy and Fig. 4.14 giving the variation with the crystal-to-source distance. (We may add here that the existence of this asymmetry was checked by us several times using different photomultipliers.) It is seen that  $\Delta$  for the lowest energy studied by us is almost unity and then it increases with energy, perhaps reaching a value of 1.1 to 1.16 (because of large errors it is difficult to establish a trend with accuracy). Furthermore,  $\Delta$  appears to be larger for larger crystal-to-source distances, almost showing a linear dependence (again large errors should not be ignored). The errors for high energy points are generally higher because of the earlier mentioned difficulty in connection with the low energy cut-off position (an uncertainty of one or two channels introduces significant error).

We cannot say much about the reasons for the existence of this asymmetry in the case of the 3" x 3" CsI(Na) crystal. It should be noted, however, that the counts under the photopeak are not only due to the one-shot photo-electric events but a significant contribution (especially for large crystals) comes from the total energy transfer through a series of interactions all taking place within a short time to give only one eventual count. Perhaps the counts due to the simple photo-electric events and due to these other events combine in such a way so as to give an overall asymmetric shape in large CsI crystals.

If our first method of analysis had given reasonable values for the photofractions of the 3" x 3" CsI(Na) crystal, there could have been some suspicion about the excess low energy counts being "spurious" but looking at the ratio of the photofractions for the 3" x 3" CsI(Na) and the 2" x 2" CsI(Tl) crystals the first method of analysis gives the unlikely values close to unity; hence the second method of analysis includes "genuine" excess counts. In this connection, for the sake of comparison, we are giving in Fig. 5.4 the ratio of the photofractions for the 3" x 3" NaI(Tl) and the 2" x 2" NaI(Tl) crystals. The theoretical values are taken from Miller and Snow (1961) and the experimental from Leutz et al (1966) and Mishra and Sadasivan (1969). On the basis of this, one would expect to obtain higher photofractions for the 3" x 3" CsI(Na) crystal compared with those of the 2" x 2" CsI(Tl) crystal.

In our view, poor energy resolution of the 3" x 3" CsI(Na) crystal could not have been responsible for the observed asymmetry because our unsealed 2" x 2" CsI(Tl) crystal with still poorer resolution gave symmetric peaks. We also checked the pulse height versus energy response of our 3" x 3" CsI(Na) crystal and found it to be linear in the energy range of interest. Thus, the possibility of a non-linear response causing this asymmetry is also ruled out.

### 5.3 Dependence of Photofractions on the Crystal-to-Source Distance:

In Table 4.9, we have presented the experimental values of the photofraction of our 2" x 2" CsI(Tl) crystal for crystal-to-source

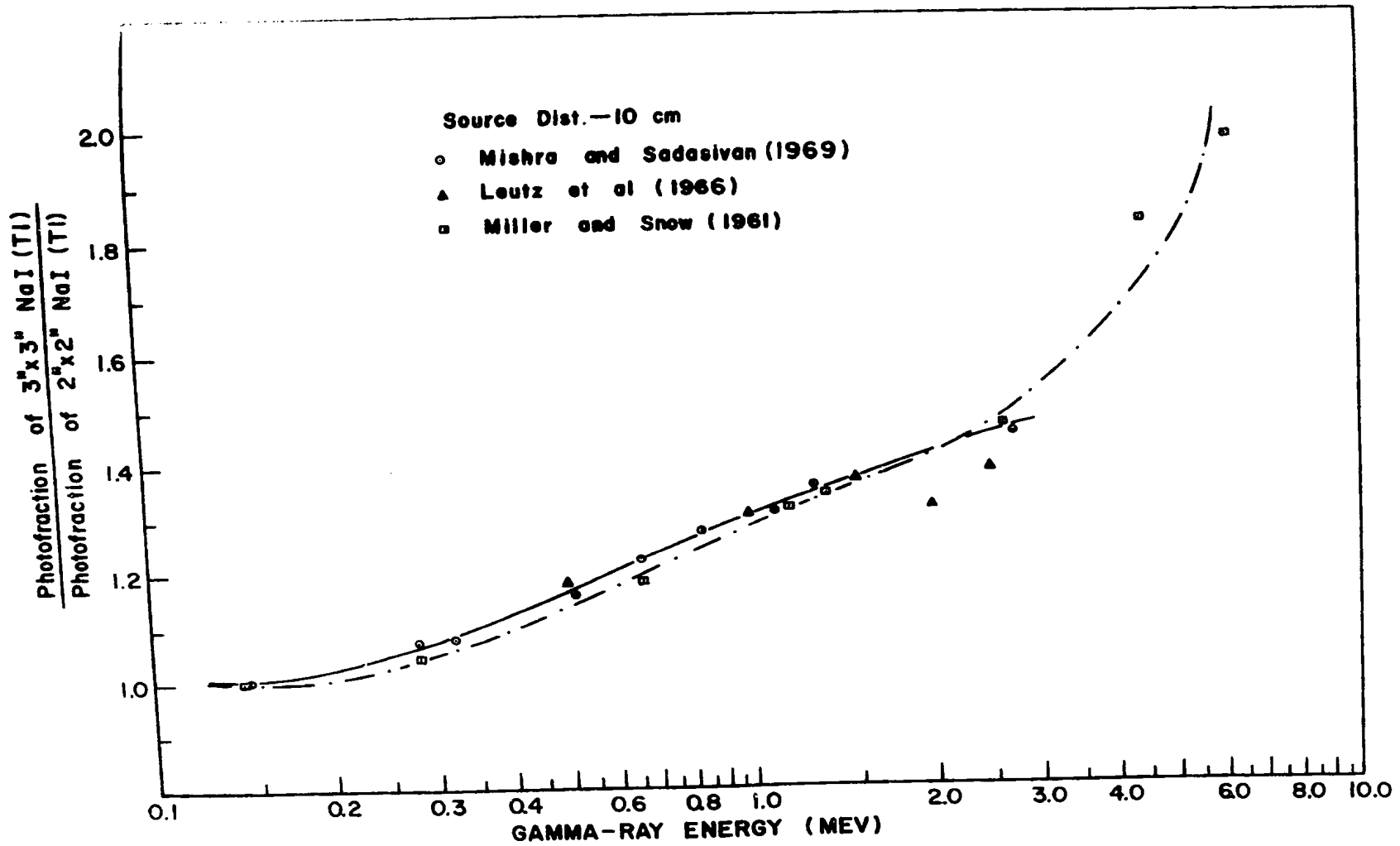


FIG. 5.4 Comparison of experimental and theoretical photofraction ratios of NaI (TI) crystals.

distances of 3 and 10 cm. The same Table also gives values for 0 and 15 cm which were obtained by extrapolation. For energy up to 1.064 Mev, the photofractions at 3 and 10 cm are not at all very different but, for higher energies, those at 3 cm may be as much as 5% lower than those at 10 cm. In general, we may say that the photofractions appear to be insensitive to crystal-to-source distance, at least in this region. The extrapolated values at 0 and 15 cm appear to be lower even after taking the maximum limit of the uncertainty (15%) in these values.

Tables 4.10 and 4.11 show the photofractions of the 3" x 3" CsI(Na) crystal for the two methods of analysis. Once again, the photofractions for low energy (up to  $\sim 1.064$  Mev) for the crystal-to-source distances of 3 and 10 cm do not appear very different. For higher energies, however, we see a difference of  $\sim 10\%$  for the first method of analysis and  $\sim 6\%$  for the second method of analysis. For 2.43 Mev in the first method of analysis, the values of the photofraction at 3 and 10 cm may differ by  $\sim 15\%$ . The photofractions at 0 and 15 cm obtained by extrapolation appear to be low. However, those at 15 cm lie within the upper limit of 15% error in these values but those at zero may not be included in this limit.

On the basis of our experimental photofractions obtained for the CsI crystals, we may say that, for low energies, the values of photofractions at 3 and 10 cm are not very different but, for higher energies, a difference of as much as 10% may be present. We may point out here that Lazar (1958) reported a difference of  $\sim 10$  to 20% in the photofractions at 3 and 9.3 cm of a 3" x 3" NaI(Tl) crystal. For

crystal-to-source distances of 3 and 10 cm for a 3" x 3" NaI(Tl) crystal, Heath (1964) obtained photofraction values differing by  $\sim 2\%$  in the energy range 0.323 Mev to 1.78 Mev.

5.4 Photofractions of CsI Crystals using the Theoretical Values of Miller and Snow for the 3" x 3" NaI(Tl) Crystal:

Our decision to use the experimental values of photofraction of a 3" x 3" NaI(Tl) crystal as given by Heath (1964) is quite simple. As far as we know, Heath's values have been obtained on the basis of very careful experiments and are considered to be quite reliable. Miller and Snow (1961) have also given the theoretical values of photofraction of a 3" x 3" NaI(Tl) crystal and for a crystal-to-source distance of 10 cm. As already discussed in Chapter II, these values have been found to be higher than the experimental values of Heath (1964) and other workers (Zerby and Moran (1961), Leutz et al (1966), Snyder (1967) and Mishra and Sadasivan (1969)). We now give the values of photofraction obtained from our results by using the theoretical values of photofraction of a 3" x 3" NaI(Tl) crystal as given by Miller and Snow instead of those given by Heath. The values for the 2" x 2" CsI(Tl) crystal are given in Table 5.2 and for the 3" x 3" CsI(Na) crystal in Table 5.3. The two values for the 3" x 3" CsI(Na) crystal correspond to the two methods of analysis. The results are shown graphically in Figs. 5.5 and 5.6 for the two crystals. We find our experimental photofraction values for the 2" x 2" CsI(Tl) crystal in excellent agreement with the values of Miller and Snow. The situation

TABLE 5.2

The Photofractions of a 2" x 2" CsI(Tl) Crystal at 10 cm

(Using the theoretical photofractions of a 3" x 3" NaI(Tl)

as given by Miller and Snow (1961))

<u>Gamma-ray Energy (Mev)</u>	<u>Photofractions</u>
0.279	0.884 ± 0.014
0.57	0.625 ± 0.031
0.662	0.556 ± 0.011
0.835	0.474 ± 0.013
1.064	0.429 ± 0.016
1.332	0.384 ± 0.019
1.837	0.315 ± 0.011
2.43	0.262 ± 0.029
2.615	0.238 ± 0.009
3.25	0.220 ± 0.014

TABLE 5.3

The Photofractions of a 3" x 3" CsI(Na) Crystal at 10 cm

(Using the theoretical photofractions of a 3" x 3" NaI(Tl)

as given by Miller and Snow (1961))

Gamma-ray Energy (Mev)	1st Method of Analysis	2nd Method of Analysis
0.279	0.862 ± 0.014	0.866 ± 0.013
0.57	0.638 ± 0.019	
0.662	0.582 ± 0.011	0.623 ± 0.011
0.835	0.508 ± 0.013	0.556 ± 0.016
1.064	0.433 ± 0.010	0.500 ± 0.013
1.332	0.392 ± 0.020	
1.837	0.308 ± 0.011	0.357 ± 0.026
2.43	0.279 ± 0.025	
2.615	0.258 ± 0.013	0.276 ± 0.017
3.25	0.249 ± 0.015	

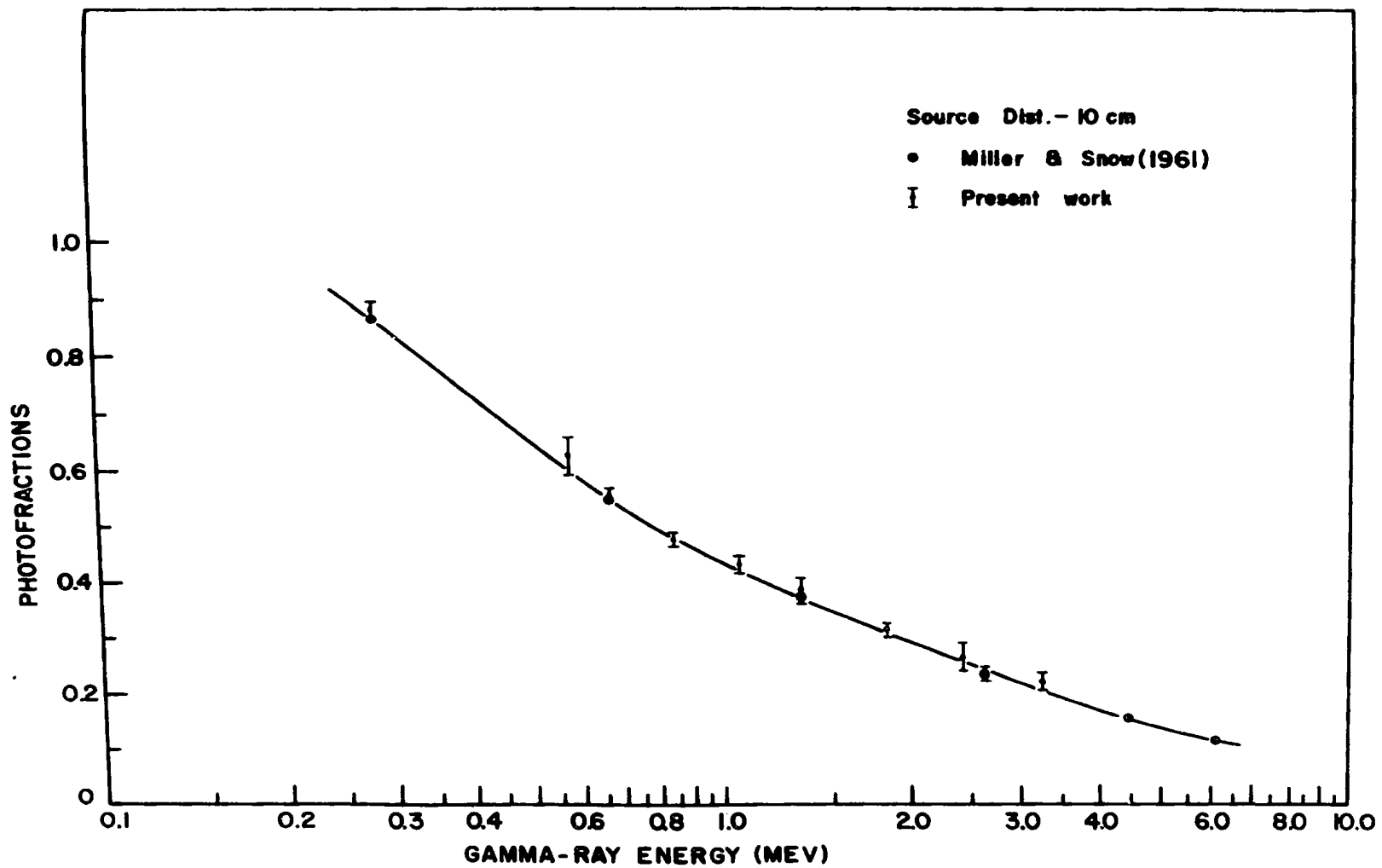


FIG. 5.5 Photofractions of 2"x2" CsI(Tl) crystal, using values of Miller and Snow(1961)

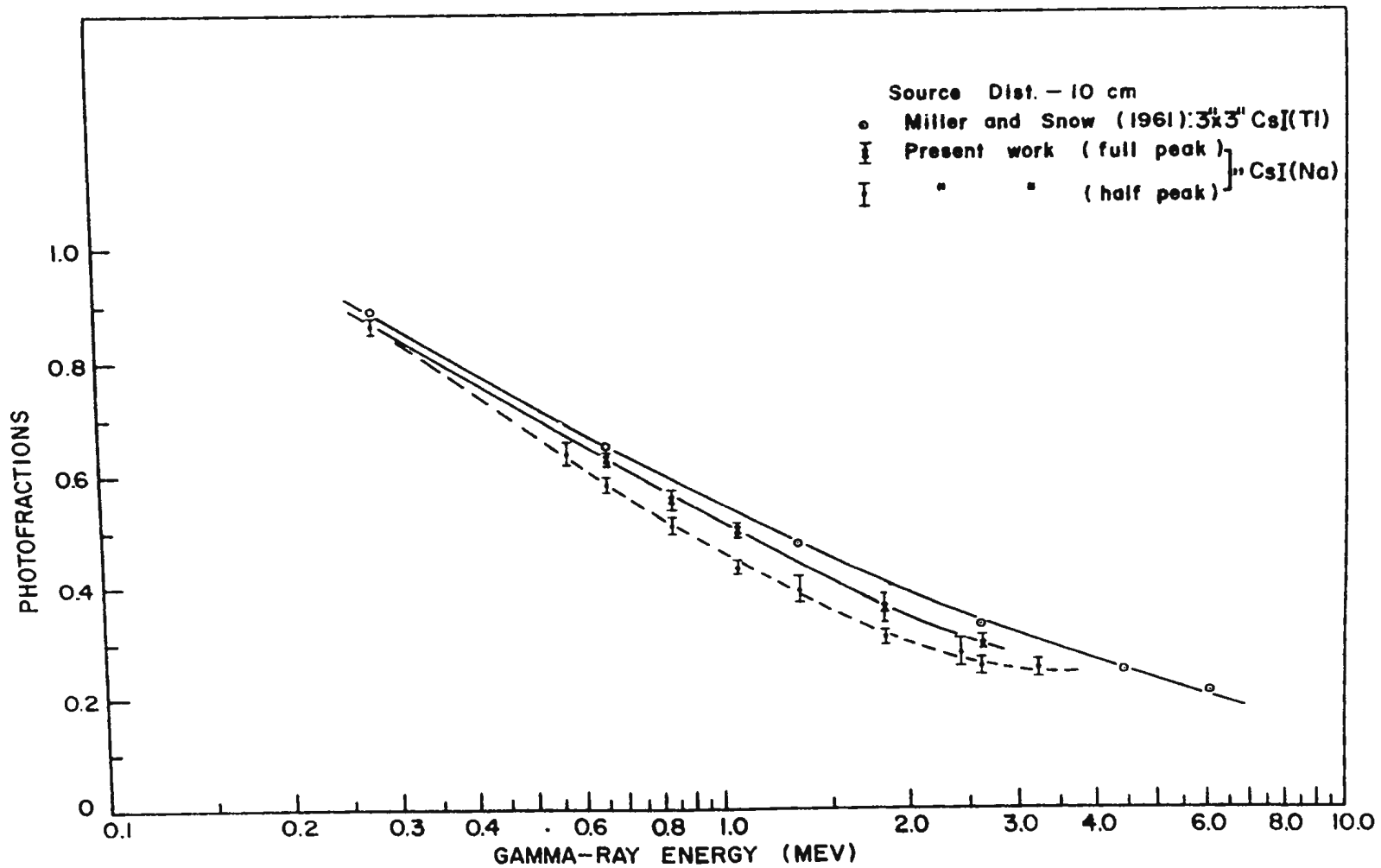


FIG. 5.6 Photofractions of  $3'' \times 3''$  CsI crystals, using values of Miller and Snow (1961).

with the 3" x 3" CsI(Na) crystal improves in general but still the photofractions are much smaller. It may be remarked that an improvement in the values of the photofraction is expected, as the theoretical photofraction values of Miller and Snow are higher than the experimental values of Heath.

5.5 The Effect of the Possible Error in the Crystal-to-Source Distance:

The crystal-to-can-top distance is known to pose difficulties in getting the accurate value of the crystal-to-source distance. We have already discussed in detail our approach to this problem (see Section 3.2). We believe that, if some systematic errors have crept in, they have compensated each other for the different crystals to yield reliable values of the relative photopeak efficiencies as long as the ratios were evaluated for the same crystal-to-source distance. It may be noted that, except for the extrapolated values of the photofractions at 0 and 15 cm, our results are based on the relative photopeak efficiencies measured for the same crystal-to-source distances. In view of the fact that we have treated all crystals according to identical criteria, we do not expect much change in these relative photopeak efficiencies if the crystal-to-can-top distances have to be altered slightly, as long as all changes are in the same direction in all the crystals. We proceed to examine this point in some detail.

We compare the relative photopeak efficiencies of the same crystal but for different distances with some sort of expected values.

We choose  $\frac{\epsilon_p(3 \text{ cm})}{\epsilon_p(10 \text{ cm})}$ ,  $\frac{\epsilon_p(3 \text{ cm})}{\epsilon_p(4 \text{ cm})}$  and  $\frac{\epsilon_p(8 \text{ cm})}{\epsilon_p(10 \text{ cm})}$ . As far as  $\frac{\epsilon_p(3 \text{ cm})}{\epsilon_p(10 \text{ cm})}$

for the 3" x 3" NaI(Tl) crystal is concerned, the comparison can be made with the values obtained from Heath's results (1964). No such values are available for direct comparisons in the case of other ratios for NaI(Tl) or CsI crystals. However, noting that the photofractions are not very sensitive to distances, we can compare these ratios (obtained from our results) with the corresponding ratios of the absolute detection efficiencies. We are restricting these comparisons to the mono-energetic sources only in order to avoid the "distance dependent" summing effects.

Table 5.4 compares the values of  $\frac{\epsilon_p(3 \text{ cm})}{\epsilon_p(10 \text{ cm})}$  for a 3" x 3" NaI(Tl) crystal obtained from our results with those obtained from Heath's results. The Table also gives the ratio of the absolute detection efficiencies  $\frac{\epsilon(3 \text{ cm})}{\epsilon(10 \text{ cm})}$ .

TABLE 5.4

Comparison of Photopeak-Efficiency Ratios  
for a 3" x 3" NaI(Tl) Crystal

Gamma-ray Energy (Mev)	$\epsilon_p(3 \text{ cm})/\epsilon_p(10 \text{ cm})$		$\frac{\epsilon(3 \text{ cm})}{\epsilon(10 \text{ cm})}$
	Present Work	Heath	
0.279	5.187	5.327	5.327
0.662	4.758	4.901	4.938
0.835	4.664	4.791	4.894

Table 5.5 compares our values for  $\frac{\epsilon_p(3 \text{ cm})}{\epsilon_p(4 \text{ cm})}$  and  $\frac{\epsilon_p(8 \text{ cm})}{\epsilon_p(10 \text{ cm})}$  for a 3" x 3" NaI(Tl) crystal with the corresponding values of  $\frac{\epsilon(3 \text{ cm})}{\epsilon(4 \text{ cm})}$  and  $\frac{\epsilon(8 \text{ cm})}{\epsilon(10 \text{ cm})}$ . Similar comparisons are given for the 2" x 2" CsI(Tl) and the 3" x 3" CsI(Na) crystals in Tables 5.6 and 5.7, respectively. (For the 3" x 3" CsI(Na), our values refer to the first method of analysis, but the situation is not materially altered if values refer to the second method of analysis.)

TABLE 5.5

Comparison of Photopeak-Efficiency Ratios with Absolute Detection  
Efficiency Ratios for a 3" x 3" NaI(Tl) Crystal

Gamma-ray Energy (Mev)	$\frac{\epsilon_p(3 \text{ cm})}{\epsilon_p(4 \text{ cm})}$	$\frac{\epsilon(3 \text{ cm})}{\epsilon(4 \text{ cm})}$	$\frac{\epsilon_p(8 \text{ cm})}{\epsilon_p(10 \text{ cm})}$	$\frac{\epsilon(8 \text{ cm})}{\epsilon(10 \text{ cm})}$
	Present Work		Present Work	
0.279	1.380	1.395	1.442	1.425
0.662	1.354	1.382	1.409	1.419
0.835	1.356	1.378	1.397	1.411

TABLE 5.6

Comparison of Photopeak-Efficiency Ratios with Absolute Detection

Efficiency Ratios for a 2" x 2" CsI(Tl) Crystal

Gamma-ray Energy (Mev)	$\frac{\epsilon_p(3 \text{ cm})}{\epsilon_p(4 \text{ cm})}$	$\frac{\epsilon(3 \text{ cm})}{\epsilon(4 \text{ cm})}$	$\frac{\epsilon_p(3 \text{ cm})}{\epsilon_p(10 \text{ cm})}$	$\frac{\epsilon(3 \text{ cm})}{\epsilon(10 \text{ cm})}$	$\frac{\epsilon_p(8 \text{ cm})}{\epsilon_p(10 \text{ cm})}$	$\frac{\epsilon(8 \text{ cm})}{\epsilon(10 \text{ cm})}$
	Present Work		Present Work		Present Work	
0.279	1.478	1.518	6.404	6.672	1.470	1.486
0.662	1.440	1.450	5.932	6.010	1.458	1.474
0.835	1.435	1.455	5.841	5.958	1.449	1.462

TABLE 5.7

Comparison of Photopeak-Efficiency Ratios with Absolute Detection

Efficiency Ratios for a 3" x 3" CsI(Na) Crystal

Gamma-ray Energy (Mev)	$\frac{\epsilon_p(3 \text{ cm})}{\epsilon_p(4 \text{ cm})}$	$\frac{\epsilon(3 \text{ cm})}{\epsilon(4 \text{ cm})}$	$\frac{\epsilon_p(3 \text{ cm})}{\epsilon_p(10 \text{ cm})}$	$\frac{\epsilon(3 \text{ cm})}{\epsilon(10 \text{ cm})}$	$\frac{\epsilon_p(8 \text{ cm})}{\epsilon_p(10 \text{ cm})}$	$\frac{\epsilon(8 \text{ cm})}{\epsilon(10 \text{ cm})}$
	Present Work		Present Work		Present Work	
0.279	1.363	1.395	5.179	5.460	1.440	1.441
0.662	1.370	1.366	4.948	5.010	1.421	1.437
0.835	1.377	1.365	4.866	4.952	1.388	1.420

Generally, our values are slightly lower than the expected values, though in most cases, the discrepancy is well within the error. Furthermore, the discrepancy for the 3 to 10 cm ratio is greater than that for the 3 to 4 cm or 8 to 10 cm ratios. This definite tendency does indicate the possibility of some systematic errors in the crystal-to-source distances, but going in the same direction for all the crystals. Thus, the relative photopeak efficiencies determined by us experimentally, referring to the same crystal-to-source distances for different crystals, are expected to be within the uncertainties quoted by us. For the extrapolated values at 0 and 15 cm, the situation is not so favourable, but we have kept an ample margin in quoting the uncertainties in the results.

We examined our set-up experimentally by another method also. Using our 3" x 3" NaI(Tl) crystal and Heath's value for photofraction, we checked the calibration of a  $Mn^{54}$  source supplied by the Radio-Chemical Centre, Amersham, England, of known activity with an overall error of + 2.9% and - 3.0%. Our measurements agreed with the lower limit of the quoted activity. If the activity measured by us is actually slightly lower than the true value, then this would indicate a slight underestimation of the crystal-to-source distance on our part. This would also agree with the above mentioned comparisons of  $\frac{\epsilon_p(3\text{ cm})}{\epsilon_p(10\text{ cm})}$ , etc., because any underestimation of distance would affect the value of  $\epsilon_p$  at smaller distances to a greater extent and, therefore, would lower the observed ratio.

Naturally, we would have been much happier if the small discrepancies mentioned in this section were not present, but we believe that most of the results are not affected by any possible systematic errors of this nature.

#### 5.6 The Effect of the Finite Dimensions of the Sources:

As already stated earlier, the gamma-ray sources used by us were point or near-point sources. In most cases the suppliers informed us that the activity was spread over a central area of diameter less than  $\frac{1}{4}$ " of the mylar discs. Using Grosjean's (1962) formula to calculate the absolute detection efficiencies of sources of finite dimensions, we calculated the absolute detection efficiencies for disc-sources of diameter 2 cm placed co-axially over both a 2" x 2" and a 3" x 3" NaI(Tl) crystal. The values of different quantities were taken from the Table of Grosjean and Bossaert (1965) and the calculations were carried out for three different crystal-to-source distances in the range of 1 to 10 cm. We found that our results cannot be influenced to any great extent because of this. For the 2" x 2" NaI(Tl) crystal at 1.0 cm, 3.0 cm and 10.0 cm, the disc-source (radius 1 cm) absolute detection efficiencies were less than the corresponding point source absolute detection efficiencies by  $\sim 3$  to 3.5%,  $\sim 2$  to 2.5% and  $\sim 0.5\%$  in the energy region of interest. For the 3" x 3" NaI(Tl) crystal, the disc-source (radius 1 cm) absolute detection efficiencies at 1.0 cm, 3.0 cm and 10.0 cm were less than the corresponding point source absolute detection efficiencies by  $\sim 1.5\%$ ,  $\sim 1.5\%$  and 0.5%. Similar calculations for CsI crystals could not be carried out, as the finite

dimension correction factors are not available for them. We expect, however, that the effect of a disc-source of radius 1 cm on the CsI absolute detection efficiencies will be similar. Again, since we are dealing with relative efficiencies, our results suffer very little from the "finite dimension" effects.

#### 5.7 Photofractions of CsI and NaI Crystals:

As a matter of interest, we compare the photofractions of our 2" x 2" CsI(Tl) with that of a 2" x 2" NaI(Tl) crystal and the photofraction of our 3" x 3" CsI(Na) crystal obtained from the second method of analysis with that of a 3" x 3" NaI(Tl). The comparison for the 2" x 2" crystals is shown in Fig. 5.7 where the data for the NaI(Tl) crystal is taken from Mishra and Sadasivan (1969). The comparison for the 3" x 3" crystals is shown in Fig. 5.8 with data for the NaI(Tl) crystal taken from Heath (1964).

We observe that in each case the CsI crystal always shows a larger photofraction in comparison to a NaI(Tl) crystal of the same size. For this comparison for the 3" x 3" CsI(Na) crystal, the photofractions evaluated by the second method of analysis, i.e. considering the full peak as the photopeak, should be considered. However, the results obtained on the basis of the first method of analysis should not be rejected for practical reasons discussed earlier and, therefore, for the sake of completeness, we have also shown the values obtained from that analysis.

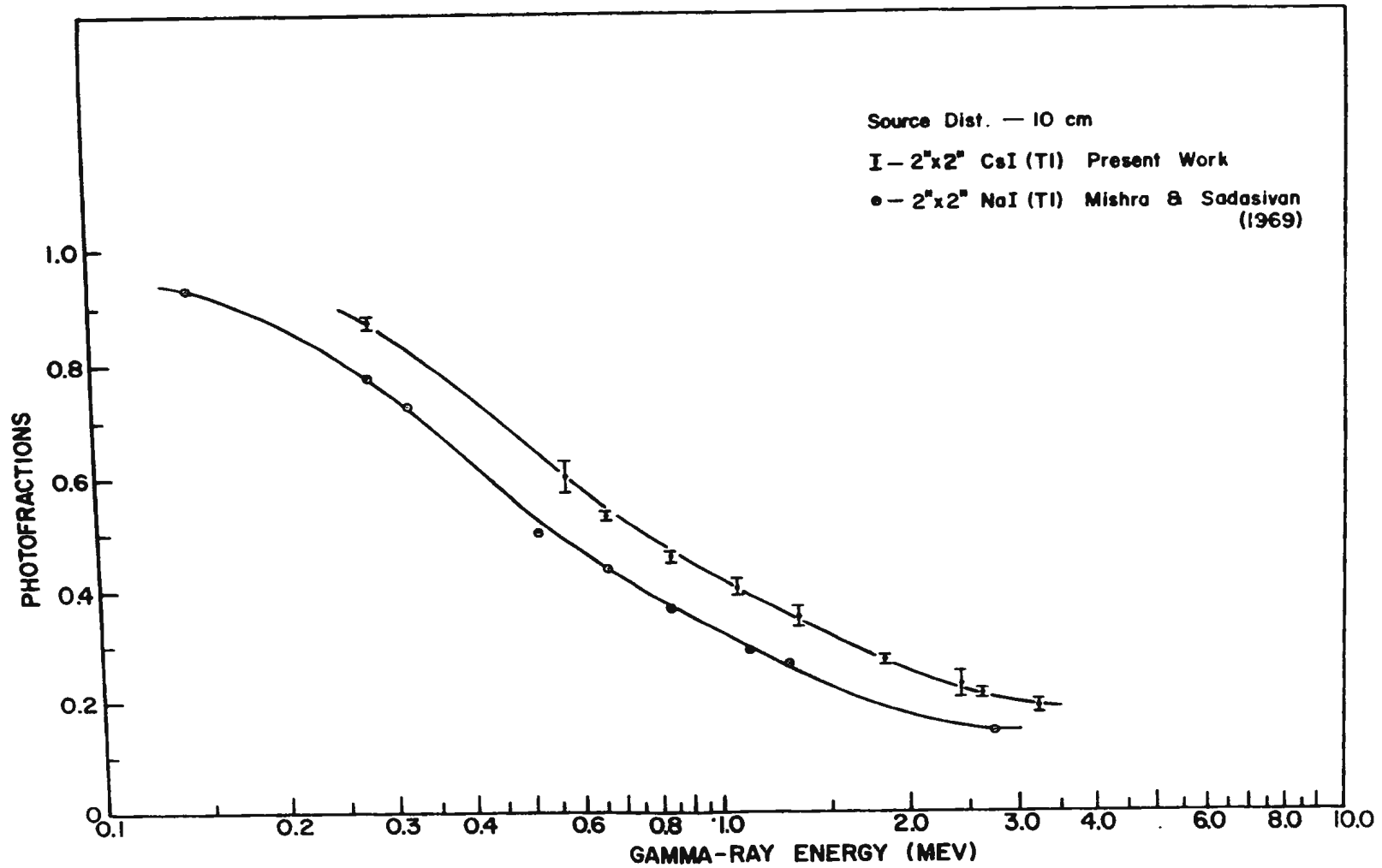


FIG. 5.7 Experimental photofractions of 2"x2" CsI (Tl) & 2"x2" NaI (Tl) crystals.

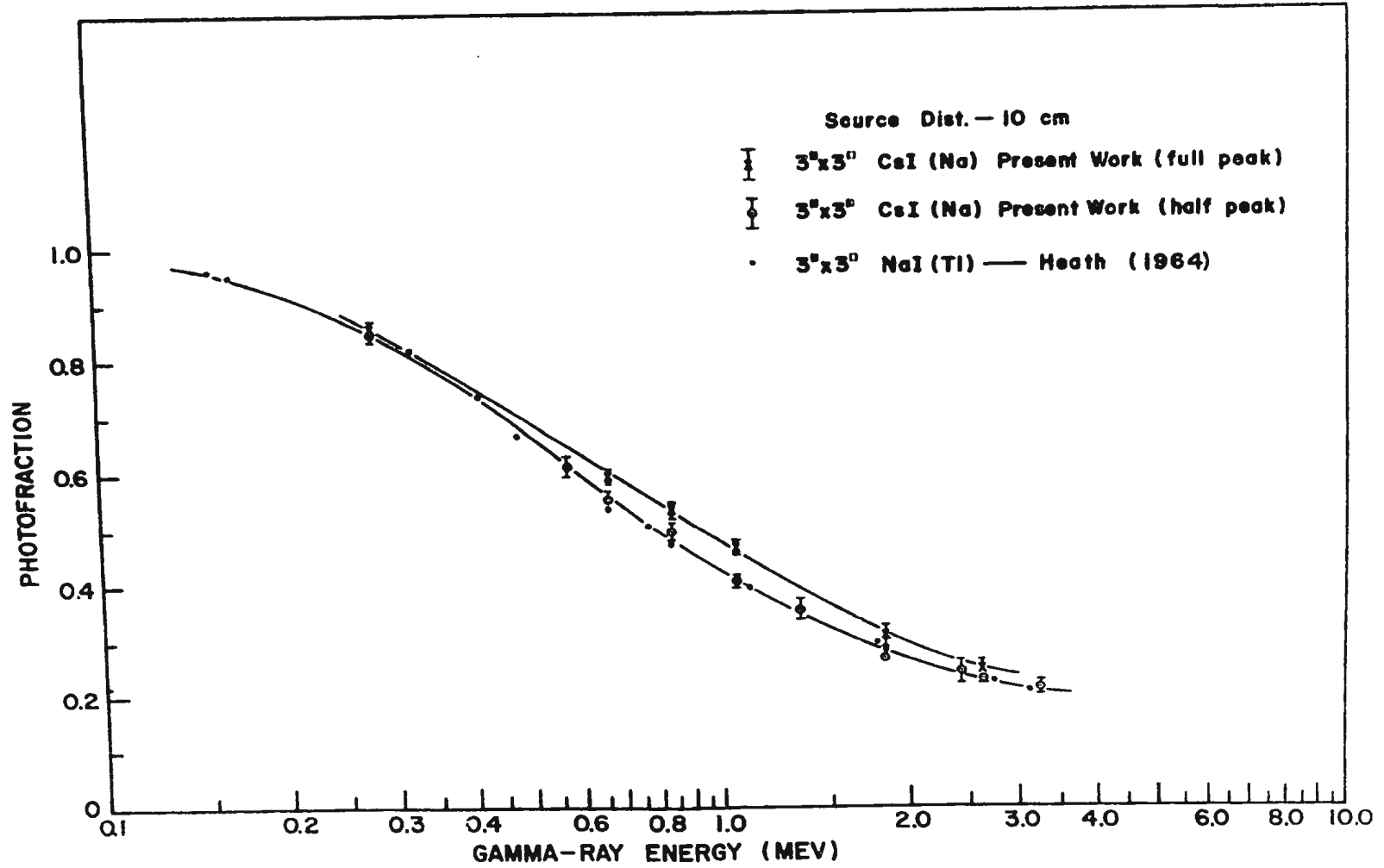


FIG. 5.8 Experimental photofractions of 3"×3" CsI(Na) and 3"×3" NaI(Tl) crystals.

5.8 The Concluding Remarks:

The technique employed by us in carrying out this project can be applied to other crystals for which the values of the photopeak efficiency and the photofraction are not known. A detailed study of the summing effects in various crystals is of great interest from the point of view of analyzing the complex spectra. In the absence of any complications due to the summing effects, our set-up can yield more accurate results if a gain stabilizer is incorporated. However, special mention has to be made of the unexpected asymmetry in the shape of the photopeaks in the 3" x 3" CsI(Na) crystal. We have not found any published reference to the existence of asymmetry of this magnitude in other crystals. Perhaps a combination of factors is responsible for this shape. We believe that the relative cross-sections of various interactions in the crystal, as well as the crystal size, play a part in this connection. Though the photofractions were found to be not too sensitively dependent on the crystal-to-source distances, we decided to carry out measurements at a large number of distances for the following reasons:

- (i) to obtain direct experimental values of the relative photopeak efficiencies for several distances,
- (ii) to be able to extrapolate the measured quantities to extend the range of our investigations, and
- (iii) to have flexibility in the schedule for carrying out measurements and, at the same time, to have provision for applying small

corrections to the crystal-to-source distances. (Need for a thorough examination of the crystal-to-can-top distance coupled with the undependable timetable for the availability of the sources made this an important factor.)

ACKNOWLEDGEMENTS

The author wishes to acknowledge with thanks the assistance received from the following members of the Department of Physics, Memorial University of Newfoundland:

Dr. M. Irfan under whose supervision the present investigations were carried out and who painstakingly guided the author at every stage of this project;

Dr. S. W. Breckon, Head of the Department, for his very keen interest throughout;

Mr. T. G. White and Mr. A. J. Walsh for their help in constructing the source-holder arrangement;

Mr. W. J. Higgins for his help in the photographic work;

Mr. R. Tucker for his help in drawing many of the diagrams;

Miss D. Janes and Mrs. G. Critch for typing the thesis;

Mr. Paul Gillard, a graduate student in Molecular Physics, for going through the manuscript and extending his help at various stages.

An acknowledgement is also extended to the Department of Technical Services, Memorial University of Newfoundland, for their help on several occasions.

Financial support received by the author from Memorial University and from the NRC Operating Grant awarded to Dr. M. Irfan is also gratefully acknowledged.

BIBLIOGRAPHY

- (1) Berger, M. J. and Doggett, J. Rev. of Scient. Instruments 27 No. 5 (1956) 269.
- (2) Breiter, G. and Schulz, G. Physics Letters 24A No. 6 (1967) 331.
- (3) Brinckmann, P. Physics Letters 15 No. 4 (1965) 305.
- (4) Chinaglia, B. and Malvano, R. Nucl. Instr. and Methods 45 (1966) 125.
- (5) Christaller, G. Nucl. Instr. and Methods 50 (1967) 173.
- (6) Coop, K. L. and Grench, H. A. Nucl. Instr. and Methods 36 (1965) 339.
- (7) Gossett, G. R. and Davisson, C. M. U. S. Naval Research Lab., Quarterly Progress Report (1961).
- (8) Grodstein, G. W. X-ray Attenuation Coefficients from 10 Kev to 100 Kev, NBS Circular 583 (1957).
- (9) Grosjean, C. C. Nucl. Instr. and Methods 17 (1962) 289.
- (10) Grosjean, C. C. The Inter. Jour. of Appl. Radiation and Isotopes 15 (1964) 239.
- (11) Grosjean, C. C. and Bossaert, W. Table of Absolute Detection Efficiencies of Cylindrical Scintillation Gamma-ray Detectors (A publication of the Computing Lab. of the Univ. of Ghent, Belgium, 1965).
- (12) Heath, R. L. AEC Report IDO-16408 (1958).
- (13) Heath, R. L. Scintillation Spectrometry Gamma-ray Spectrum Catalogue, AEC R and D Report IDO-16880 (1964).

- (14) Jarczyk, L., Knoepfel, H., Lang, J., Müller, R. and Wölfi, W.  
Nucl. Instr. and Methods 17 (1962) 310.
- (15) Korda, Yu S., Timoshevskii, G. F. and Remaev, V. V. Trans. from  
Atomnaya Energiya (USSR) 14 (1963) 319.
- (16) Kreger, W. E. and Brown, R. M. Nucl. Instr. and Methods 11 (1961)  
290.
- (17) Lazar, N. H., Davis, R. C. and Bell, P. R. IRE Trans. on Nucl.  
Science, NS-3 No. 4 (1956) 136.
- (18) Lazar, N. H. IRE Trans. on Nucl. Science, NS-5 No. 3 (1958) 138.
- (19) Leutz, H., Schulz, G. and Van Gelderen, L. Nucl. Instr. and  
Methods 40 (1966) 257.
- (20) McGinnies, Rosemary T. X-ray Attenuation Coefficients from 10 Kev  
to 100 Mev, NBS Supplement to 583 (1959).
- (21) Menefee, J., Cho, Y. and Swinehart, C. IEEE Trans on Nucl. Science,  
NS-14 No. 1 (1967) 464.
- (22) Miller, W. F. and Snow, William J. Rev. of Scient. Instruments 31  
No. 8 (1960) 861.
- (23) Miller, W. F. and Snow, William J. Nucleonics 19 No. 11 (1961) 174.
- (24) Miller, W. F. and Snow, William J. Monte-Carlo Calculation of the  
Energy Loss Spectra for Gamma-rays in Sodium Iodide and Cesium  
Iodide, AEC Report ANL-6318 (1961).
- (25) Mishra, U. C. and Sadasivan, S. Nucl. Instr. and Methods 69 (1969)  
330.
- (26) Polevoi, R. M. Pribory i Tekh. Eksper. (USSR) No. 4 (1961) 47.  
(Engl. Trans.: Instr. Exper. Tech. (USA) No. 4 (1962) 668).

- (27) Schmidt, C. T. IRE Trans. on Nucl. Science, NS-7 No. 2-3 (1960) 25.
- (28) Snyder, B. J. Nucl. Instr. and Methods 46 (1967) 173.
- (29) Stanford, A. L., Jr. and Rivers, W. K., Jr. Rev. of Sci. Instruments 29 No. 5 (1958) 406.
- (30) Steyn, J. J. and Andrews, D. G. Nucl. Instr. and Methods 68 (1969) 118.
- (31) Storm, E., Gilbert E. and Israel, H. Gamma-ray Absorption Coefficients for Elements 1 through 100, Report LA-2237 (1958).
- (32) Van Oostrum, K. J. and Meijer, A. C. Nucl. Instr. and Methods 10 (1961) 31.
- (33) Vartanov, N. A. and Samoilov, P. S. Pribory i Tekh. Eksper. (USSR) No. 2 (1965) 69 (Engl. Trans.: Instr. Exper. Tech. (USA) No. 2 (1965) 310).
- (34) Vegors, S. H., Marsden, L. L. and Heath, R. L. Calculated Efficiencies of Cylindrical Radiation Detectors, AEC Report IDO-16370 (1958).
- (35) Weitkamp, C. Nucl. Instr. and Methods 23 (1963) 10.
- (36) Weitkamp, C. Nucl. Instr. and Methods 23 (1963) 13.
- (37) Wolicki, E. A., Jastraw, R. and Brooks, F. Calculated Efficiencies of NaI Crystals, NRL Report-4833 (1956).
- (38) Young, F. C., Heaton, H. T., Phillips, G. W., Forsyth, P. D. and Marion, J. B. Nucl. Instr. and Methods 44 (1966) 109.
- (39) Zerby, C. D. and Moran, H. S. Calculation of the Pulse-Height Response of NaI(Tl) Scintillation, AEC Report ORNL-3169 (1961).

ADDITIONAL GENERAL REFERENCES

- (1) Birks, J. B. The Theory and Practice of Scintillation Counting  
(A Pergamon Press Book, The Macmillan Co., New York, 1964).
- (2) Chase, Robert L. Nuclear Pulse Spectrometry (McGraw-Hill Book Co.,  
Inc., New York, Toronto and London, 1961).
- (3) Crouthamel, C. E. (Ed). Applied Gamma-ray Spectrometry (Pergamon  
Press, New York, Oxford, London and Paris, 1960).
- (4) Fenyves, E. and Haiman, O. The Physical Principles of Nuclear  
Radiation Measurements (Academic Press, New York and London,  
1969).
- (5) Harshaw Scintillation Phosphors (The Harshaw Chemical Co., Cleveland,  
Ohio, 1962).
- (6) Shafroth, Stephen M. (Ed.). Scintillation Spectroscopy of Gamma  
Radiation (Gordon and Breach, 1966).
- (7) Siegbahn, Kai (Ed.).  $\alpha$ ,  $\beta$ ,  $\gamma$  Ray Spectroscopy, Vol. I (North-  
Holland Publishing Co., Amsterdam, 1965).
- (8) Snell, Arthur H. (Ed.). Nuclear Instruments and Their Uses (John  
Wiley and Sons, 1962).



